INFORMATION TO USERS

This manuscript has been reproduced from the microfilm master. UMI films the text directly from the original or copy submitted. Thus, some thesis and dissertation copies are in typewriter face, while others may be from any type of computer printer.

The quality of this reproduction is dependent upon the quality of the copy submitted. Broken or indistinct print, colored or poor quality illustrations and photographs, print bleedthrough, substandard margins, and improper alignment can adversely affect reproduction.

In the unlikely event that the author did not send UMI a complete manuscript and there are missing pages, these will be noted. Also, if unauthorized copyright material had to be removed, a note will indicate the deletion.

Oversize materials (e.g., maps, drawings, charts) are reproduced by sectioning the original, beginning at the upper left-hand corner and continuing from left to right in equal sections with small overlaps. Each original is also photographed in one exposure and is included in reduced form at the back of the book.

Photographs included in the original manuscript have been reproduced xerographically in this copy. Higher quality 6" x 9" black and white photographic prints are available for any photographs or illustrations appearing in this copy for an additional charge. Contact UMI directly to order.

UMI

A Bell & Howell Information Company
300 North Zeeb Road, Ann Arbor MI 48106-1346 USA
313/761-4700 800/521-0600

A

Quantum Optical Tests of Complementarity: Quantum Eraser and The Decoherence Time of a Local Measurement Process

by
Yonatan Abranyos

A dissertation submitted to the Graduate Faculty in Physics in partial fulfillment of the requirements for the degree of Doctor of Philosophy, The City University of New York

1999

This manuscript has been read and accepted for the Graduate Faculty in Physics in satisfaction of the dissertation requirement for the degree of Doctor of Philosophy.

4/8/99
Date

Professor János A. Bergou
Chair of Examining Committee

4/20/99
Date

Professor Louis S. Celenza
Executive Officer

Professor Mark Hillery

Professor Ying-Chin Chen

Professor Leon Cohen

Professor Edward Whittaker

Supervisory Committee

THE CITY UNIVERSITY OF NEW YORK

Abstract

Quantum Optical Tests of Complementarity: Quantum Eraser and The Decoherence Time of a Local Measurement Process

by

Yonatan Abranyos

Adviser: Professor János A. Bergou

Quantum optical tests of the fundamental principles of quantum mechanics, in particular, complementarity, entanglement and non-locality, are the central themes of this dissertation. A which-path experiment is implemented based on a recent experiment by Eichmann *et al.* [1] involving two four-level atoms. In the version considered here a continuous Broad Band Excitation field drives the two trapped atoms and, depending on the type of scattering, information about which atom scattered the light is stored in the internal degrees of the atoms. Entanglement of the atoms-photon system is intimately connected to the availability of "which way" information. The quantum eraser disentangles the atoms-photon system and consequently "which way" information is lost leading to interference. Two different experimental schemes based on the Eichmann *et al.* experiment are proposed for the implementation of

the quantum eraser. The quantum eraser schemes erase the "which way" information and interference is observed in the second order correlation function. With a slight modification of the experiment, a scheme that allows to verify recently derived inequalities by Englert [2] in connection with distinguishability and visibility in a two-way interferometer is proposed. These inequalities, in some sense, can be regarded as quantifying the notion of wave-particle duality. The visibility of interference depends on the detected polarization direction of the scattered light, and a reading out of the internal atomic states of one of the two atoms provides for partial "which way" information or distinguishability of the two different paths. Finally, the quantum eraser is used to measure the decoherence time of a local measurement process. The experiment proposed is similar to the quantum eraser setup and contains the complete measurement process of system-meter-environment interaction. The decoherence time is quantitatively expressed in the amount of reduction of the visibility in the second order correlation function. In addition, it explores how we can cast the question of quantum coherence of mesoscopic or macroscopic systems with a quantum eraser or in general interference experiments.

Acknowledgements

I would like to express my deepest gratitude and appreciation to my adviser Professor János A. Bergou. His support, suggestions and advice were invaluable and his warm and friendly interaction were indispensable. I am grateful to Professor Mark Hillery for the lectures and seminars he organized through the years, the committee members for their time and energy, Dr. Matthias Jakob of Ulm, Germany, for the numerous discussions we had and his ideas, and Jozef Skvarcek for introducing me to Linux and helping me with application softwares. I am deeply indebted to Cristina for her constant support and encouragement. And finally, I am very grateful to my family for their support.

Table of contents

List of Figures

Chapter I

1 Introduction

1.1 Complementarity

Recently there has been a growing number of experiments and theoretical models in quantum optics which are used to test the fundamental principles of quantum mechanics. Some of the implications and counter intuitive results of quantum mechanics, which are demonstrated through gedanken experiments such as the EPR paradox and Bell's Theorem, are still explored at the present time. In this dissertation we develop a scheme to implement one such process, *The Quantum Eraser*, to demonstrate the principle of complementarity and to explore a local measurement process. The quantum eraser gives a clear demonstration of the non-local behavior of quantum systems, via entanglement of separate quantum systems. The application of the quantum eraser as a tool to study the decoherence in a local measurement process also helps to investigate the transitions from microscopic to mesoscopic to macroscopic systems.

Bohr's principle of complementarity [3] is vividly manifested in the classic double-slit experiment. The central point is that quantum systems exhibit properties which are both equally real but mutually exclusive. In the case of the double-slit experiment, these two realities are manifested via visibility of fringes (wave-like property)

or " which way" information (particle-like property). Depending on the type of experimental setup, one can observe either wave-like or particle-like property. This is commonly termed *duality*. The decision to observe wave-like or particle-like behavior can be made at any time during the course of the experiment. As J. A. Wheeler [4] showed in a beam splitter experiment, one can arrange to observe either of the dual behaviors of a photon after the photon has left the source and is on the way to a measuring apparatus. This *delayed choice* shows that before measurement is done (irreversible interaction with the environment) either one of the two properties can be realized. Even though these two realities are mutually exclusive, it has been shown [2] that there is a certain degree of flexibility in which the two properties are realized. In other words, one can have a certain amount of "which way" information while preserving some visibility of fringes.

1.2 Entanglement, "Which-Way" Information and Quantum Eraser

Complementarity is a general concept with the traditional wave-particle duality being one common example. In general, two observables are complementary if exact knowledge of one precludes any precise knowledge of the other. For example, the presence of interference in a two-way interferometry and the knowledge of which path the particle took illustrate the concept. In the double-slit experiment any measurement of position (slit) to determine which path the particle took through the double-slit appa-

ratus destroys the interference pattern. In which-path experiments, such as Einstein's recoiling slit [3] and Feynman's light microscope [5], the destruction of interference is explained in terms of uncontrolled classical momentum kicks to the particle. This random momentum transfer in such experiments amounts to at least $\pi\hbar/2d$ where d is the slit width in accordance to the uncertainty principle and is sufficient to smear the interference pattern.

Recently, the question whether the destruction of the interference pattern in a which-path experiment necessarily involves momentum transfer has been raised. According to Scully *et al.* [6], the destruction of interference can occur without any momentum transfer and gave as an example a which-path experiment scheme involving an interaction between an atom and a microwave cavity field where the states of the cavity field serve as which-path flags. By exploring the states of the cavity field it is possible to know the path of the atom, and they point out that no momentum transfer to the atom occurs. Wiseman *et al.* [7, 8] argue that the destruction of interference in a which-path experiment due to measurement can always be attributed to momentum transfer depending on how one defines momentum transfer. Accordingly, they gave two ways of defining random momentum transfer. The first definition corresponds to the classical convolution of the particle's momentum probability distribution with a momentum transition probability distribution, and the second as the convolution of the particle's momentum space wave function with a set of momen-

tum transfer amplitudes [7]. In the older which-path experiments, such as Einstein's recoiling slit and Feynman's light microscope, the destruction of the interference pattern involves local random momentum transfer corresponding to the first definition, while in the scheme of Scully *et al.* the momentum transfer is of a peculiar quantum, nonlocal nature, corresponding to the second definition [7, 8].

We will see next that whether we have a which-path experiment involving local momentum transfer or a nonlocal momentum transfer, entanglement plays a crucial role in deciding if either of the complementary behaviors is exhibited. In other words, regardless of how complementarity is enforced in a which-path experiment, the absence or presence of interference pattern is determined by whether the quantum sub-systems describing the system are entangled or not. In general, non-entanglement of quantum sub-systems leads to interference, and entanglement of quantum sub-systems leads to "which way" information. A quantum system of two or more sub-systems is said to be entangled if the state vector describing the quantum system is not factorizable. For example, for a two-particle system the state $\alpha|a,b\rangle + \beta|b,a\rangle$ is entangled for α and β non zero, and is maximally entangled for $\alpha = \beta = 1/\sqrt{2}$ and is not entangled if either α or $\beta = 0$.

In order to illustrate this point, we consider a quantum system with two sub-systems, A and B, in a two-way interferometric setup with an optional which-path detector Fig. 1. We denote the two possible paths of the interferometer by 1 and 2,

and the state vectors for a particle to go through either of the two paths by $|\psi_1(\mathbf{r})\rangle$ and $|\psi_2(\mathbf{r})\rangle$.

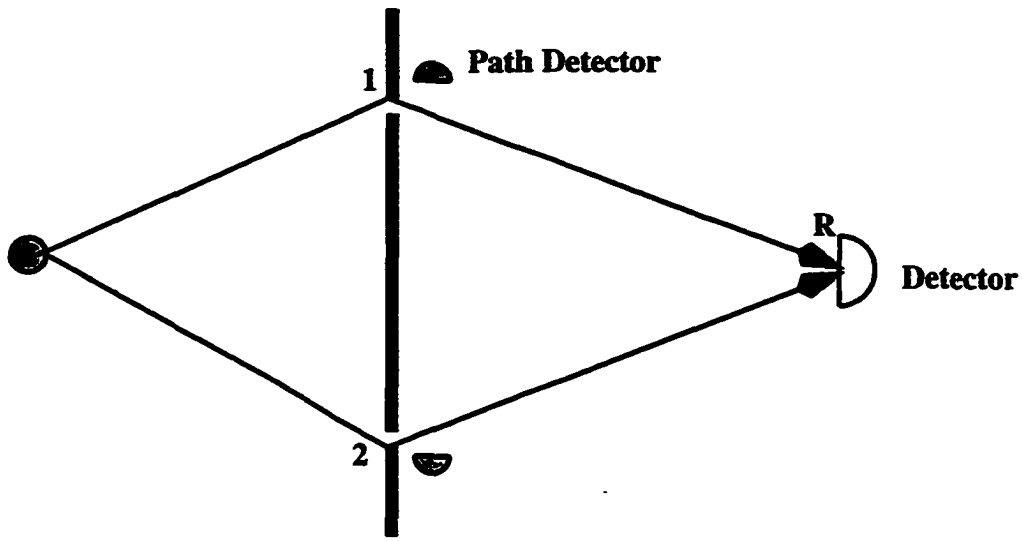

Figure 1: Two-way interferometer with optional path-detectors. Depending on whether the path-detectors are active or not interference is observed at the detector at position R. Entanglement of the quantum sub-systems (particle and detector) leads to noninterference, and non-entanglement of the quantum sub-systems leads to interference.

The state vector for the two-way interferometer (sub-system A) is then

$$|\psi_A(\mathbf{r})\rangle = |\psi_1(\mathbf{r})\rangle + |\psi_2(\mathbf{r})\rangle, \tag{1.2.1}$$

and the state vector for the path detector (sub-system B) is given by

$$|\psi_B\rangle = |l_1, k_1\rangle, \tag{1.2.2}$$

where, $l, k = 0, 1$ with $|1_1, 0_2\rangle$ and $|0_1, 1_2\rangle$ indicate a detection of the particle through path 1 or 2 respectively. If the path detector is inactive, the state vector of the

composite system is

$$|\Psi(\mathbf{r})\rangle = (|\psi_1(\mathbf{r})\rangle + |\psi_2(\mathbf{r})\rangle)|0_1, 0_2\rangle. \tag{1.2.3}$$

The state vector for the detector is $|0_1, 0_2\rangle$ since it is inactive and did not detect the particle. We then get for the probability density at position $\mathbf{R}$ the following

$$\begin{aligned} P(\mathbf{R}) &= \langle\Psi(\mathbf{R})|\Psi(\mathbf{R})\rangle \\ &= \big(\langle\psi_1(\mathbf{R})|\psi_1(\mathbf{R})\rangle + \langle\psi_2(\mathbf{R})|\psi_2(\mathbf{R})\rangle \\ &+ \langle\psi_1(\mathbf{R})|\psi_2(\mathbf{R})\rangle + \langle\psi_2(\mathbf{R})|\psi_1(\mathbf{R})\rangle\big)\langle 0_1, 0_2|0_1, 0_2\rangle \\ &= \langle\psi_1(\mathbf{R})|\psi_1(\mathbf{R})\rangle + \langle\psi_2(\mathbf{R})|\psi_2(\mathbf{R})\rangle + \langle\psi_1(\mathbf{R})|\psi_2(\mathbf{R})\rangle + \langle\psi_2(\mathbf{R})|\psi_1(\mathbf{R})\rangle. \end{aligned} \tag{1.2.4}$$

Here, we get interference (the last two terms) and we note the state of the two sub-systems is not entangled. It is also important to recognize that when the path detectors are inactive, it is not possible to know which path of the interferometer is taken. In other words, no "which way" information leads to interference. We consider now the situation where the path detector is active, so that we can know which path of the interferometer is taken. In this case, the state vector of the system is

$$|\Psi(\mathbf{r})\rangle = |\psi_1(\mathbf{r})\rangle|1_1, 0_2\rangle + \psi_2(\mathbf{r})|0_1, 1_2\rangle. \tag{1.2.5}$$

The probability density is then

$$\begin{aligned} P(\mathbf{R}) &= \langle \Psi(\mathbf{R}) | \Psi(\mathbf{R}) \rangle \\ &= \langle \psi_1(\mathbf{R}) | \psi_1(\mathbf{R}) \rangle + \langle \psi_2(\mathbf{R}) | \psi_2(\mathbf{R}) \rangle \\ &+ \langle \psi_1(\mathbf{R}) | \psi_2(\mathbf{R}) \rangle \langle 1_1, 0_2 | 0_1, 1_2 \rangle + \langle \psi_2(\mathbf{R}) | \psi_1(\mathbf{R}) \rangle \langle 0_1, 1_2 | 1_1, 0_2 \rangle \\ &= [\langle \psi_1(\mathbf{R}) | \psi_1(\mathbf{R}) \rangle + \langle \psi_2(\mathbf{R}) | \psi_2(\mathbf{R}) \rangle. \end{aligned} \tag{1.2.6}$$

In this case, the interference terms vanish due to the orthogonality of the detector states. We note that when the two sub-systems are entangled, we can know which path the particle took, i.e. by reading the state of the detector, and consequently there is no interference. We do not need to actually know which path the particle took, only the possibility is sufficient to remove the interference.

We now consider the question of the quantum eraser. We have seen earlier that non-entanglement leads to interference and entanglement leads to non-interference or "which way" information. If we consider the case where we have entanglement implying "which way" information, we are led to investigate if it is possible, by some means, to reinstate the interference term, that is to erase the "which way" information after the process has already occurred. In order to erase the information, we need to disentangle the system so that we cannot know, even in principle, which path the particle took. So a quantum eraser is a device which disentangles originally entangled sub-systems, therefore interference is restored. In other words, a quantum eraser can

be described as a device in which coherence appears to be lost in a quantum subsystem, but in which the coherence can be restored by erasing the information which originally destroyed it.

To illustrate the essential points, we discuss an experiment originally proposed by Scully [6] involving the scattering of light from two 4-level atoms. The atoms play the role of the slits in an analogous way as Youngs's double-slit experiment, and the internal states serve as possible which-path flags. We will discuss schemes to implement a quantum eraser using a pair of 4-level atoms in detail in subsequent chapters. Here we will outline the basic ideas involved in a qualitative way. The experimental setup is shown in Fig. 2.

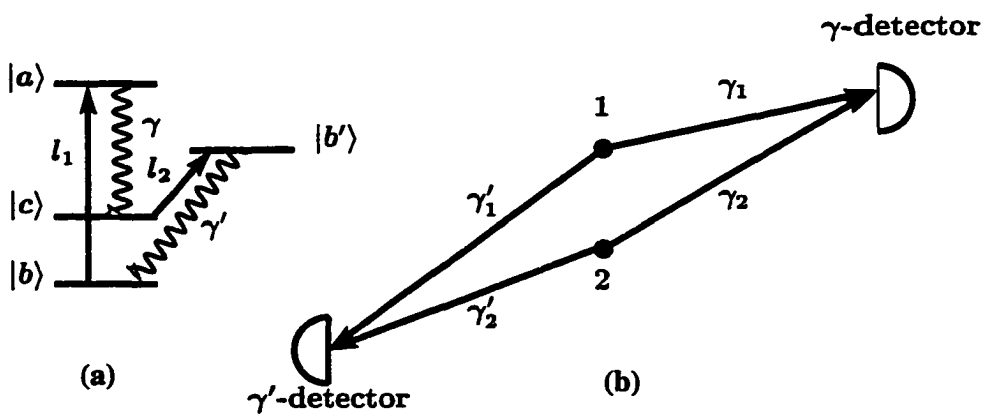

Figure 2: (a) Internal structure of a 4-level atom for the implementation of a quantum eraser proposed by Scully *et al.*. (b) The scattering photons are detected at the γ-detector and the erasing photons are detected at the γ'-detector, and interference occurs in the coincidence measurement of the γ and γ' photons.

The two 4-level atoms are situated at sites 1 and 2. The separation between the atoms is assumed to be very large compared to the wavelength of the laser pulses used to excite them. A laser pulse l_1, short enough to excite only one atom, excites one of the atoms from level $|b\rangle$ to level $|a\rangle$ followed by a spontaneous emission to level $|c\rangle$ of a $|\gamma\rangle$ photon which is detected at the γ-detector. The state vector of the atoms-photon system is then

$$|\psi_1\rangle = |c_1, b_2\rangle|\gamma_1\rangle + |b_1, c_2\rangle|\gamma_2\rangle. \tag{1.2.7}$$

We note that we have entanglement of the atoms-photon system, therefore we have "which way" information. It is possible to know which atom is involved in the scattering process by exploring the internal levels of the atoms, and consequently, a measurement of the first order correlation function (field correlation) at the $|\gamma\rangle$-detector yields no interference. How can we erase the information contained in the internal levels of the atoms so that we cannot know which atom scattered the photon? To accomplish this, a second laser pulse l_2 which is tuned to take state $|c\rangle$ to $|b'\rangle$ is applied. It is assumed that $|b'\rangle$ is strongly coupled to $|b\rangle$ so that we have a spontaneous decay from $|b'\rangle$ to $|b\rangle$ with an emission of $|\gamma'\rangle$ photon. The state vector of the system is then

$$|\psi_2\rangle = |b_1, b_2\rangle(|\gamma_1, \gamma_1'\rangle + |\gamma_2, \gamma_2'\rangle). \tag{1.2.8}$$

Here, we note that the atoms-photons system is disentangled, and it is not possible to know which atom scattered the photon if we detect the $|\gamma\rangle$ photons at the γ-

detector and $|\gamma'\rangle$ photons at the γ'-detector. Measurement of intensity correlation of $|\gamma\rangle$ photons at the γ-detector and $|\gamma'\rangle$ photons at the γ'-detector exhibits interference.

We gave here a qualitative description of the quantum eraser. The detailed analysis and implementation of the quantum eraser based on the experiment of Eichmann *et al.* [1] is one of the main goals of this thesis and will be presented in subsequent chapters. We outline here the general setup of the thesis. Chapter II is devoted to the dynamical behavior of a 4-level atom where the upper and lower states, which are two fold-degenerate, are driven by a linearly polarized monochromatic laser that is in near resonance with the transition frequency between the upper and lower states. This is important because our implementation of the quantum eraser is based on a pair of 4-level atoms. In Chapter III we show what happens to the interference pattern when we drive two 4-level atoms, especially in the saturated or steady state regime. We show that a continuous monochromatic driving field cannot be used to implement an experiment where the lack of interference is due to the presence of "which way" information. Conversely, the presence of interference is not due to the lack of "which way" information, but is a consequence of the steady state behavior of the atoms. In chapter IV we will investigate if there is still the possibility of having "which way" information in the case when there is no interference. A Broad Band Excitation (BBE) of the two atoms is shown to give a possible scheme for an interference experiment where the lack of interference is due to the availability

of "which way" information. This consideration shows that there is a possibility, even in the long time regime, to use the Eichmann *et al.* [1] description if we use BBE of the two atoms. For such kind of excitation, it is possible to talk about independent excitation and scattering of photons (one at a time), which is necessary in the quantum eraser. Proceeding from these clarifications, we show in Chapter V two possible schemes to implement a quantum eraser where the two atoms are continually driven as in the experiment of Eichmann *et al.*. The first scheme uses a general initial condition of the atoms and the second scheme uses a special initial condition of the atoms where the degeneracy of the two 4-level atoms is removed with the application of a magnetic field. Chapter VI has two parts. In the first part, we show how the quantum eraser scheme can be used to display anti-fringes [9] with intensity minimum at the center. The second and main part is devoted to developing a scheme to quantify the duality concept of complementarity. We use the schemes of the previous chapters with slight modifications to get partial "which way" information and partial fringe visibility. A fundamental inequality relating distinguishability and visibility is verified. In Chapter VII we use the quantum eraser as a tool to visualize the decoherence of a local measurement process and explore the measurement process itself. In addition, it contains how we can cast the question of quantum coherence of mesoscopic or macroscopic systems with a quantum eraser or in general interference experiments. Finally we offer a discussion and conclusion in Chapter VIII.

In order to maintain the flow of the thesis, we include many important detailed calculations in the appendix. Appendix A contains calculations of solutions of the equations of motion of two atoms in a BBE field. In appendix B we show that a general incoherent initial condition of the two atoms can give rise to interference. And finally, in appendix C, we provide the calculations of the second order correlation function for a general incoherent initial condition for the quantum eraser.

Chapter II

2 Dynamics of a Driven 4-Level Atom

2.1 Introduction

We have seen in the introduction that in order to implement "which way" experiments with possible quantum eraser schemes via scattering of light a 4-level atomic structure can be used [6]. We dedicate this chapter to study the dynamics of a single driven 4-level atom. The dynamical equations for a 4-level atom driven by a monochromatic field and coupled to a reservoir at zero temperature have an important role in our implementation of a "which way" experiment. Here we give a solution to the system and find the expectation values of the radiated field in different polarization directions. These results will be used in subsequent chapters. A thorough understanding of the 4-level system reveals the essential issue involved in the implementation of "which way" experiments, if and when we can use such a system to implement a "which way" experiment. As we will see later, the availability of a "which way" information, whether we know the actual path or not, is a necessary condition for implementation of a quantum eraser.

We consider a 4-level atom with two lower states and two upper states which are degenerate with respect to the magnetic quantum number m_j (see Fig. 3). As a result

of the internal structure, the resonance fluorescence contains π-polarized scattered field ($|\Delta m_j| = 0$) and σ-polarized scattered field ($|\Delta m_j| = 1$), when the incident light is linearly polarized. Due to this level structure, the interference properties of the scattered light are sensitive to polarization-sensitive detection schemes [1, 10, 11, 12]. The interference pattern comes only from the π-polarized coherent part of the scattered field ($|\Delta m_j| = 0$), while the σ-polarized incoherent part ($|\Delta m_j| = 1$) gives no contribution to the interference pattern.

The dynamical equations for a driven 4-level atom were derived by Polder and Schurmann [11] in the context of fluorescence. The master equation describing the system was derived by Walls and *et al* [12] in the context of interference in their analysis of the experiment of Eichmann *et al.* [1]. Here we use the results of Polder and Schurmann [11] to derive explicitly the time dependence and expectation values of the electric field components in different polarization directions. These results are needed when we consider interference effects in the resonance fluorescence from two atoms, especially in the steady state regime.

2.2 Master Equation

We consider an atom at rest at the position $\mathbf{r} = 0$ which is coupled to the electromagnetic field in the dipole approximation by the interaction Hamiltonian

$$H_{int} + H_{dri} = -\boldsymbol{\mu} \cdot \mathbf{E}(\mathbf{r} = 0, \mathrm{t}). \tag{2.2.1}$$

Here μ is the electric dipole operator $e\mathbf{r}$ and the electric field is the sum of the classical x-polarized driving field and the quantized field of all modes in free space at zero temperature. The classical x-polarized driving field is given by

$$\mathbf{E}_c(\mathbf{r},t) = \hat{\mathbf{x}}\mathbf{E}_o(\mathbf{r})\cos(\omega t),$$

and the quantized field is given by

$$\mathbf{E}_q(\mathbf{r}) = \sum_{\mathbf{k}} \hat{e}_{\mathbf{k}s}\{g_{\mathbf{k}}(\mathbf{r})b_k + g^*_{\mathbf{k}}(\mathbf{r})b^\dagger\}. \tag{2.2.2}$$

Here

$$g_k(\mathbf{r}) = \left(\frac{\hbar\omega_k}{2\epsilon_0 V}\right)^{\frac{1}{2}} e^{i\mathbf{k}\cdot\mathbf{r}},$$

and $b_{\mathbf{k}}$ and $b^\dagger_{\mathbf{k}}$ are the annihilation and creation operators for the quantized field, respectively, with the boson commutation relations

$$[b_{\mathbf{k}}, b_{\mathbf{k}'}] = [b^\dagger_{\mathbf{k}}, b^\dagger_{\mathbf{k}'}] = 0, \qquad [b_{\mathbf{k}}, b^\dagger_{\mathbf{k}'}] = \delta_{\mathbf{k}\mathbf{k}'}.$$

We denote the two lower states with $|1\rangle$ and $|2\rangle$ with magnetic quantum numbers $m_j = -1/2$ and $m_j = +1/2$, respectively, and the two upper states with $|3\rangle$ and $|4\rangle$ with the corresponding magnetic quantum numbers $m_j = -1/2$ and $m_j = +1/2$. The frequency splitting between the lower and upper states is ω_0. We consider the quantized field as a reservoir at zero temperature coupled to the atom in the Markoff approximation. In addition, we use the rotating wave approximation in the interaction Hamiltonian which describes the interaction of the field with the atom. The dipole

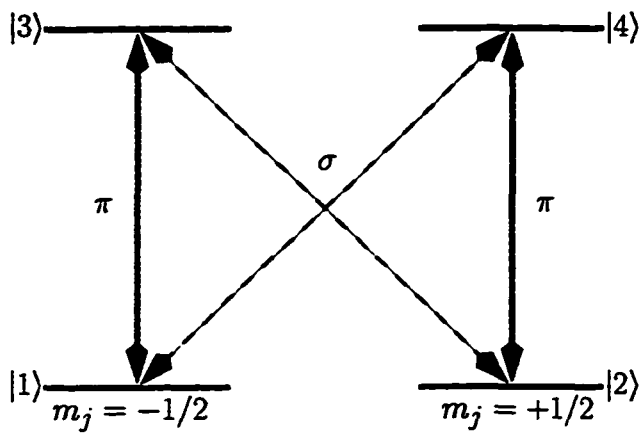

Figure 3: Internal structure of the 4-level atom with polarization sensitive transitions: π-polarized transition for $|\Delta m_j| = 0$ and σ-polarized transition for $|\Delta m_j| = 1$.

operator for our system can be written as follows

$$\begin{aligned} \mu &= \mu\{\hat{\mathbf{x}}(|1\rangle\langle 4| + |2\rangle\langle 3|) \\ &+ i\hat{\mathbf{y}}(|1\rangle\langle 4| - |2\rangle\langle 3|) \\ &+ \hat{\mathbf{z}}(|1\rangle\langle 3| - |2\rangle\langle 4|)\} + H.c. \quad . \end{aligned} \tag{2.2.3}$$

Here we have expanded μ in the atomic basis and $\mu = e\langle 1|x|4\rangle$ (assumed the same for all transitions). We then have for the total Hamiltonian

$$H = H_A + H_F + H_{dri} + H_{int}. \tag{2.2.4}$$

Here H_A is the unperturbed atomic Hamiltonian, H_F is the field Hamiltonian, H_{driv} and H_{int} describe the interactions of the atom with the classical driving field and the

quantized field, respectively,

$$\begin{aligned} H_0 &= H_A + H_F = \frac{\hbar\omega_0}{2}\{|4\rangle\langle 4| + |3\rangle\langle 3| - |2\rangle\langle 2| - |1\rangle\langle 1|\} + \hbar\sum_{\mathbf{k}} \omega_k b_{\mathbf{k}}^\dagger b_{\mathbf{k}}, \\ H_{dri} &= -\hbar v\{(|1\rangle\langle 4| + |2\rangle\langle 3|)e^{i\omega t} + (|4\rangle\langle 1| + |3\rangle\langle 2|)e^{-i\omega t}\}, \\ H_{int} &= -\hbar\sum_{\mathbf{k}}\sum_{i,j=1}^{4}\langle i|\boldsymbol{\mu}\cdot\hat{\mathbf{e}}_{\mathbf{k}}|j\rangle(g_{\mathbf{k}}(\mathbf{r})b_{\mathbf{k}} + g_{\mathbf{k}}^*(\mathbf{r})b_{\mathbf{k}}^\dagger)|i\rangle\langle j|. \end{aligned} \tag{2.2.5}$$

We now make a transformation to an interaction picture and eliminate H_0 with the following

$$\begin{aligned} |\Psi_S\rangle &= \exp\{-i\Phi t/\hbar\}|\Psi_I\rangle, \\ \Phi &= H_0 + \frac{\hbar\Delta}{2}\{|4\rangle\langle 4| + |3\rangle\langle 3| - |2\rangle\langle 2| - |1\rangle\langle 1|\}, \end{aligned} \tag{2.2.6}$$

and we get an interaction Hamiltonian

$$\begin{aligned} H_I(t) &= -\hbar\Delta\{|4\rangle\langle 4| + |3\rangle\langle 3| - |2\rangle\langle 2| - |1\rangle\langle 1|\} \\ &+ \hbar v\{|1\rangle\langle 4| + |2\rangle\langle 3| + |4\rangle\langle 1| + |3\rangle\langle 2|\} \\ &+ \hbar\sum_{k}\left\{\tilde{g}_{\mathbf{k}}^* b_{\mathbf{k}}^\dagger[(1-i)|1\rangle\langle 4| + (1+i)|2\rangle\langle 3| + |2\rangle\langle 4| - |1\rangle\langle 3|]e^{i(\omega_k-\omega)t} + H.c.\right\}. \end{aligned} \tag{2.2.7}$$

Here $\tilde{g}_{\mathbf{k}}^* = \mu g_{\mathbf{k}}^*(\hat{\mathbf{e}}_{\mathbf{i}}\cdot\hat{\mathbf{e}}_{\mathbf{k}})_{av}$ where the average is over polarization angles, $\hat{\mathbf{e}}_{\mathbf{i}}$ is a unit vector ($\hat{\mathbf{x}}, \hat{\mathbf{y}}$, or $\hat{\mathbf{z}}$), $v = \boldsymbol{\mu}\cdot\mathbf{E}_0/2\hbar$ is the interaction parameter (Rabi frequency) and $\Delta = \omega - \omega_0$ is the detuning.

The derivation of the master equation for the system " 4-level atom coupled to the quantized reservoir field of all modes at zero temperature" is accomplished by

the standard procedure using Born-Markoff approximation. We solve for the total density operator of system-reservoir to second order and use the Markoff's approximation. After tracing over the reservoir, we obtain the equation of motion for the system density operator which is the master equation. The first two parts of the Hamiltonian do not contain reservoir operators, therefore their contribution is trivial. The contribution of the last term gives rise to damping [12]. The master equation is then

$$\begin{aligned}\frac{d}{dt}\rho &= i\frac{\Delta}{2}\Big[\rho,\ |4\rangle\langle 4| + |3\rangle\langle 3| - |2\rangle\langle 2| - |1\rangle\langle 1|\Big] \\ &+ iv\Big[\rho,\ |1\rangle\langle 4| + |2\rangle\langle 3| + |4\rangle\langle 1| + |3\rangle\langle 2|\Big] \\ &+ \mathcal{L}\rho. \end{aligned} \tag{2.2.8}$$

Here $\mathcal{L}\rho$ is the Liouvillian operator given by

$$\begin{aligned}\mathcal{L}\rho &= -3\gamma\Big[(|4\rangle\langle 4| + |3\rangle\langle 3|)\rho + \rho(|4\rangle\langle 4| + |3\rangle\langle 3|)\Big] \\ &+ 2\gamma\Big[2|1\rangle\langle 4|\rho|4\rangle\langle 1| + 2|2\rangle\langle 3|\rho|3\rangle\langle 2| \\ &+ (|2\rangle\langle 4| - |1\rangle\langle 3)\rho(|4\rangle\langle 2| - |3\rangle\langle 1)|\Big]. \end{aligned} \tag{2.2.9}$$

Here $2\gamma = \frac{4}{3}\mu^2\omega_0^3 c^{-3}\hbar^{-1}$ is one third of the spontaneous decay rate of the upper to lower level. Taking matrix elements of the master equation we get equations for the matrix elements of the system density operator. The x-polarized scattered field, which is proportional to μ_x, and the y-polarized scattered field, which is proportional to μ_y, are σ-polarized with ($|\Delta m_j| = 1$), while the z-polarized scattered field is π-polarized ($|\Delta m_j| = 0$). From general consideration, it is clear that only the x-

polarized scattered field is coherent to the incident light, while the y- or z-component scattered fields are not coherent. As was shown by Polder and Schurmann, the two incoherent parts behave in the same way (i.e, have the same spectra), therefore it is sufficient to consider only one incoherent component. We restrict our consideration to the coherent E_x-component and the incoherent E_y-component, and obtain

$$\begin{aligned}
\frac{d}{dt}\hat{\rho}_{14} &= (i\Delta - 3\gamma)\hat{\rho}_{14} + iv(\rho_{44} - \rho_{11}), \\
\frac{d}{dt}\hat{\rho}_{23} &= (i\Delta - 3\gamma)\hat{\rho}_{23} + iv(\rho_{33} - \rho_{22}), \\
\frac{d}{dt}\rho_{11} &= 4\gamma\rho_{44} + 2\gamma\rho_{33} + iv(\hat{\rho}_{41} - \hat{\rho}_{14}), \\
\frac{d}{dt}\rho_{22} &= 4\gamma\rho_{33} + 2\gamma\rho_{44} + iv(\hat{\rho}_{32} - \hat{\rho}_{23}), \\
\frac{d}{dt}\rho_{33} &= -6\gamma\rho_{33} + iv(\hat{\rho}_{23} - \hat{\rho}_{32}), \\
\frac{d}{dt}\rho_{44} &= -6\gamma\rho_{44} + iv(\hat{\rho}_{14} - \hat{\rho}_{41}).
\end{aligned} \tag{2.2.10}$$

Here $\rho_{kl} = \rho_{lk}^*$, $\hat{\rho}_{14} = \rho_{14}e^{-i\omega t}$ and $\hat{\rho}_{23} = \rho_{23}e^{-i\omega t}$. The equations for $\rho_{24}, \rho_{13}, \rho_{12}$ and ρ_{34} necessary for the calculation of $\langle E_z(t)\rangle$ are not needed because $\langle E_y(t)\rangle = \langle E_z(t)\rangle$ as shown in [11]. As a consequence of Eqs. (2.2.10), the matrix elements $\rho_{kl}(t)$ can be expressed as a linear combination of matrix elements at an earlier time t'.

2.3 Expectation Values of the Radiated Field in the Weak Field Limit

We start with the following expression for $\rho(t)$,

$$\begin{aligned}\rho(t) &= \mathrm{Tr}_R\{U((t,t')\rho(t')_{SR}U^\dagger(t,t')\} \\ &= \mathrm{Tr}_R\sum_{mn}\{U((t,t')|m\rangle\langle m|\rho(t')_{SR}|n\rangle\langle n|U^\dagger(t,t')\} \\ &= \mathrm{Tr}_R\sum_{mn}\{U((t,t')|m\rangle\langle n|U^\dagger(t,t')\}\langle m|\rho(t')_{SR}|n\rangle, \qquad (2.3.1)\end{aligned}$$

where $U(t,t')$ is the time evolution operator for the system-reservoir and $\rho(t)_{SR}$ is the system-reservoir density operator. Applying the Markoff approximation in the third line by replacing $\rho_{SR}(t')$ with $\rho_R(0)\otimes\rho(t')$ we obtain

$$\rho(t) = \mathrm{Tr}_R\sum_{mn}\{U((t,t')|m\rangle\langle n|U^\dagger(t,t')\rho_R(0)\}\langle m|\rho(t')|n\rangle. \qquad (2.3.2)$$

Taking matrix elements we obtain the relationships at two different times for the elements of the density matrix

$$\rho_{kl}(t) = \sum_{mn} G_{kl,mn}(t,t')\rho_{mn}(t') \quad (t>t'), \qquad (2.3.3)$$

with

$$\begin{aligned}G_{kl,mn}(t,t') &= \mathrm{Tr}_R\{\langle k|U(t,t')|m\rangle\langle n|U^\dagger(t,t')|l\rangle\rho_R(0)\}, \\ G_{kl,mn}(t',t') &= \delta_{km}\delta_{ln}. \qquad (2.3.4)\end{aligned}$$

$G_{kl,mn}(t',t')$ is a propagator (Green's function) of the equation of motion and satisfies

$$\frac{d}{dt}G_{kl,mn}(t,t') - A_{ij}G_{ij,mn}(t,t') = \delta(t-t')\delta_{km}\delta_{ln}, \qquad (2.3.5)$$

where A_{ij} is the matrix of the equation of motion and the Green's function $G_{kl,mn}(t,t)$ gives a solution of Eqs. (2.2.10) with inhomogeneity $\delta(t-t')\delta_{km}\delta_{ln}$ which arises from $G_{kl,mn}(t',t') = \delta_{km}\delta_{ln}$. This allows us to solve the equations of motion for the Green's function. We can find the expectation values $\langle E_x(t)E_x(t+\tau)\rangle$ and $\langle E_y(t)E_y(t+\tau)\rangle$ for the field correlations. Their Fourier transform gives the spectrum of the different polarization components of the resonance fluorescence field. Here we are interested in the field radiated in different polarization directions. We specify our initial conditions of the atom as $\rho_{kl}(0) = \delta_{k1}\delta_{l1}$ and restrict the treatment to the Green's function $G_{kl,11}(t,0)$. In the Fourier space we find the following equations

$$i\nu\tilde{G}_{kl,11}(\nu) = \sum_{ij} A_{ij}\tilde{G}_{ij,11}(\nu) + \delta_{k1}.\delta_{l1} \tag{2.3.6}$$

Because we are interested in interference properties of two 4-level atoms we restrict our treatment to the weak field limit of the driving field. The reason is that it is necessary to have a coherent part in the spectrum to get interference. The coherent part is, however, vanishing if the atom becomes strongly saturated. We then get in

the weak field limit $v^2 \ll \Delta^2 + 9\gamma^2$, the following

$$\begin{aligned}
\rho_{14}(t) + \rho_{23}(t) &= e^{i\omega t}\frac{v(\Delta - 3i\gamma)}{9\gamma^2 + \Delta^2 + 2v^2}[1 - e^{-(3\gamma - i\Delta)t}], \\
\rho_{14}(t) - \rho_{23}(t) &= e^{i\omega t}\frac{v(\Delta - 3i\gamma)}{9\gamma^2 + \Delta^2 + 2v^2} \\
&\quad \times [e^{-4v^2\gamma t/9\gamma^2 + \Delta^2} - e^{-(3\gamma - i\Delta)t}], \\
\rho_{33}^{ss} &= \frac{v^2}{2(9\gamma^2 + \Delta^2 + 2v^2)} = \rho_{44}^{ss}, \\
\rho_{11}^{ss} &= \frac{\Delta^2 + 9\gamma^2 + v^2}{2(9\gamma^2 + \Delta^2 + 2v^2)} = \rho_{22}^{ss}. \qquad (2.3.7)
\end{aligned}$$

Here ρ_{11}^{ss}, ρ_{22}^{ss}, ρ_{33}^{ss} and ρ_{44}^{ss} are the steady state populations. The equations for $\rho_{24}(t)$ and $\rho_{13}(t)$ have the same time dependence as those for $\rho_{23}(t)$ and $\rho_{14}(t)$. We notice from Eqs. (2.3.7) that steady state is reached for times larger than $\left[\frac{4v^2\gamma}{9\gamma^2+\Delta^2}\right]^{-1}$. We note, however, that the probability to observe one photon in the incoherent part is also connected to this expression. The expression $\frac{4v^2\gamma}{9\gamma^2+\Delta^2}$ is the probability per unit time that a Raman scattering occurs, and after a few Raman transitions, or observation of a few incoherent photons, the atom reaches a steady state.

We now give expressions for the expectation values of the electric fields. They will be important for the interference effects in the scattered fields from two atoms, starting from the ground states $|1\rangle$ at $t = 0$. The expression for the radiated field is obtained by solving the Heisenberg equations for the field operators. In the radiation zone or far field region the positive frequency part of the field is given by the following

expression [13]

$$\mathbf{E}^{(+)}(\mathbf{r},t) = \mathbf{E}_f^{(+)}(\mathbf{r},t) - \Theta(t - r/c)\frac{\omega_0^2}{4\pi r^3 \epsilon_0 c^2}\Big[\mathbf{r}\times(\mathbf{r}\times\mu^{(-)}(t - |\mathbf{r}|/c)\Big]. \quad (2.3.8)$$

Here $\mu^{(-)}$ is the dipole operator, related to the atomic lowering operator $\sigma^{(-)}$, $\mathbf{r}$ is the vector from the atom to the observation point and $\Theta(t-r/c)$ is the step function which preserves causality. $\mathbf{E}_f^{(+)}(\mathbf{r},t)$ is the freely evolving part which does not contribute to normally (Fig. 4) ordered expectation values.

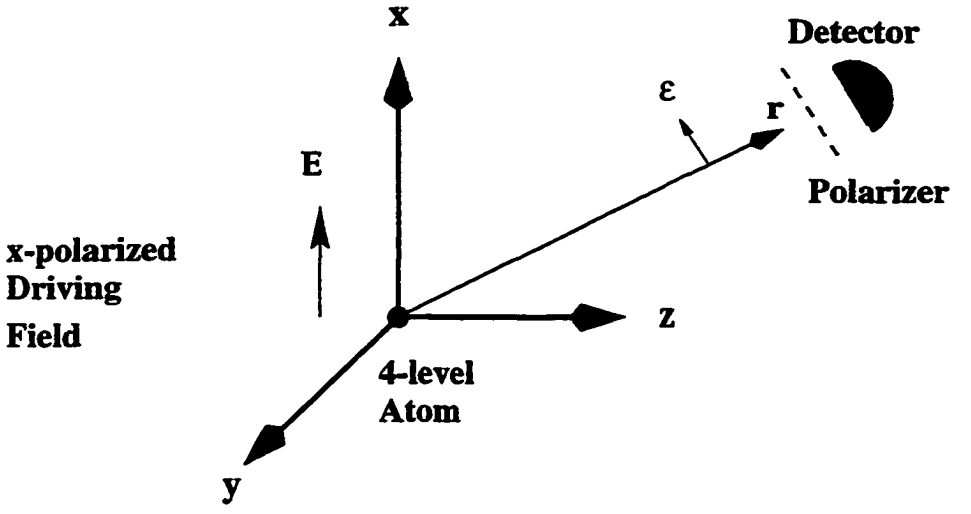

Figure 4: Geometry of the scattering process. The scattered field has a polarization direction along $\hat{\epsilon}$. The three orthogonal components of the field ($\hat{\mathbf{x}}$, $\hat{\mathbf{y}}$ and $\hat{\mathbf{z}}$) have the following properties. The $x-(\pi-)$polarized component contain the coherent part while the y- and $z-(\sigma-)$polarized components are incoherent. Polarization sensitive measurement is performed at the detector with the a polarizer in front of the detector.

We define the following

$$\Psi(\mathbf{r}) = \frac{-\mu\omega_0^2}{4\pi r^3 \epsilon_0 c^2}\Big[(\hat{\epsilon}\times\mathbf{r})\times\mathbf{r}\Big], \tag{2.3.9}$$

where $\hat{\epsilon}$ is a unit vector ($\hat{\mathbf{x}}$, $\hat{\mathbf{y}}$, or $\hat{\mathbf{z}}$, depending on the polarization direction under consideration). We note that the expression is reminiscent of the classical field from a radiating dipole. With this we get, for the expectation values of the radiated field in different polarization directions, the following

$$\begin{aligned}
\langle E_x^{(-)}(t,\mathbf{r})\rangle &= \Theta(t-|\mathbf{r}|/c)\Psi_x(\mathbf{r})\langle\sigma_x^{(+)}(t-|\mathbf{r}|/c)\rangle \\
&= \Theta(t-|\mathbf{r}|/c)\Psi_x(\mathbf{r})(\rho_{14}(t-|\mathbf{r}|/c)+\rho_{23}(t-|\mathbf{r}|/c)) \\
&= \Theta(t-|\mathbf{r}|/c)\Psi_x(\mathbf{r})\frac{v(\Delta-3i\gamma)}{9\gamma^2+\Delta^2+2v^2}e^{(i\omega t-|\mathbf{r}|/c)} \\
&\qquad\qquad \times\left[1-e^{-(3\gamma-i\Delta)(t-|\mathbf{r}|/c)}\right] \\
&\to \Theta(t-|\mathbf{r}|/c)\Psi_x(\mathbf{r})\frac{v(\Delta+3i\gamma)}{9\gamma^2+\Delta^2+2v^2}e^{i\omega(t-|\mathbf{r}|/c)}, \quad \text{as} \quad t\to\infty,
\end{aligned} \tag{2.3.10}$$

and

$$\begin{aligned}
\langle E_y^{(-)}(t,\mathbf{r})\rangle &= i\Theta(t-|\mathbf{r}|/c)\Psi_y(\mathbf{r})\langle\sigma_y^{(+)}(t-|\mathbf{r}|/c)\rangle \\
&= \Theta(t-|\mathbf{r}|/c)\Psi_y(\mathbf{r})(\rho_{14}(t-|\mathbf{r}|/c)-\rho_{23}(t-|\mathbf{r}|/c)) \\
&= \Theta(t-|\mathbf{r}|/c)\Psi_y(\mathbf{r})\frac{v(\Delta+3i\gamma)}{9\gamma^2+\Delta^2+2v^2}e^{(i\omega t-|\mathbf{r}|/c)} \\
&\qquad\qquad \times\left[e^{-4v^2\gamma(t-|\mathbf{r}|/c)/(9\gamma^2+\Delta^2)}-e^{-(3\gamma-i\Delta)(t-|\mathbf{r}/c)}\right] \\
&\to 0, \quad \text{as} \quad t\to\infty.
\end{aligned} \tag{2.3.11}$$

For the intensity we give only the steady state results

$$\begin{aligned}\langle E_x(t)E_x(t)\rangle &= |\Psi(\mathbf{r})|^2\langle\sigma_x^{(+)}\sigma_x^{(-)}\rangle_{ss} \\ &= |\Psi(\mathbf{r})|^2(\langle\rho_{44}\rangle_{ss}+\langle\rho_{33}\rangle_{ss}) \\ &= v^2|\Psi(\mathbf{r})|^2(9\gamma^2+\Delta^2+2v^2)^{-1} \\ &= \langle E_y(t)E_y(t)\rangle. \qquad (2.3.12)\end{aligned}$$

We recognize from Eqs. (2.3.11) that the expectation value of the incoherent part of the electric field vanishes in steady state. We can only have fluctuations from this part in steady state. However, it is important to note that steady state is reached only within few Rabi cycles or Raman transitions in the incoherent part of the spectrum and the incoherent part contributes to the spectrum.

Chapter III

3 Interference of Light Scattered from Two Independent 4-Level Atoms

3.1 Introduction

We now consider the problem of the scattering of light from two 4-level atoms. The theory of light scattering from two atoms has first been dealt with by Heitler [14] in the context of coherent scattering. A recent experiment by Eichmann *et al.* [1] reports on the first observation of interference effects in the light scattered from two trapped ions. In the experiment two $^{198}Hg^{+}$ ions were trapped along the axis of a linear trap [1, 15, 16]. The $^{198}Hg^{+}$ ion has an interesting internal level structure with lower state $6s^2s_{1/2}$ and an excited state $6p^2s_{1/2}$, both degenerate with respect to the magnetic quantum number $m_j = \pm 1/2$. Due to the internal structure the resonance fluorescence contains $\pi-$ and $\sigma-$ polarized light ($|\Delta m_j| = 0$ and $|\Delta m_j| = 1$), when the incident light is linearly polarized. Because of this level structure, the interference properties of the scattered light can be observed by polarization sensitive detection [1, 10]. The interference pattern comes only from the coherent part of the scattered field, while the incoherent part gives no contribution.

There seems to be a certain ambiguity whether the experiment of Eichmann *et al.*[1] can be used to implement a which-path experiment, and by what mechanism complementarity is enforced. The explanation in Ref. [1] (see also [10]) indicates that the experiment offers the possibility to obtain which way information by exploring the internal structure of the atom. As we will see, this description is, however, only valid as long as the atom is not saturated. The assumption is that only one photon scattered at a time. This enables, in principle (by comparing the initial internal states with the final states of the atoms), to decide if interference is possible or not. However, one must be careful with such a description. Because of the continuous monochromatic excitation laser, the assumption of independently scattered photons, i. e. one at a time, is not valid. For a monochromatic excitation we have a coherent oscillation between the ground states and the excited states [11, 12, 17]. Due to the interaction with the reservoir, after a few Rabi cycles, the atom reaches a steady state. In this chapter we want to investigate what happens to the interference picture when the atoms have evolved in a steady state. When is it necessary to talk about saturated atoms or how long is the description of scattering of independent photons valid [18, 19, 20]? Is it possible in the long time regime, in particular, to get "which way" information about the photon? The clarification of these problems is important for a possible realization of the quantum eraser [6, 21, 22, 23, 24, 25, 26, 27, 28, 29, 30], which stores erasable information about which path the particle took. It is also important to clarify whether the destruction of interference is due to the mere

existence of "which way" information, or due to random momentum transfers in the scattering process [7, 8, 22, 27, 31, 32].

3.2 Steady State Interference for $\pi-$ and $\sigma-$Scatterings

Here we consider the question of the interference of light scattered from two independent 4-level atoms. We will consider the experimental situation of Ref. [1] and assume the atoms are at rest at positions $\mathbf{r}_A$ and $\mathbf{r}_B$ (Fig. 5). We will also neglect thermal

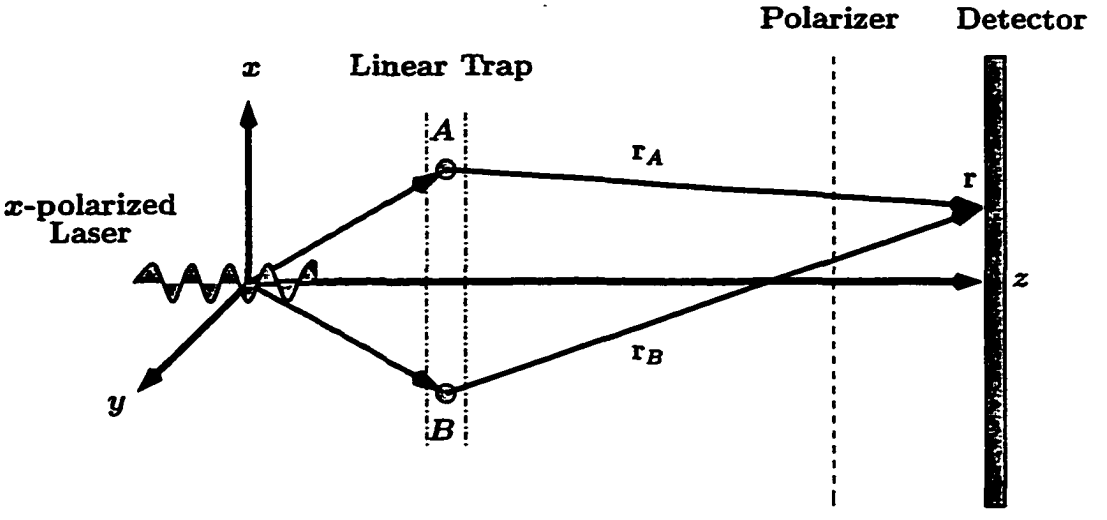

Figure 5: Schematic diagram depicting an experimental setup for the scattering of light from two trapped atoms (ions). The axis of the trap is along the x-axis, the two atoms are designated by A and B. An x-polarized laser drives the two atoms and polarization sensitive detection of the scattered fields takes place at the detector at the point $\mathbf{r}$. For a more complete description of the experiment see Eichmann *et al.* [1, 10].

fluctuations of the center of mass of the atoms. The thermal fluctuation will reduce the fringe visibility via the Debye-Waller factor, analogously to neutron scattering from a crystal, and for the experimental setup of Eichmann *et al.* in the Doppler limit of the two trapped atoms, it does not affect the basic "which way" argument [10]. The two atoms are driven by an x-polarized monochromatic weak laser, so we can use the results of the previous section. The interaction Hamiltonian is

$$H = -\boldsymbol{\mu}_A \cdot \mathbf{E}(\mathbf{r}_A, t) + \boldsymbol{\mu}_B \cdot \mathbf{E}(\mathbf{r}_B, t). \tag{3.2.1}$$

For a monochromatic transition we have a coherent oscillation between the ground and the excited states [11, 12]. This implies, if we can neglect direct interaction between the two atoms, then each atom is driven independently, therefore we can use the results of Chapter II. In particular, no entanglement will arise between the two atoms with such kind of monochromatic continuous driving and both atoms evolve independent of each other into a steady-state. We start with an initial density operator for the two independent atoms, given by

$$\rho(t) \;=\; \rho_A(t) \otimes \rho_B(t). \tag{3.2.2}$$

The field scattered from the two atoms has now two contributions to the resonance fluorescence and the intensity at the detector at position $\mathbf{r}$ is given by

$$\begin{aligned} \langle I(\mathbf{r},t)\rangle &= \langle [\mathbf{E}_A^{(-)}(\mathbf{r},t) + \mathbf{E}_B^{(-)}(\mathbf{r},t)] \cdot [\mathbf{E}_A^{(+)}(\mathbf{r},t) + \mathbf{E}_B^{(+)}(\mathbf{r},\mathrm{t})] \rangle \\ &= \langle I_A(\mathbf{r},t)\rangle + \langle I_B(\mathbf{r},t)\rangle \\ &+ \langle \mathbf{E}_A^{(-)}(\mathbf{r},t) \cdot \mathbf{E}_B^{(+)}(\mathbf{r},t)\rangle + \langle \mathbf{E}_A^{(+)}(\mathbf{r},t) \cdot \mathbf{E}_B^{(-)}(\mathbf{r},t)\rangle. \end{aligned} \tag{3.2.3}$$

The scattered fields from atoms A and B are given in terms of the lowering operators of the two atoms and for the positive frequency part we have

$$\mathbf{E}^{(+)}_{A,B}(\mathbf{r},t) = \Theta(t-|\mathbf{r}_{A,B}|/c)\Psi(\mathbf{r})\sigma^{(-)}_{A,B}\Big(t-\frac{|\mathbf{r}_{A,B}|}{c}\Big). \tag{3.2.4}$$

The last two terms of Eq.(3.2.3) are responsible for interference. We want to see the effect of detecting a specific polarization direction of the scattered field, specifically the x-polarized and the y-polarized fields.

$\pi-$Scattering

The x-polarized part of the scattered field is responsible for the coherent part of the spectrum [11], and therefore interference is expected in this polarization. From Eq. (3.2.3) we can express these terms as

$$\begin{aligned}
&\langle E^{(-)}_{x,A}(\mathbf{r},t)\cdot E^{(+)}_{x,B}(\mathbf{r},t)\rangle + c.c.,\\
=\ &\Theta(t-|\mathbf{r}_A|/c)\Theta(t-|\mathbf{r}_B|/c)|\Psi(\mathbf{r})|^2\\
\times\ &\langle\sigma^{(+)}_{x,A}(t')\sigma^{(-)}_{x,B}(t'+\tau)+\sigma^{(-)}_{x,A}(t')\sigma^{(+)}_{x,B}(t'+\tau)\rangle,\\
=\ &\Theta(t-|\mathbf{r}_A|/c)\Theta(t-|\mathbf{r}_B|/c)|\Psi(\mathbf{r})|^2\\
&\times\frac{2v^2(9\gamma^2+\Delta^2)}{(9\gamma^2+\Delta^2+2v^2)^2}\cos[\mathbf{k}\cdot(\mathbf{r}_A-\mathbf{r}_B)].
\end{aligned} \tag{3.2.5}$$

Here, $t' = t - |\mathbf{r}_A|/c$ is the retarded time and we have introduced the delay time $\omega\tau = \omega(|\mathbf{r}_A| - |\mathbf{r}_B|)/c \approx \mathbf{k}\cdot(\mathbf{r}_A - \mathbf{r}_B)$. As expected, the coherent part of the spectrum gives rise to interference, and this is in accord with Young's double slit experiment. Note that the coherent π-polarized contribution vanishes in the strong field limit,

implying that the interference pattern disappears. The vanishing of the coherent part is not due to the appearance of "which way"information in the π-scattering, rather, it is simply due to the fact in the high field limit there is no more coherent scattering.

$\sigma-$Scattering

Next we turn to the incoherent part of the scattered field and consider, e.g, the y-polarization component. The z-polarized field has the same properties, so it is sufficient to consider only one of the two incoherent components representative for both. Treating the y-component in the same fashion as the x-component of the RF field we get

$$\begin{aligned} & \langle E^{(-)}_{y,A}(\mathbf{r},t)\cdot E^{(+)}_{y,B}(\mathbf{r},t)\rangle + c.c., \\ = \;& \Theta(t-|\mathbf{r}_A|/c)\Theta(t-|\mathbf{r}_B|/c)|\Psi(\mathbf{r})|^2 \\ & \times\frac{2v^2(9\gamma^2+\Delta^2)}{(9\gamma^2+\Delta^2+2v^2)^2}\exp\left[\frac{-8v^2\gamma t'}{9\gamma^2+\Delta^2}\right]\cos[\mathbf{k}\cdot(\mathbf{r}_A-\mathbf{r}_B)] \\ \to \;& 0, \quad \text{as} \quad t\to\infty. \end{aligned} \tag{3.2.6}$$

We note that the observation of an interference pattern usually requires several scattered photons. On the other hand, the excitation time of an incoherent photon is related to $t_c = \frac{9\gamma^2+\Delta^2}{4v^2\gamma}$, so we must assume $t \gg t_c$ to have any incoherent excitation. The consequence is that Eq. (3.2.6) goes to zero and the incoherent part does not contribute to the interference. At this point it is worth comparing our results

to the interpretation of Eichmann *et al.* [1]. Both considerations lead to the same conclusion, viz., the existence of interference in the coherent part of the spectrum and no interference in the incoherent part. There is, however, an important difference between the two approaches. According to our results, the presence or lack of interference is a consequence of the steady state behavior of the two atoms. In the interaction of a monochromatic laser with an atom coupled to a reservoir steady state is reached in a few Rabi cycles. In the steady state regime, however, there is no "which way" information any longer, and thus one cannot invoke "which way" arguments to explain the presence or lack of interference [1, 10, 12]. Simply, there is a coherent component in the $\pi-$polarized part of the RF field for a weak driving field and it leads to interference between the fields scattered by the two atoms. The $\sigma-$polarized parts of the RF field are entirely incoherent and exhibit no interference. There is no entanglement between the two atoms in steady-state and consequently no "which way" information.

Chapter IV

4 Interference due to lack of "Which Way" Information.

4.1 Introduction

We now look for a possible modification of the experiment of Eichmann *et al.* [1] to implement a "which way" experiment. First, we cannot consider a continuous monochromatic driving field, the infinite long coherence time in such a field leads to coherent Rabi flopping of the atoms with spontaneous decay, leading to a steady state of the two atoms after some time. Therefore, we need laser pulses weak enough to excite only one atom per pulse and separated well enough to complete spontaneous emission before the next pulse arrives or, alternatively, we can use a continuous broad band incoherent excitation (BBE). The interaction of a 4-level atom with a BBE is discussed in detail in Ref [18]. We therefore give only the main results. The coherence time of the broad band field is given by $\tau_c = 1/\delta$ where δ is the bandwidth (not to be confused with the detuning in the previous sections) and the excitation time is $T_D = \frac{1}{\gamma_D} \approx \frac{\delta}{v^2}$ where v is the coupling parameter between the atoms and the BBE field in frequency units. We assume that $T_D \gg \gamma^{-1}$, therefore we can neglect stimulated emission by the broad band field. Furthermore, since $\tau_c \ll T_D$, (and also $\tau \ll \gamma^{-1}$) we can regard the broad band field as a reservoir which leads to absorption of one

photon at a time, followed by spontaneous decay. The time-sequence for the the interaction of the atoms with the broad band field and the vacuum is scheduled in Fig. 6. Approximately every time T_D one of the two atoms is excited according to the broad band field interaction and decays into the lower states due to the interaction with the vacuum. For such a system the interpretation in [1] is applicable, and we can talk about interference effects due to the indistinguishability of the possible paths. In other words, for such a system a "which way" argument is applicable which is required for the implementation of a quantum eraser [6, 21, 22, 23, 24, 25, 26, 27, 28, 29, 30]. The reason for the applicability of a "which way" argument is the entanglement between the two atoms due to the nature of the BBE, since we do not know which atom absorbed the photon. We note that a BBE has the advantage over laser pulses, in that it allows a continuous monitoring of the atoms. With a BBE the atoms do not saturate.

4.2 Interaction of Two 4-Level Atoms with a Broad Band Excitation Field

The interaction Hamiltonian with the broad band driving field $\mathbf{E}_D$ is

$$H_{int}(t) = -\left(\boldsymbol{\mu}^{(-)} \cdot \mathbf{E}_D^{(+)} + \boldsymbol{\mu}^{(+)} \cdot \mathbf{E}_D^{(-)}\right). \tag{4.2.1}$$

Here $\boldsymbol{\mu} = (\boldsymbol{\mu}_A + \boldsymbol{\mu}_B)$ and $\mathbf{E}_D$ is the broad band excitation field. In the second order of the interaction we get for the time-evolution of the reduced density operator $\rho(t)$

$$\frac{d}{dt}\rho(t) = -\frac{1}{\hbar^2}\int dt' \mathrm{Tr}_R\big[H_{int}(t), [H_{int}(t'), \rho_T(t')]\big]. \tag{4.2.2}$$

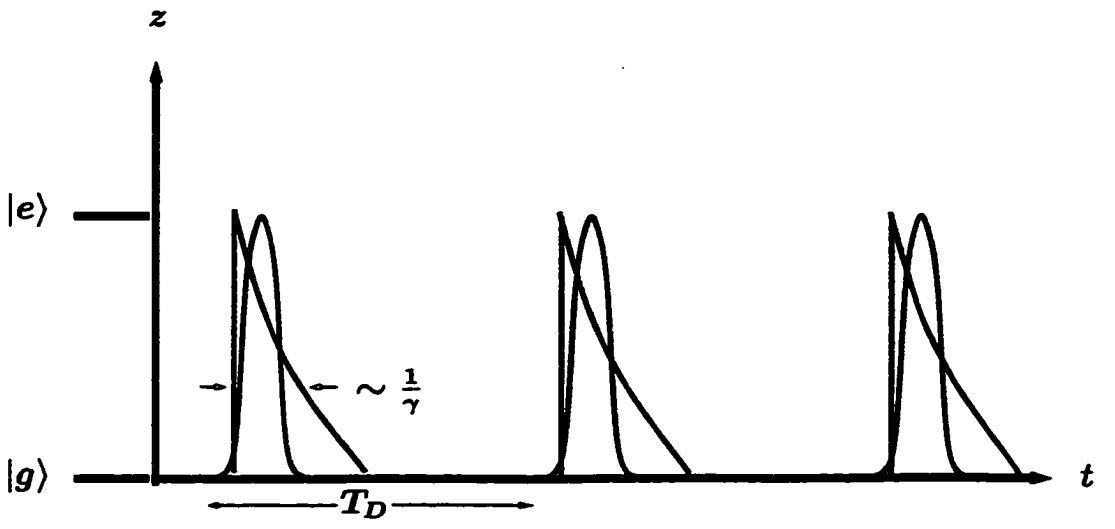

Figure 6: Time-schedule for the atomic transitions of one of the two atoms induced by the interaction with the continuous BBE excitation and the vacuum (thick lines). The interaction with the BBE causes a transition from the lower states $|g\rangle = |1\rangle, |2\rangle$ to the upper states $|e\rangle = |3\rangle, |4\rangle$ approximately every time $T_D \gg 1/\gamma$ which is followed by a spontaneous transition into the lower states $|g\rangle$ induced by the interaction with the vacuum (thin lines). Due to the condition $T_D \gg 1/\gamma$ we can neglect stimulated emissions into the BBE.

Here $\rho_T(t) = \rho(t) \otimes \rho_R(t)$ where $\rho(t)$ is the atomic density operator and $\rho_R(t)$is the density operator for the reservoir (BBE field). We now consider the two time correlation of the BBE field. The two time correlation for the incoherent BBE field can be evaluated, and for appropriate parameters (see Cohen-Tannoudji [18]) can be expressed as follows

$$\langle E_D^{(-)}(t) E_D^{(+)}(t') \rangle = \mathcal{E}_0^2 \delta(t - t'). \tag{4.2.3}$$

Here $\mathcal{E}_0$ is an electric field amplitude related to the BBE field. With this we can replace $\rho(t')$ by $\rho(t)$, which is the Markoff's approximation for the BBE field. We take the BBE field to be z-polarized and get finally for the master equation

$$\frac{d}{dt}\rho(t) = -\gamma_D \sum_{k,k'=A,B} [\ \sigma_{zk}^{(-)}\sigma_{zk'}^{(+)}\rho(t) + \rho(t)\sigma_{zk}^{(-)}\sigma_{zk'}^{(+)} - 2\sigma_{zk}^{(+)}\rho(t)\sigma_{zk'}^{(-)}]. \tag{4.2.4}$$

Here $\gamma_D = \frac{1}{T_D}$ and depends on the parameters of the BBE field. The interaction with the vacuum leads to the following master equation

$$\frac{d}{dt}\rho(t) = -\gamma \sum_{k=A,B}\sum_{j=x,y,z} [\ \sigma_{j;k}^{(+)}\sigma_{j;k}^{(-)}\rho(t) + \rho(t)\sigma_{j;k}^{(+)}\sigma_{j;k}^{(-)} - 2\sigma_{j;k}^{(-)}\rho(t)\sigma_{j;k}^{(+)}]. \tag{4.2.5}$$

The interaction with $\mathbf{E}_D$ leads to mixed terms which connect the two atoms, while for the vacuum we have no mixed terms. The mixed terms indicate that there arises a correlation between the two atoms, while for the vacuum each atom is independently coupled to the reservoir and no correlations arise between them. In other words the interaction with the BBE leads to the entanglement between the two atoms. This entanglement is the crucial point for the applicability of a "which way" argument. In the case of a continuous BBE, independent scattering events occur for which we can apply "which way" arguments and a quantum eraser can be implemented.

We consider a special initial condition for the density operator of the two atoms,

which is given by

$$\rho_{AB}(t_0) = |1\rangle_{AA}\langle 1| \otimes |1\rangle_{BB}\langle 1|. \tag{4.2.6}$$

After the absorption of one photon at time $t_1 \approx t_0 + T_D$ of the BBE field, the density operator of the two atoms A and B is entangled due to the non-local behavior of a single absorbed photon

$$\begin{aligned}\rho_{AB}(t_1) &= \frac{1}{2}\left[|1\rangle_{AA}\langle 1| \otimes |3\rangle_{BB}\langle 3| + |3\rangle_{AA}\langle 3| \otimes |1\rangle_{BB}\langle 1|\right. \\ &\quad \left. + |1\rangle_{AA}\langle 3| \otimes |3\rangle_{BB}\langle 1| + |3\rangle_{AA}\langle 1| \otimes |1\rangle_{BB}\langle 3|\right].\end{aligned}$$

The coupling to the vacuum leads to decay of the excited states. This means, immediately after the absorption of a photon at the time t_1, the density operator evolves according to the master equation, which describes the interaction of an excited atom with the vacuum. We give the details of the calculations for the interaction of the BBE field with the two atoms in Appendix A. Here, we give the relevant equations for the coupling with the vacuum. Since each atom is coupled independently we have

for either of the atoms A or B, the following

$$\begin{aligned}
\frac{d\hat{\rho}_{42}(t)}{dt} &= -3\gamma\hat{\rho}_{42}(t), \\
\frac{d\hat{\rho}_{31}(t)}{dt} &= -3\gamma\hat{\rho}_{31}(t), \\
\frac{d\rho_{11}(t)}{dt} &= 2\gamma\rho_{33}(t) + 4\gamma\rho_{44}(t), \\
\frac{d\rho_{22}(t)}{dt} &= 2\gamma\rho_{44}(t) + 4\gamma\rho_{33}(t), \\
\frac{d\rho_{33}(t)}{dt} &= -6\gamma\rho_{33}(t), \\
\frac{d\rho_{44}(t)}{dt} &= -6\gamma\rho_{44}(t). \qquad (4.2.7)
\end{aligned}$$

With these equations we get the following time evolution of the density matrix

$$\begin{aligned}
\rho_{42}(t) &= \rho_{42}(0)e^{-(i\omega+3\gamma)t}, \\
\rho_{31}(t) &= \rho_{31}(0)e^{-(i\omega+3\gamma)t}, \\
\rho_{11}(t) &= \frac{1}{3}\rho_{33}(0)(1-e^{-6\gamma t}) + \frac{2}{3}\rho_{44}(0)(1-e^{-6\gamma t}), \\
\rho_{22}(t) &= \frac{1}{3}\rho_{44}(0)(1-e^{-6\gamma t}) + \frac{2}{3}\rho_{33}(0)(1-e^{-6\gamma t}), \\
\rho_{44}(t) &= \rho_{44}(0)e^{-6\gamma t}, \\
\rho_{33}(t) &= \rho_{33}(0)e^{-6\gamma t}. \qquad (4.2.8)
\end{aligned}$$

4.3 Interference and Non-Entanglement for π-Scattering

The interference part of the intensity is given by the expression

$$\Theta(t'+\tau)\Theta(t')|\Psi(\mathbf{r})|^2\left(\langle\sigma_A^{(+)}(t')\sigma_B^{(-)}(t'+\tau)\rangle + c.c.\right).$$

Here $t' = t - t_1 - |\mathbf{r}_A|/c$ is again the retarded time and $\tau = (|\mathbf{r}_A| - |\mathbf{r}_B|)/c$ the delay time. We consider the case of π-polarized scattering starting with the "initial" condition (4.2.6). The details for general initial conditions are given in Appendix B. This is related to the z-polarized scattering or $\pi - (|\Delta m_j| = 0)$ transition. We get for the interfering part for π-scattering the following

$$\begin{aligned}
&\frac{1}{2}\Theta(t'+\tau)\Theta(t')|\Psi(\mathbf{r})|^2\Big(\langle\sigma^{(+)}_{A,z}(t')\sigma^{(-)}_{B,z}(t'+\tau)\rangle + c.c.\Big) \\
&= \frac{1}{2}\Theta(t'+\tau)\Theta(t')|\Psi(\mathbf{r})|^2 \\
&\quad \times \mathrm{Tr}_{A,B}\langle\rho^A_{13}(t')\rho^B_{31}(t'+\tau)|1\rangle_{AA}\langle 1|\otimes|1\rangle_{BB}\langle 1| + c.c.\rangle \\
&= \Theta(t'+\tau)\Theta(t')|\Psi(\mathbf{r})|^2\cos[\mathbf{k}\cdot(\mathbf{r}_A-\mathbf{r}_B)]e^{-6\gamma(t'+\frac{\tau}{2})} \\
&\quad \times \mathrm{Tr}_{A,B}|1\rangle_{AA}\langle 1|\otimes|1\rangle_{BB}\langle 1|. \qquad (4.3.1)
\end{aligned}$$

Thus, for π-scattering we get interference during the coherence time $\frac{1}{6\gamma}$. The reason is that it is indistinguishable what path the photon took. Note that the final total density matrix is disentangled between the atoms and the photon, and therefore interference takes place. This can be readily recognized from the expression for the complete first-order correlation function (3.2.3) which can be expressed as

$$\begin{aligned}
I(\mathbf{r},t',\tau) &= \frac{1}{2}\mathrm{Tr}_{A,B}(|1\rangle_{AA}\langle 1|\otimes|1\rangle_{BB}\langle 1|) \\
&\quad \times|\Psi(\mathbf{r})|^2\Big[\Theta(t'_A)e^{-6\gamma t'_A} + A\leftrightarrow B \\
&\quad 2\Theta(t'_A+\tau)\Theta(t'_A)e^{-6\gamma(t'_A+\frac{\tau}{2})}\cos[\mathbf{k}\cdot(\mathbf{r}_A-\mathbf{r}_B)]\Big], \qquad (4.3.2)
\end{aligned}$$

where we have introduced the retarded times $t'_{A,B} = t - t_1 - |\mathbf{r}_{A,B}|/c$. In Eq. (4.3.2) the atomic density operator is factored out, which expresses the disentanglement of the atoms-photon system. Indeed, there are two different possibilities which lead to the same final atomic density operator and it is impossible to know which of the two atoms scattered the photon. Consequently, interference occurs due to the superposition of two ways.

4.4 Non-Interference and Entanglement for σ-Scattering

We now consider the case of σ-polarized scattering and obtain, for the x-polarized scattered light,

$$\begin{aligned} & \frac{1}{2}\Theta(t'+\tau)\Theta(t')|\Psi(\mathbf{r})|^2 \left(\langle \sigma^{(+)}_{A,x}(t')\sigma^{(-)}_{B,x}(t'+\tau)\rangle + c.c. \right) \\ = \; & \frac{1}{2}\Theta(t'+\tau)\Theta(t')|\Psi(\mathbf{r})|^2 e^{-6\gamma(t'+\frac{\tau}{2})} \\ \times \; & \mathrm{Tr}_{A,B}(|1\rangle_{AA}\langle 2| \otimes |2\rangle_{BB}\langle 1|e^{-i\omega\tau} + |1\rangle_{BB}\langle 2| \otimes |2\rangle_{AA}\langle 1|e^{i\omega\tau}) \\ = \; & 0. \end{aligned} \tag{4.4.1}$$

We recognize that the σ-polarized scattered light cannot lead to interference. The reason is that the scattering process brings one of the two atoms to a final state which is orthogonal to the initial state. From another point of view, the scattering process of σ-polarized photon leads to two distinguishable paths of the photon giving no interference. This, again, can be recognized most easily when we consider the

first-order correlation, which is the following

$$
\begin{aligned}
I(\mathbf{r},t',\tau) &= \frac{1}{2}|\Psi(\mathbf{r})|^2 \\
&\times\Big[\Theta(t'_A)e^{-6\gamma t'_A}\mathrm{Tr}_{A,B}\left(|2\rangle_{AA}\langle 2|\otimes|1\rangle_{BB}\langle 1|+A\leftrightarrow B\right) \\
&\quad+\Theta(t'_A+\tau)\Theta(t'_A)e^{-6\gamma\left(t'_A+\frac{\tau}{2}\right)} \\
&\times\mathrm{Tr}_{A,B}(|1\rangle_{AA}\langle 2|\otimes|2\rangle_{BB}\langle 1|e^{-i\omega\tau}+|1\rangle_{BB}\langle 2|\otimes|2\rangle_{AA}\langle 1|e^{i\omega\tau})\Big].
\end{aligned}
\tag{4.4.2}
$$

Here, due to the entanglement between the atoms-photon system there are two distinguishable events leading to two different final atomic density operators, and, consequently no interference occurs. It is, however, not necessary to have an actual knowledge of the path. The mere existence of "which way" information, whether we choose to know it or not, is enough to destroy the interference.

Chapter V

5 Quantum Eraser

5.1 Introduction

After the discussions in Chapter IV we have now the necessary setup to implement a quantum eraser using the Eichmann *et al.* experiment. This chapter is divided into two sections. The first section deals with the implementation of a quantum eraser for general atomic initial condition of the two degenerate 4-level atoms. The second section deals with a quantum eraser for a special initial condition which is achieved by removing the degeneracy of the 4-level atoms with a magnetic field. The removal of the degeneracy allows us to consider the special initial condition that the atoms populate exclusively the lower atomic state $|1\rangle$ in thermal equilibrium. After these preliminaries we now show that a modification of the experiment in [1] allows one to implement a quantum eraser with a delayed choice set up, in the sense proposed originally [25]. The first requirement for the implementation of the quantum eraser is a non-unitary time evolution to erase the information through an irreversible process, and the second is a measurement of the second order (or intensity) correlation function. The first condition is required because a unitary time evolution is reversible and in any reversible process information is not "lost" and can be recovered by an inverse

transformation which is again unitary. The second condition is required because of the orthogonality of the photon states $|\gamma_A\rangle$ and $|\gamma_B\rangle$ of the photons scattered from atoms A and B. A detection of the photons $|\gamma_A\rangle$ and $|\gamma_B\rangle$ reduces the infinite number of possible ways they can take to one specific way, they have actually taken.

Irreversibility is brought in by a non-unitary transformation such as a decay process, which is detected, so there is a non-unitary state reduction. Because of the internal structure of the 4-level atoms, we do not need additional levels to erase the information, the 4-level structure is enough for the realization of a quantum eraser. We use the same experimental setup that was originally suggested by Scully and Drühl, with a slight variation, where a π-polarization sensitive detector is placed equidistantly between atoms A and B (Fig. 9). The detection scheme allows us to distinguish between a π-polarized erasing photon and a σ-polarized interference photon. The erasing photon produces a final density matrix which is disentangled between the two subsystems, atoms and scattered photons. The detection of the erasing photon ensures the specific final state of the density operator, i.e. the disentanglement of the two subsystems atoms and the scattered (interference) photon.

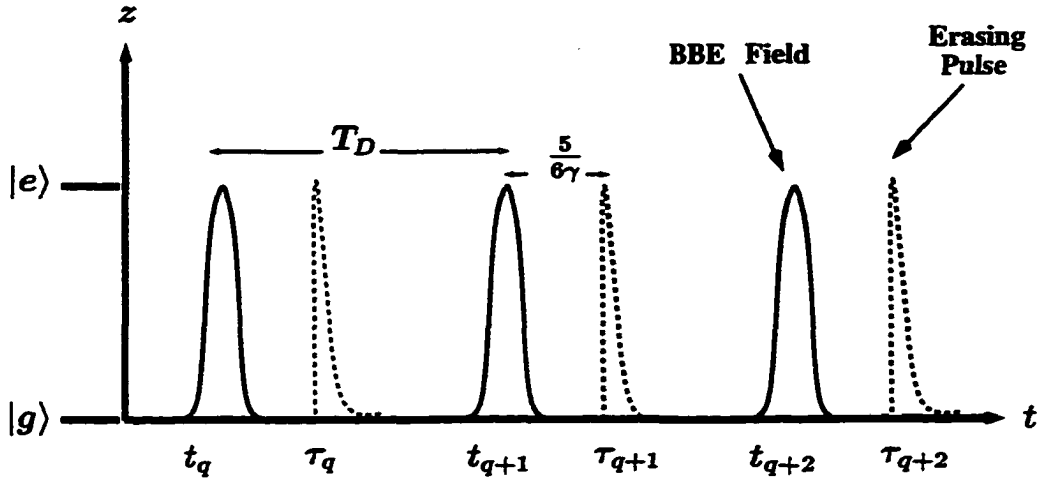

Figure 7: Time-schedule for the quantum eraser experiment. One of the two atoms is excited due to the interaction with the BBE approximately at times $t_q \approx t_0 + q \times T_D$ (solid lines) $q = 1, 2, 3, \ldots$. At times $\tau_q = t_q + 5/(6\gamma)$ we apply the erasing pulse (dashed lines). The arising photons are detected in a second order correlation measurement.

5.2 Quantum Eraser Scheme for Arbitrary Atomic Density Operator Initial Condition

We start to drive the atoms at t_0 with the broad band light which excites one of the two atoms at the time $t_1 = t_0 + T_D$. After this free evolution takes place and the excited atom decays into the specific ground state connected with the relevant polarization of the detected interference photon. At the time $t_2 \approx t_0 + T_D + 5(6\gamma)^{-1}$, which ensures that the excited atom has decayed, we apply a strong, erasing pulse which is assumed to be short enough to excite only one of the two atoms (see also Fig. 7). The requirement to excite only one of the two atoms at a time can also be achieved by applying a second broadband field pulse. After this excitation time there is no

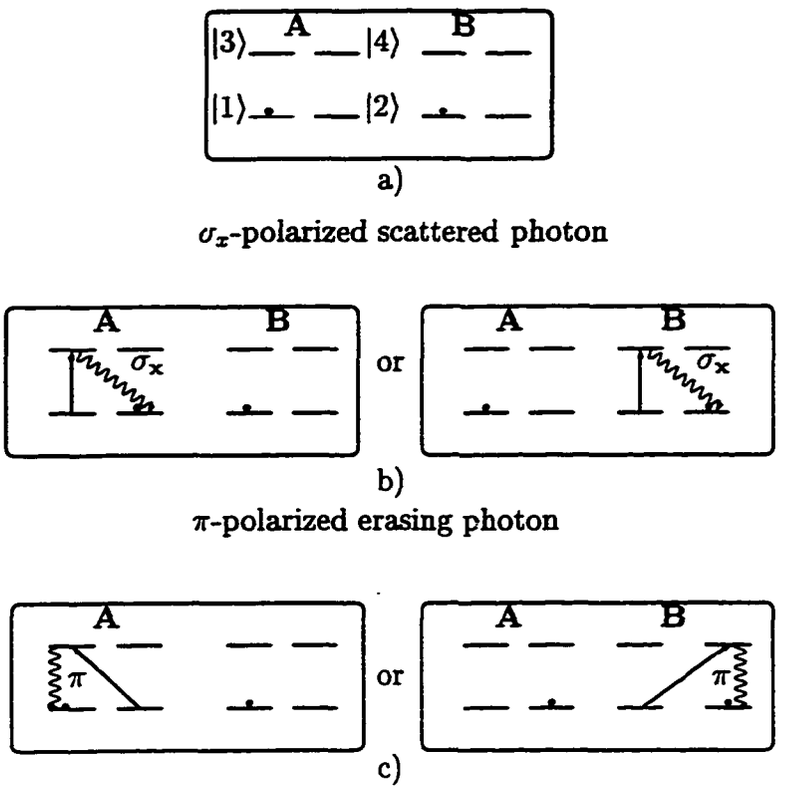

Figure 8: a) We start initially in the state $|1\rangle_A \otimes |1\rangle_B$ of the two atoms. b) A z-polarized BBE induces σ_x-polarized scattering from atom A or B leading to state $|2\rangle_A \otimes |1\rangle_B$ or $|1\rangle_A \otimes |2\rangle_B$ followed by c), a π-polarized scattering erasing photon bringing the final atomic states to $|1\rangle_A \otimes |1\rangle_B$ or $|2\rangle_A \otimes |2\rangle_B$.

interaction with the broadband pulse and the only interaction is the interaction with the reservoir field so that spontaneous emission takes place. The correlated detection of the erasing and scattered photons ensures that we have the required final state of the density operator which disentangles the atoms and photons system. Fig. 8 depicts the relevant atomic transitions in the implementation of the quantum eraser. Starting with the density operator $|1\rangle_{AA}\langle 1| \otimes |1\rangle_{BB}\langle 1|$, due to the interaction with

the BBE at time $t_1 \approx t_0 + T_D$, the density operator evolves to $|1\rangle_{AA}\langle 1| \otimes |2\rangle_{BB}\langle 2| + |1\rangle_{AA}\langle 2| \otimes |2\rangle_{BB}\langle 1| + A \leftrightarrow B$. After the application of the erasing pulse we have, at time $t_2 = t_1 + 5/6\gamma$, the final density operator $|1\rangle_{AA}\langle 1| \otimes |1\rangle_{BB}\langle 1| + 1 \leftrightarrow 2$.

We want to express the above qualitative description mathematically and point out the important ideas necessary to erase the information. We consider the calculations of the second order correlation function in detail in Appendix C.

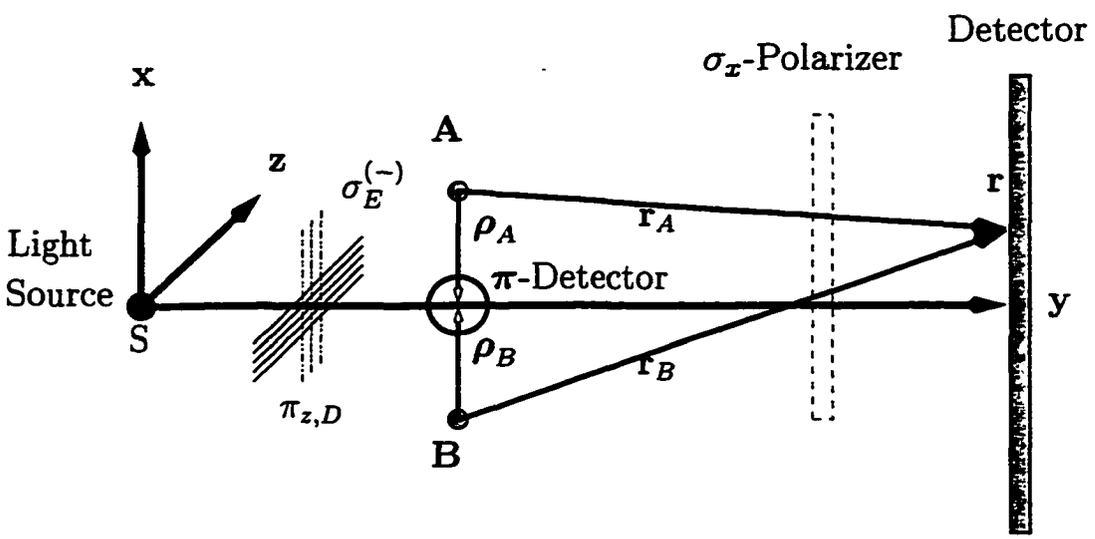

Figure 9: Arrangement for the quantum eraser where S is the light source which can have different polarization directions (using $\sigma_E^{(-)}$ and $\pi_{z,D}$ polarizers). σ_x is an x-polarizer for the scattering photons and π-Detector is a π-polarization dependent detector for the erasing photon.

The measurement of σ-polarized scattered photons at $(\mathbf{r}, t)$ and π-polarized erasing

photons at $(\boldsymbol{\rho}, \tau)$ is expressed by the second order correlation function defined as

$$\begin{aligned} G^{(2)}(\mathbf{r}, t; \boldsymbol{\rho}, \tau) &= \langle [\hat{E}_A^{(-)\sigma}(\mathbf{r}, t) + \hat{E}_B^{(-)\sigma}(\mathbf{r}, t)] \\ &\quad \cdot [\hat{E}_A^{(-)\pi}(\boldsymbol{\rho}, \tau) + \hat{E}_B^{(-)\pi}(\boldsymbol{\rho}, \tau)] \\ &\quad \cdot [\hat{E}_A^{(+)\pi}(\boldsymbol{\rho}, \tau) + \hat{E}_B^{(+)\pi}(\boldsymbol{\rho}, \tau)] \\ &\quad \cdot [\hat{E}_A^{(+)\sigma}(\mathbf{r}, t) + \hat{E}_B^{(+)\sigma}(\mathbf{r}, t)] \rangle, \end{aligned} \tag{5.2.1}$$

where π denotes the π-polarized photons which are used to erase the information, σ denotes σ-polarized scattered photons which are observed at the detector and $\boldsymbol{\rho}$ is the distance of the π detector from either atom. The part of the second order correlation function $G^{(2)}(\mathbf{r}, t; \rho, \tau)$ that produces interference is given by

$$\begin{aligned} G_{int}^{(2)}(\mathbf{r}, t; \boldsymbol{\rho}, \tau) &= \langle E_A^{(-)\sigma}(\mathbf{r}, t) [E_A^{(-)\pi}(\boldsymbol{\rho}, \tau) E_B^{(+)\pi}(\boldsymbol{\rho}, \tau) \\ &\quad + A \leftrightarrow B] E_B^{(+)\sigma}(\mathbf{r}, t) \\ &\quad + E_B^{(-)\sigma}(\mathbf{r}, t) [E_A^{(-)\pi}(\boldsymbol{\rho}, \tau) E_B^{(+)\pi}(\boldsymbol{\rho}, \tau) \\ &\quad + A \leftrightarrow B] E_A^{(+)\sigma}(\mathbf{r}, t) \rangle. \end{aligned} \tag{5.2.2}$$

This term describes the interference because both atoms A and B contribute to the π- and σ-polarized light, respectively. As it is shown in Appendix C, we can express the field operators in terms of Heisenberg dipole moment operators. The calculation of the second-order correlation function on the basis of Heisenberg dipole moment operators is performed in detail in Appendix C and we give, here, only the final result and point out the erasing scheme. We get, for the second-order correlation

function

$$
\begin{aligned}
G^{(2)}_{int}(\mathbf{r},t;\boldsymbol{\rho},\tau_2) \quad &= \quad \frac{1}{4}\Theta(t-t_1-|\mathbf{r}_A|/c)\Theta(t-t_1-|\mathbf{r}_B|/c)\Theta(\tau_2-|\boldsymbol{\rho}|/c) \\
&\times \quad |\Psi(\mathbf{r})|^2|\Psi(\boldsymbol{\rho})|^2 e^{-6\gamma[t-t_1-\frac{1}{2}(|\mathbf{r}_A+\mathbf{r}_B|)/c]}e^{-6\gamma(\tau_2-|\boldsymbol{\rho}|/c)} \\
&\times \quad Tr_{A,B}\Big\{|1\rangle_{AA}\langle 1|\otimes|1\rangle_{BB}\langle 1| + |2\rangle_{AA}\langle 2|\otimes|2\rangle_{BB}\langle 2| \\
&\qquad +A\leftrightarrow B\Big\}\times\cos[\omega(|\mathbf{r}_A|-|\mathbf{r}_B|)/c] \\
&= \quad \Theta(t-t_1-|\mathbf{r}_A|/c)\Theta(t-t_1-|\mathbf{r}_B|/c)\Theta(\tau_2-|\boldsymbol{\rho}|/c) \\
&\qquad \times|\Psi(\mathbf{r})|^2|\Psi(\boldsymbol{\rho})|^2 e^{-6\gamma(\tau_2-|\boldsymbol{\rho}|/c)}e^{-6\gamma[t-t_1-\frac{1}{2}(|\mathbf{r}_A|+|\mathbf{r}_B|)/c]} \\
&\qquad \times\cos[\mathbf{k}\cdot(\mathbf{r}_A-\mathbf{r}_B)]. \qquad (5.2.3)
\end{aligned}
$$

Here we have introduced the time delay $\tau_2 = t - t_2$ between the detection of the erasing photon and application of the erasing pulse. We have neglected in the above expression for τ_2 the excitation time $T_{D_2} \approx 10^{-10}$s of the atoms due to the erasing pulse which is much smaller than the relevant time-scale $1/6\gamma$. It is important to recognize in the above Eq. (5.2.3) that the atomic density operator which occurs in the second order correlation before tracing over the atomic subsystem is given as

$$\rho_{A,B} = \frac{1}{4}(|1\rangle_{AA}\langle 1|\otimes|1\rangle_{BB}\langle 1| + |2\rangle_{AA}\langle 2|\otimes|2\rangle_{BB}\langle 2| + A\leftrightarrow B). \qquad (5.2.4)$$

We see that the final atomic density operator contains only populations of the two atoms leading to interference. We recognize that there is our erasing of the information if we detect the π-polarized erasing photons before the scattered or interfering photons. The detection before is necessary because only this detection ensures our

atomic system state to be in the final state.

It is important to recognize that the quantum eraser disentangles the two subsystems atoms and scattered photons. This disentanglement makes it impossible to know which of the two atoms scattered the photon and consequently interference occurs. The disentanglement between photons and atoms is most obvious in the total second order correlation function which is given as

$$
\begin{aligned}
& G^{(2)}(\mathbf{r},t;\boldsymbol{\rho},\tau_2) = \frac{1}{4}\mathrm{Tr}_{A,B}\langle|1\rangle_{AA}\langle 1|\otimes|1\rangle_{BB}\langle 1| + 1 \leftrightarrow 2\rangle \\
\times\ & |\Psi(\mathbf{r})|^2|\Psi(\boldsymbol{\rho})|^2\Big\{\Theta(t-t_1-|\mathbf{r}_A|/c)\Theta(\tau_2-|\boldsymbol{\rho}|/c) \\
\times\ & e^{-6\gamma(t-t_1-|\mathbf{r}_A|/c)}e^{-6\gamma(\tau_2-|\boldsymbol{\rho}|/c)} + A \leftrightarrow B \\
& +2\Theta(t-t_1-|\mathbf{r}_A|/c)\Theta(t-t_1-|\mathbf{r}_B|/c)\Theta(\tau_2-|\boldsymbol{\rho}|/c) \\
& \times e^{-6\gamma\left[t-t_1-\frac{1}{2}(|\mathbf{r}_A|+|\mathbf{r}_B|)/c\right]}e^{-6\gamma(\tau_2-|\boldsymbol{\rho}|/c)} \\
& \times\cos[\mathbf{k}\cdot(\mathbf{r}_A-\mathbf{r}_B)]\Big\}. \qquad (5.2.5)
\end{aligned}
$$

Here, we can recognize the disentanglement between the photons and atoms. There is no possibility of knowing which atom has scattered. The superposition of two indistinguishable paths leading to the same final atomic density matrix is the reason for the occurrence of interference. The quantum eraser can be understood as a scheme which disentangles a previous entanglement between two subsystems. As a result of this disentanglement interference is brought back.

5.3 Quantum Eraser Scheme for Non-Degenerate 4-Level Atoms

In this section we consider a special quantum eraser scheme valid in the case when the 4-level atoms are non-degenerate. The removal of the degeneracy can be achieved with the application of a magnetic field in z-direction which shifts the atomic levels by an amount of $\pm\Delta/2 = \pm 1/(2\hbar)\mu_0 B_0$, where μ_0 is the magnetic moment of the electron and B_0 is the strength of the magnetic field (Fig. 10). In thermal equilibrium it is sufficient to consider the following initial atomic density operator

$$\rho_{A,B}(t_0) = |1\rangle_{AA}\langle 1| \otimes |1\rangle_{BB}\langle 1|, \tag{5.3.1}$$

which is valid for strong enough detuning Δ since $\exp(-\hbar\Delta/k_B T) \approx 0$, where k_B is the Boltzmann constant and T is the temperature, The non-degenerate 4-level atoms allow us to selectively drive certain transitions. In addition, we can use frequency selective detectors for the erasing photons and interference photons which results in a high efficiency measurement of the second-order correlation function in the quantum eraser scheme.

Let us consider the following quantum eraser scheme. We drive the atoms with a BBE field starting at t_0 and apply it continuously during the whole measurement of the second-order correlation function. Then at the time $t_1 \approx t_0 + T_D$ we can expect one of the two atoms to be excited. After a time $t_2 = t_0 + T_D + 5/(6\gamma)$, which ensures that the atoms have decayed to the ground states, we apply a strong and short $\frac{\pi}{2}$-

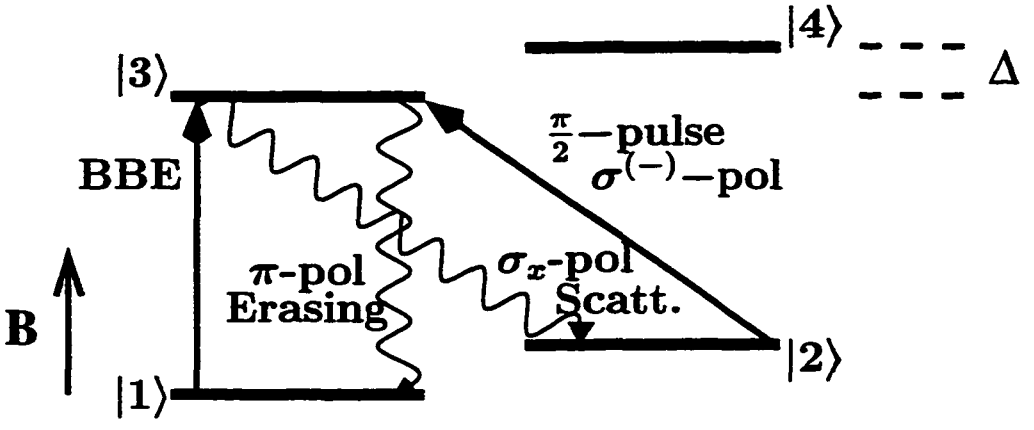

Figure 10: Quantum eraser scheme for a non degenerate initial condition. The degeneracy is removed by the application of a magnetic field B in the z-direction inducing a shift of Δ (Zeeman split). The BBE field induces a σ_x-polarized scattered field. The erasing is accomplished with the application of $\frac{\pi}{2}$-pulse inducing a π-polarized erasing pulse.

pulse which is $\sigma^{(-)}$-circular polarized and selectively drive the transition $|2\rangle \leftrightarrow |3\rangle$. After this excitation again decay into the vacuum occurs and we detect the emerging erasing photon as a π-polarized photon. The two photons are measured in the second-order correlation measurement, i.e. we measure the correlated photon emission of the two emerging photons. Due to our assumption, $T_D \gg 1/(6\gamma)$, it does not matter that the BBE is continuously applied because stimulated emission by the BBE can be neglected against spontaneous emission into the vacuum. The above time schedule is applied until we have enough data to get the second-order correlation function, i.e., the erasing pulse is applied at times $t_0+q\times T_D+5/(6\gamma)$, where $q = 1, 2, 3, \ldots$ (see Fig. 5). As we measure the interference as σ_x-polarized photons and the erasing photons

as π-polarized photons, we can use frequency selective detectors. The frequency of the π-polarized photons is equal to ω_0, while the frequency of the σ_x-polarized photons [only the $|2\rangle\langle 3| + |3\rangle\langle 2|$ part of the σ_x-dipole moment operator is relevant for the special initial condition (5.3.1)] is equal to $\omega_0 - \Delta$. This frequency difference allows for an efficient quantum eraser scheme because we can collect all the erasing photons by using a frequency selective elliptical reflector at the π-detector [6].

The calculations for the second-order correlation function are similar to the previous subsection and we give here only a qualitative description. We consider therefore only the atomic density operator and give the final result for the second-order correlation function. After the excitation with the BBE our density operator reads at the time $t_1 \approx t_0 + T_D$ starting from the initial condition (5.3.1) as

$$\begin{aligned} \rho_{A,B}(t_1) &= \frac{1}{2}\left(|1\rangle_{AA}\langle 1| \otimes |3\rangle_{BB}\langle 3| + |3\rangle_{AA}\langle 1| \otimes |1\rangle_{BB}\langle 3|\right. \\ &\quad \left. + A \leftrightarrow B\right). \end{aligned} \tag{5.3.2}$$

Then a transition from level $|3\rangle \rightarrow |2\rangle$ takes place. The probability of this transition event is 2/3 of all possible scattering events. After a sufficiently long free evolution time, which we take to be five times the decay-time $1/(6\gamma)$ of the atoms, it is ensured that the atomic density operator has decayed into the following density operator

$$\begin{aligned} \rho_{A,B}(t_2) &= \frac{1}{2}\left(|1\rangle_{AA}\langle 1| \otimes |2\rangle_{BB}\langle 2| + |2\rangle_{AA}\langle 1| \otimes |1\rangle_{BB}\langle 2|\right. \\ &\quad \left. + A \leftrightarrow B\right). \end{aligned} \tag{5.3.3}$$

The erasing pulse which is a circularly polarized $\sigma^{(-)}$ pulse drives the atomic transition

$|2\rangle \rightarrow |3\rangle$. Because of the form of the atomic density operator Eq. (5.3.3) we can apply a $\pi/2$ pulse that ensures one of the two atoms will be excited, the one which was involved in the scattering process. It is however unknowable which of the two atoms will be excited, and therefore it is possible to dientangle the atomic subsystem from the photon subsystem. The excitation time T_{D_2} of the atoms by the $\frac{\pi}{2}$-pulse is assumed to be very short compared to the life-time $1/(6\gamma)$. This can be achieved with a sufficient strong laser pulse due to the relation $\Omega T_{D_2} = \pi/2$ where Ω is the interaction parameter in frequency units of the laser pulse and the atoms. Immediately after the application of the strong $\pi/2$–$\sigma^{(-)}$ laser pulse at the time $t_2 = t_0 + T_D + 5/(6\gamma)$ the atomic density operator reads as

$$\begin{aligned} \rho_{A,B}(t_2) &= \frac{1}{2}\left(|1\rangle_{AA}\langle 1| \otimes |3\rangle_{BB}\langle 3| + |3\rangle_{AA}\langle 1| \otimes |1\rangle_{BB}\langle 3|\right. \\ &\quad \left. + A \leftrightarrow B\right). \end{aligned} \tag{5.3.4}$$

Again free evolution takes place and a photon appears which is detected as a π-polarized photon at the erasing detector in the second-order correlation function. The probability of scattering a π-polarized photon is equal to 1/3 (it is however important that only π-polarized photons contribute in the second-order correlation function). The probability of detection events in the second-order correlation function is therefore equal to $1/3 \times 2/3 = 2/9$ of all possible scattering events assuming we can collect all the erasing and scattering photons, which can be achieved by using the frequency selective elliptical reflector for the erasing photons (see above). The other

scattering events do not contribute to the second-order correlation and therefore do not disturb the experiment. After free evolution our atomic density operator evolves finally into

$$\rho_{A,B} = |1\rangle_{AA}\langle 1| \otimes |1\rangle_{BB}\langle 1|. \tag{5.3.5}$$

In other words, all scattering events in the second-order correlation function lead to the same final atomic density operator (5.3.5), and consequently, interference occurs as the result of different possible paths starting from the initial density operator (5.3.1) and leading to the same final density operator (5.3.5). The atomic density operator (5.3.5) is therefore disentangled from the photon subsystem leading to the following final result for the second-order correlation function

$$\begin{aligned} G^{(2)}(\mathbf{r},t;\boldsymbol{\rho},\tau_2) &= \frac{1}{2}\mathrm{Tr}_{A,B}\langle|1\rangle_{AA}\langle 1|\otimes|1\rangle_{BB}\langle 1|\rangle \\ \times\ & |\Psi(\mathbf{r})|^2|\Psi(\boldsymbol{\rho})|^2\Big\{\Theta(t-t_1-|\mathbf{r}_A|/c)\Theta(\tau_2-|\boldsymbol{\rho}|/c) \\ \times\ & e^{-6\gamma(t-t_1-|\mathbf{r}_A|/c)}e^{-6\gamma(\tau_2-|\boldsymbol{\rho}|/c)} + A\leftrightarrow B \\ & +2\Theta(t-t_1-|\mathbf{r}_A|/c)\Theta(t-t_1-|\mathbf{r}_B|/c)\Theta(\tau_2-|\boldsymbol{\rho}|/c) \\ & \times e^{-6\gamma\left[t-t_1-\frac{1}{2}(|\mathbf{r}_A|+|\mathbf{r}_B|)/c\right]}e^{-6\gamma(\tau_2-|\boldsymbol{\rho}|/c)} \\ & \times\cos[\mathbf{k}\cdot(\mathbf{r}_A-\mathbf{r}_B)]\Big\}. \end{aligned} \tag{5.3.6}$$

Here, again $\tau_2 = t-t_2$ is the delay time after the excitation with the erasing pulse at t_2 and detecting our erasing photon. We recognize immediately the disentanglement of our two subsystems atoms and photons. Again, the quantum eraser has disentangled these two subsystems and consequently interference occurs in the scattered field.

Chapter VI

6 Schemes for Displaying of Anti-Fringes and Partial "Which Way" Information

6.1 Scheme for Displaying Anti-Fringes

This chapter is divided into two parts. In the first part we devise a scheme to display anti-fringes using the two 4-level atoms by a slight variation of the earlier setup we used in Chapter IV. The second and main part is devoted to possible experimental schemes which can be used to test a recently derived inequality which quantifies the concept of complementarity [2].

Recently, a scheme to display anti-fringes in the light scattered from two two-level atoms in a cavity was proposed [9]. Here, we present a scheme with two 4-level atoms, which is different from the one considered previously in [9], which can display a minimum at the center of the arising Young interference picture. The scheme, which does not need a cavity, depends however on the initial atomic density operator. Instead of applying a π-polarized BBE, we employ here a σ_x-polarized BBE. In addition, unlike the previous case, here we measure the interference fringes which arise in the σ_y-polarized scattering light. The occurrence of interference in

the σ_y-polarized light depends on the initial atomic density operator. In particular the arising interference picture can display anti-fringes, fringes, or non-interference as a result of the superposition of both, anti-fringes and fringes. We start with the following special initial condition

$$\rho_{AB}(t_0) = |1\rangle_{AA}\langle 1| \otimes |2\rangle_{BB}\langle 2|. \tag{6.1.1}$$

After the excitation by the σ_x-polarized BBE we have at the time $t_1 \approx t_0 + T_D$

$$\begin{aligned} \rho_{AB}(t_1) &= \frac{1}{2}\left(|4\rangle_{AA}\langle 4| \otimes |2\rangle_{BB}\langle 2| + |1\rangle_{AA}\langle 1| \otimes |3\rangle_{BB}\langle 3|\right. \\ &+ \left. |4\rangle_{AA}\langle 1| \otimes |2\rangle_{BB}\langle 3| + |1\rangle_{AA}\langle 4| \otimes |3\rangle_{BB}\langle 2|\right). \end{aligned} \tag{6.1.2}$$

This is followed by a free evolution and a final detection of σ_y-polarized light at the detector at time t. The first order correlation function with the initial condition (6.1.1) is evaluated in a similar fashion as in Chapter V, however, here we will have σ_y dipole operators instead of σ_z dipole operators and we have

$$\begin{aligned} G^{(1)}(\mathbf{r}_A, \mathbf{r}_B; t) &= \langle [\mathbf{E}_A^{(-)}(\mathbf{r}, t) + \mathbf{E}_B^{(-)}(\mathbf{r}, t)] \\ &\cdot [\mathbf{E}_A^{(+)}(\mathbf{r}, t) + \mathbf{E}_B^{(+)}(\mathbf{r}, \mathbf{t})]\rangle. \end{aligned} \tag{6.1.3}$$

Here, the electric fields are expressed by the appropriate electric dipole operator, and

we obtain for the interfering part

$$G^{(1)}_{int}(\mathbf{r}_A,\mathbf{r}_B;t) = \frac{1}{2}|\Psi(\mathbf{r})|^2\Big\{\Theta(t-t_1-|\mathbf{r}_A|/c)\Theta(t-t_1-|\mathbf{r}_B|/c) \langle\sigma^{(+)}_{A,y}(t')\sigma^{(-)}_{B,y}(t'+\tau)\rangle + \langle\sigma^{(+)}_{B,y}(t')\sigma^{(-)}_{A,y}(t'+\tau)\Big\}, \tag{6.1.4}$$

where, $t' = t - t_1 - |\mathbf{r}_{A,B}|/c$ for atom A and atom B, respectively and $\sigma^{(+)}_y = i(|3\rangle\langle 2| - |4\rangle\langle 1|)$. The factor i which appears for y-scattered light which arises from $\sigma^{(+)}_y$ is responsible for the anti-fringes ($i^2 = -1$, and a minus sign appears in the expression of the interfering part). The above expression can be further calculated by using the results of Section 4.2 for the solutions of the matrix elements of the density operator. We also include the non-interfering part and obtain

$$\begin{aligned} &G^{(1)}(\mathbf{r}_A,\mathbf{r}_B;t) = \\ &\frac{1}{2}|\Psi(\mathbf{r})|^2 \times \Big\{\Theta\Big(t-t_1-\frac{|\mathbf{r}_A|}{c}\Big)e^{-6\gamma(t-t_1-|\mathbf{r}_A|/c)} + A \leftrightarrow B \\ &-\Theta\Big(t-t_1-\frac{|\mathbf{r}_A|}{c}\Big)\Theta\Big(t-t_1-\frac{|\mathbf{r}_B|}{c}\Big) \\ &2 \times e^{-\gamma[t-t_1-(|\mathbf{r}_A|+|\mathbf{r}_B|)/2c]}\cos[\mathbf{k}\cdot(\mathbf{r}_A-\mathbf{r}_B)]\Big\}. \end{aligned} \tag{6.1.5}$$

We note that we have an intensity minimum when $|\mathbf{r}_A| = |\mathbf{r}_B|$, implying an anti-fringe at the center [9]. This is valid for the special initial condition $|2\rangle_{AA}\langle 2| \otimes |1\rangle_{BB}\langle 1|$ and also for the initial condition $|1\rangle_{AA}\langle 1| \otimes |2\rangle_{BB}\langle 2|$. For the initial conditions $|1\rangle_{AA}\langle 1| \otimes |1\rangle_{BB}\langle 1|$ and $|2\rangle_{AA}\langle 2| \otimes |2\rangle_{BB}\langle 2|$ we have fringes with an intensity maximum at the center. For a more likely initial condition (which is more probable in the case of a

degenerated 4-level atom) given by the following,

$$\rho_{AB}(t_0) = \frac{1}{4}(|1\rangle_{AA}\langle 1| \otimes |1\rangle_{BB}\langle 1| + |2\rangle_{AA}\langle 2| \otimes |2\rangle_{BB}\langle 2| + |2\rangle_{AA}\langle 2| \otimes |1\rangle_{BB}\langle 1| + |1\rangle_{AA}\langle 1| \otimes |2\rangle_{BB}\langle 2|), \quad (6.1.6)$$

we get no interference since we have an equal contribution to fringes and anti-fringes [9]. In general we have something in between with reduced fringe visibility depending on the initial condition.

We note that the quantum erasing scheme of section 5.3 allows us to display anti-fringes. This can be achieved with a simple shifting of the position of the erasing detector out of the center between the two atoms. The shifting of the erasing π-detector results in a shift in the argument of the cosine function of Eq. (5.3.6),

$$\cos[\mathbf{k}\cdot(\mathbf{r}_A - \mathbf{r}_B)] \rightarrow \cos[\mathbf{k}\cdot(\mathbf{r}_A - \mathbf{r}_B) + \mathbf{k}'\cdot(\boldsymbol{\rho}_A - \boldsymbol{\rho}_B)], \quad (6.1.7)$$

where $|\mathbf{k}|/c = \omega_0 - \Delta$ and $|\mathbf{k}'|/c = \omega_0$. If we shift the erasing detector out of the center between the two atoms so that $\mathbf{k}'\cdot(\boldsymbol{\rho}_A - \boldsymbol{\rho}_B) = \pi$ the resulting interference pattern of the scattering photons in the second-order correlation function displays anti-fringes, i.e. a minimum at the center of the interference picture. It is important to recognize that this simple scheme to display anti-fringes or, in general, phase-shifted interference fringes with the quantum eraser is only possible with the quantum eraser scheme of subsection 5.3. In the quantum eraser scheme of section 5.2 a shifting of the erasing detector would merely reduce the visibility of the interference fringes. The reason is that two cosine functions appear in the second-order correlation function of Eq.

(5.2.5) when the erasing detector is shifted out of the center between the two atoms as

$$\cos[\mathbf{k}\cdot(\mathbf{r}_A-\mathbf{r}_B)]\rightarrow\cos[\mathbf{k}\cdot(\mathbf{r}_A-\mathbf{r}_B)]\cos[\mathbf{k}'\cdot(\boldsymbol{\rho}_A-\boldsymbol{\rho}_B)]. \tag{6.1.8}$$

Consequently, a shifting of the erasing detector out of the center between the two atoms results in a reduction of the interference fringes by the amount $\cos[\mathbf{k}'\cdot(\boldsymbol{\rho}_A-\boldsymbol{\rho}_B)]$. Nevertheless, a shifting of the erasing detector so that $\cos[\mathbf{k}'\cdot(\boldsymbol{\rho}_A-\boldsymbol{\rho}_B)]=\pi$ results also in the displaying of anti-fringes for the scattering photons in the quantum eraser scheme of section 5.2. However, a shifting of the erasing detector so that $\cos[\mathbf{k}'\cdot(\boldsymbol{\rho}_A-\boldsymbol{\rho}_B)]=\pi/2$ results in the vanishing of the interference fringes in the quantum eraser scheme of section 5.2 while it only shifts the interference fringes of the scattering photons by a phase of $\pi/2$ in the quantum erasing scheme of section 5.3. The quantum eraser scheme of section 5.2, on the other hand could be employed to verify an inequality due to Englert [2] which quantifies the general complementarity principle "which way information $\leftrightarrow$ no interference" and "no which way information $\leftrightarrow$ interference". We now turn to the scheme which can be used for this experimental test of Englert's inequality .

6.2 Scheme for Partial "Which Way" Information

Wave-particle duality is a concept which is usually connected to a two-way interferometer such as Young's double-slit experiment. It is a famous example of Bohr's

principle of complementarity [3] which states that quantum systems possess properties that are equally real but mutually exclusive. The duality concept states that the observation of an interference pattern and the acquisition of which-way information are mutually exclusive.

Recently, an inequality was derived by Englert [2] which quantifies this duality concept in the sense to what extent partial fringe visibility and partial which-way knowledge are compatible. This inequality allows us to consider intermediate stages of the extreme situations "perfect fringe visibility and no interference" and "full which-way information and no fringes" which are familiar from textbooks.

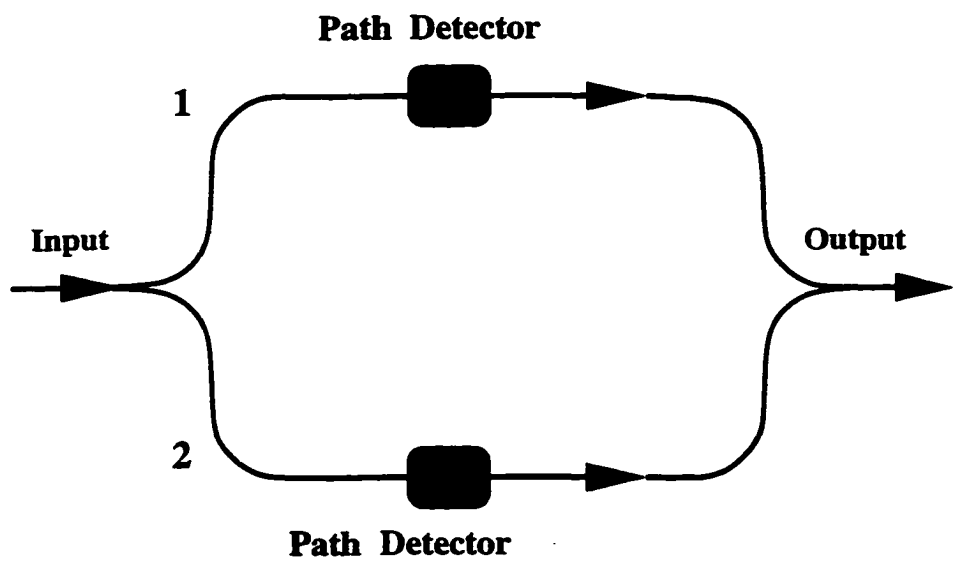

Figure 11: Scheme for partial "which way" information and partial interference. With the use of the path detectors, both partial "which way" information and partial interference patterns is obtained within the limits set by duality.

The main effort of this section is the implementation of an experiment which allows us to consider the intermediate stages of the duality concept, i.e. partial which-way information and partial interference fringes (Fig. 11). The proposal is again based on the experiment of Eichmann *et al.* [1]. The continuous, coherent monochromatic excitation is again replaced by a continuous, incoherent broadband excitation as in Chapter IV. In addition, we have a linear polarizer in front of the detection screen as indicated in Fig. 8 which allows us to measure certain polarization directions of the scattered light with an angle of φ relative to the z-axis. Therefore, we are not restricted to the two extreme cases of the observation of x- or z-polarized scattered light but can consider also intermediate cases where the scattered light has a polarization direction at a certain angle of φ with respect to the z-axis in the z-x-plane. As it turns out, this provides for partial which-way information and partial fringe visibility depending on the polarization angle φ. The extreme cases, measurement of the z-polarized light or measurement of the x-polarized light, correspond, to the extreme duality cases "perfect fringe visibility and no which-way information" or "full which-way information and no fringe visibility". To get an actual partial which-way information it is necessary to measure the internal atomic states of one of the two atoms, e.g. atom A, as indicated in Fig. 12.

In general, the expectation value of the intensity $\langle I(\mathbf{r},t)\rangle$ of the scattered light

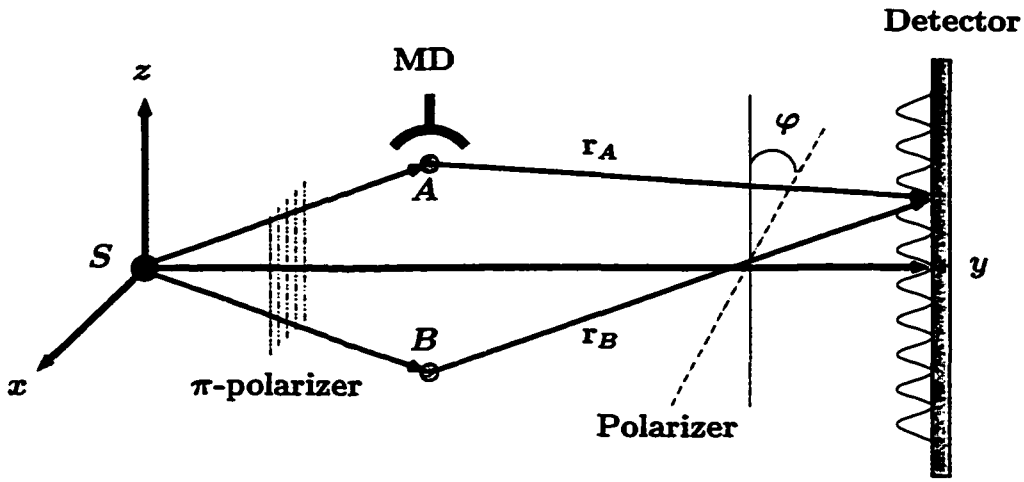

Figure 12: Setup for getting partial which way information. The atoms denoted as A and B, are excited by a π-polarized broadband light which excites one of the two atoms at a time. The scattered light, after passing through the polarizer at an angle φ with respect to the z-axis in the $x-z$-plane is measured at the detector. The internal atomic states of atom A, which serve as the detector states, are measured with MD. This can be experimentally realized if we excite atom A with an excitation pulse after the scattering process which can only excite the ground-state $|1\rangle$ (i.e. a σ^+-circularly polarized $\pi/2$-pulse) and determine if resonance light occurs or not.

from the two atoms A and B at a position $\mathbf{r}$ is determined by

$$\begin{aligned}\langle I(\mathbf{r},t)\rangle &= \langle[\mathbf{E}_A^{(-)}(\mathbf{r},t)+\mathbf{E}_B^{(-)}(\mathbf{r},t)] \\ &\quad \cdot[\mathbf{E}_A^{(+)}(\mathbf{r},t)+\mathbf{E}_B^{(+)}(\mathbf{r},t)]\rangle, \\ &= \langle I_A(\mathbf{r},t)\rangle + \langle \mathbf{E}_A^{(-)}(\mathbf{r},t)\cdot\mathbf{E}_B^{(+)}(\mathbf{r},t)\rangle + A \leftrightarrow B.\end{aligned} \tag{6.2.1}$$

In the case of the experimental setup of Fig. 8 where we measure a certain linear polarization direction in the x-z plane, with angle φ relative to the z-axis, the intensity

of the scattered light is expressed as

$$\begin{aligned}\langle I(\mathbf{r},t)\rangle &= \langle I_A(\mathbf{r},\varphi,t)\rangle + \langle I_B(\mathbf{r},\varphi,t)\rangle \\ &+ \{(\langle E^{(-)}_{A,z}(\mathbf{r},t)E^{(+)}_{B,z}(\mathbf{r},t)\rangle \cos^2\varphi \\ &+ \langle E^{(-)}_{A,x}(\mathbf{r},t)E^{(+)}_{B,x}(\mathbf{r},t)\rangle \sin^2\varphi) \quad + A \leftrightarrow B\}, \end{aligned} \tag{6.2.2}$$

where

$$\langle I_A(\mathbf{r},\varphi,t)\rangle = \langle E^{(-)}_{A,z}(\mathbf{r},t)E^{(+)}_{A,z}(\mathbf{r},t)\rangle \cos^2\varphi + \langle E^{(-)}_{A,x}(\mathbf{r},t)E^{(+)}_{A,x}(\mathbf{r},t)\rangle \sin^2\varphi, \tag{6.2.3}$$

is the intensity solely due to atom A and we have a similar expression for $\langle I_B(\mathbf{r},\varphi,t)\rangle$.

The scattered fields from atoms A and B can be expressed again in terms of atomic lowering operators in the Heisenberg picture

$$\mathbf{E}^{(+)}_{A,B}(\mathbf{r},t) = \Theta\Big(t - \frac{|\mathbf{r}_{A,B}|}{c}\Big)\Psi(\mathbf{r})\sigma^{(-)}_{A,B}\Big(t - \frac{|\mathbf{r}_{A,B}|}{c}\Big).$$

The lowering operators $\sigma^{(-)}_{A,B}\Big(t - \frac{|\mathbf{r}_{A,B}|}{c}\Big)$ are the time-dependent, negative-frequency part Heisenberg lowering operators and depend on the polarization directions

$$\begin{aligned}\sigma^{(-)}_{A,B}\Big(t - \frac{|\mathbf{r}_{A,B}|}{c}\Big) &= \sigma^{(-)}_{A,B,x}\Big(t - \frac{|\mathbf{r}_{A,B}|}{c}\Big)\hat{\mathbf{x}} \\ &+\sigma^{(-)}_{A,B,y}\Big(t - \frac{|\mathbf{r}_{A,B}|}{c}\Big)\hat{\mathbf{y}} \\ &+\sigma^{(-)}_{A,B,z}\Big(t - \frac{|\mathbf{r}_{A,B}|}{c}\Big)\hat{\mathbf{z}}. \end{aligned} \tag{6.2.4}$$

Inserting this in the expression for the intensity (6.2.2) we get, starting with the initial density operator $\rho_{A,B}(t_0) = |1\rangle_{AA}\langle 1| \otimes |1\rangle_{BB}\langle 1|$ at the time t_0, the following which

can be derived in a similar way as shown in [33, 34, 35]

$$\begin{aligned}\langle I(\mathbf{r},t',\tau)\rangle &= \frac{1}{2}|\Psi(\mathbf{r})|^2 \mathrm{Tr}_{A,B}\Big\{ \cos^2\varphi |1\rangle_{AA}\langle 1|1\rangle_{BB}\langle 1| \\ &\times \big[\Theta(t'_A)e^{-6\gamma t'_A} + \Theta(t'_B)e^{-6\gamma t'_B} \\ &\quad +2\Theta(t'_A+\tau)\Theta(t'_A)e^{-6\gamma\left(t'_A+\frac{\tau}{2}\right)}\cos(\omega\tau)\big] \\ &+ \sin^2\varphi\big[\Theta(t'_A)e^{-6\gamma t'_A}|2\rangle_{AA}\langle 2|1\rangle_{BB}\langle 1| \\ &\quad +\Theta(t'_B)e^{-6\gamma t'_B}|2\rangle_{BB}\langle 2|1\rangle_{AA}\langle 1| \\ &\quad +\Theta(t'_A+\tau)\Theta(t'_A)e^{-6\gamma\left(t'_A+\frac{\tau}{2}\right)} \\ &\quad \times(|2\rangle_{AA}\langle 1|1\rangle_{BB}\langle 2|e^{i\omega\tau} \\ &\quad +|1\rangle_{AA}\langle 2|2\rangle_{BB}\langle 1|e^{-i\omega\tau})\big]\Big\}, \end{aligned} \tag{6.2.5}$$

which can be derived in a similar way as in Refs. [33, 34, 35]. Here, we have introduced the retarded times $t'_{A,B} = t - t_1 - |\mathbf{r}_{A,B}|/c$, as well as the delay time $\tau = (|\mathbf{r}_A| - |\mathbf{r}_B|)/c$.

Equation (6.2.5) contains a part leading to interference and a part which does not lead to interference. The part which leads to interference is connected to π- or z-polarized scattering while the non-interfering part is connected to σ- or x-polarized scattering. Due to the polarizer directed at an angle φ with respect to the z-axis, it is impossible to know which part of the polarization direction contributes to the scattered light. It can be the z-polarized part or the x-polarized part with a certain probability. The probability that the z-polarization part of the scattered light contributes is equal to $\frac{1}{3}\cos^2\varphi$, while the probability for the x-polarized part of the

scattered light is $\frac{1}{3}\sin^2\varphi$. The part which contains the x-polarized scattered light offers the possibility to get "which way" information out of the internal atomic states. However, it is not an actual "which way" information so far but only the possibility. In the part containing the z-polarized light it is impossible to get "which way" information and consequently interference occurs.

The two extreme cases of measuring either the z-polarized part or the x-polarized part are connected to the two extreme cases of complementarity: possibility of full "which way" information–no interference and no possibility of "which way" information–full interference fringes as shown previously [1, 10, 33, 34, 35]. Due to the introduction of a polarizer, however, we have the possibility to get intermediate situations between the above extreme cases. Depending on the angle φ of the polarizer we obtain reduced fringe visibility at the expense of getting partial "which way" information.

The above system allows the verification of an earlier inequality by Greenberger and Yasin [36] connecting with predictability (of which way the photon took) and the visibility of interference fringes. This inequality is also implicitly contained in the work of Wooters and Zurek [37] and also in a paper by Mandel [38]. It was experimentally confirmed by Rauch, Summhammer, and Tuppinger [39]. The predictability $\mathcal{P}$ is defined as the difference of the probabilities which way the photon took through the interferometer

$$\mathcal{P} = |w_+ - w_-|, \tag{6.2.6}$$

where w_+ is the probability of the upper path and w_- is the probability of the lower path through the interferometer, respectively. The inequality by Greenberger and Yasin [36] connects the predictability $\mathcal{P}$ with the visibility $\mathcal{V}$ and is given as

$$\mathcal{P}^2 + \mathcal{V}^2 \leq 1. \tag{6.2.7}$$

In the above considered interferometer the predictability of which way the photon took is equal to zero as long as we are not doing a measurement of the internal atomic states of one of the two atoms as in the sense discussed earlier (symmetric interferometer). The fringe visibility is, however, reduced because of the possibility of getting partial "which way" information. Depending on the direction of the polarizer in front of the detector, the fringe visibility in this interferometric setup is

$$\mathcal{V} = \frac{\langle I \rangle_{max} - \langle I \rangle_{min}}{\langle I \rangle_{max} + \langle I \rangle_{min}} = \cos^2 \varphi, \tag{6.2.8}$$

while the predictability $\mathcal{P}$ is always equal to zero. Thus, the above interferometer satisfies the inequality of Greenberger and Yasin [36]

$$\mathcal{P}^2 + \mathcal{V}^2 = \cos^4 \varphi \leq 1. \tag{6.2.9}$$

The polarizer in front of the detector allows us to verify the above inequality experimentally.

In the next section we consider the inequality derived by Englert [2]. It was derived for the case when the symmetric interferometer, which has no a priori which-way information, is coupled to another physical system that is meant to serve as a

"which way" detector. The detector allows one to get actual "which way" information out of the symmetric interferometer. Due to the interaction with the detector, the ways the photon took become distinguishable depending on the observable which is measured by the detector. The detector consists of reading out certain internal states of atom A with a certain polarization direction of the polarizer in front of the detector. The polarizer setting determines the degree of "which way" information or distinguishability provided by to the detector.

6.3 Verification of the Englert-Inequality

Recently, Englert derived an inequality which allows one to quantify, in some sense, the wave-particle duality concept [2]. The inequality combines the fringe visibility $\mathcal{V}$ and the distinguishability $\mathcal{D}$ of which way the photon took in an interferometer induced by a detector. The distinguishability depends strongly on the observable which is measured by the detector. It is defined as

$$\mathcal{D} = \frac{1}{2}\mathrm{Tr}_{Det}\left\{|\rho_{Det}^{(+)} - \rho_{Det}^{(-)}|\right\}, \tag{6.3.1}$$

where $\rho_{Det}^{(+)}$ and $\rho_{Det}^{(-)}$ are the density operators for the detector states for the upper way $^+$ and lower way $^-$ through the interferometer, respectively. The quantity $\mathcal{D}$ which is the distance between $\rho_{Det}^{(+)}$ and $\rho_{Det}^{(-)}$ in the trace-class norm gives a quantitative measure of the amount of "which way" information that has become available due to the detector. The fringe visibility $\mathcal{V}$, which is defined as the absolute of the complex

contrast factor, and the distinguishability $\mathcal{D}$ obey the following inequality (Englert, [2])

$$\mathcal{D}^2 + \mathcal{V}^2 \leq 1. \tag{6.3.2}$$

This inequality is a fundamental statement about the duality concept. An important quantity, which is closely related to the distinguishability, is the maximum likelihood of guessing the way right which way the photon took through the interferometer. This quantity is defined as [2]

$$\mathcal{L}_{\text{opt}} = \frac{1}{2}(1 + D). \tag{6.3.3}$$

The purpose of this section is the verification of the inequality (6.3.2) in the interferometer considered in the previous section. The detector states of this interferometer are determined by the internal atomic states of the two atoms. In particular, we can derive the following density operator for the detector

$$\begin{aligned} \rho_{Det}^{final} &= \frac{1}{2}\left(\rho_{Det}^{(+)} + \rho_{Det}^{(-)}\right) \\ &= \frac{1}{2}(\cos^2\varphi|1\rangle_{AA}\langle 1| \otimes |1\rangle_{BB}\langle 1| + \sin^2\varphi|2\rangle_{AA}\langle 2| \otimes |1\rangle_{BB}\langle 1|)^{(+)} \\ &+ \frac{1}{2}(\cos^2\varphi|1\rangle_{AA}\langle 1| \otimes |1\rangle_{BB}\langle 1| + \sin^2\varphi|1\rangle_{AA}\langle 1 \otimes ||2\rangle_{BB}\langle 2|)^{-}, \end{aligned} \tag{6.3.4}$$

where we have defined as the "upper way" when atom A is scattering and as the "lower way" when atom B is scattering, respectively.

The "which way" information is stored in the 4-level atoms which serve as our detectors. However, it is only partial information because we cannot get "which way" information from the z-polarized scattering. The extraction of the "which way" information stored in the detectors requires the measurement of a suitable observable. A suitable observable in the above interferometric scheme is the reading out of the internal states of one of the two atoms, i.e. atom A. This can be done if we exclusively excite atom A after the scattering process with, i.e. a σ^--pulse which drives the $|1\rangle \leftrightarrow |4\rangle$-transition and determine if resonance-light occurs or not. If resonance light occurs atom A was in the state $|1\rangle$, while atom A was in the state $|2\rangle$ if no resonance light occurs.

What is the available "which way" information from such a measurement? Let us assume we find atom A in the state $|1\rangle$, that is a resonance photon occurs after the excitation with the σ^--pulse. The extractable which-way information $\mathcal{I}^+$ through the upper and $\mathcal{I}^-$ through the lower interferometer or path in this case are determined by

$$\begin{aligned} \mathcal{I}_{11}^{+} &= \frac{1}{2}\cos^2\varphi \\ \mathcal{I}_{11}^{-} &= 1 - \mathcal{I}_{11}^{+} = \frac{1}{2}\cos^2\varphi + \sin^2\varphi, \end{aligned} \tag{6.3.5}$$

In other words if we find the atom A in the ground-state $|1\rangle$ we know we can guess the way right (through the lower interferometric arm) with the probability given in

equation (6.3.5). Similarly, we can guess the way right through the upper interferometric arm if we find atom A in the ground-state $|2\rangle$. In this case the extractable which-way information is

$$\begin{aligned} \mathcal{I}_{22}^{+} &= 1, \\ \mathcal{I}_{22}^{-} &= 0. \end{aligned} \tag{6.3.6}$$

In other words, we can be sure that the photon goes through the upper interferometric arm in this case. The distinguishability can be determined from Eq. (6.3.4) as

$$\begin{aligned} \mathcal{D} &= \frac{1}{2}\mathrm{Tr}_{Det}\left\{|\rho_{Det}^{(+)} - \rho_{Det}^{(-)}|\right\} \\ &= \frac{1}{2}\sin^2\varphi \mathrm{Tr}_{AB}\Big||2\rangle_{AA}\langle 2| \otimes |1\rangle_{BB}\langle 1| - |1\rangle_{AA}\langle 1| \otimes |2\rangle_{BB}\langle 2|\Big| \\ &= \sin^2\varphi, \\ &= \left|\mathcal{I}_{11}^{+} - \mathcal{I}_{11}^{-}\right|. \end{aligned} \tag{6.3.7}$$

This is in accordance with the above considerations about the extractable which way information as indicated by the last line of Eq. (6.3.7). The visibility $\mathcal{V}$ of the above interferometer is determined by

$$\mathcal{V} = \cos^2\varphi. \tag{6.3.8}$$

The optimum of likelihood for guessing the way right $\mathcal{L}_{\mathrm{opt}}$ is determined as

$$\begin{aligned} \mathcal{L}_{\mathrm{opt}} &= \frac{1}{2}(1 + D) \\ &= \frac{1}{2}\left(1 + \sin^2\varphi\right). \end{aligned} \tag{6.3.9}$$

This follows also from the extractable which way informations

$$\begin{aligned}
\mathcal{L}_{\text{opt}} &= \text{Tr}_{Det}\left\{\mathcal{I}_{11}^{+}|1\rangle\langle 1| + \mathcal{I}_{22}^{+}\sin^2\varphi|2\rangle\langle 2|\right\}, \\
&= \text{Tr}_{Det}\left\{\mathcal{I}_{11}^{-}|1\rangle\langle 1| + \mathcal{I}_{22}^{-}\sin^2\varphi|2\rangle\langle 2|\right\}, \\
&= \frac{1}{2}\cos^2\varphi + \sin^2\varphi, \\
&= \frac{1}{2}\left(1 + \sin^2\varphi\right). \qquad (6.3.10)
\end{aligned}$$

Inserting eqs. (6.3.7) and (6.3.8) in the inequality (6.3.2) we derive

$$\begin{aligned}
\mathcal{D}^2 + \mathcal{V}^2 &= \sin^4\varphi + \cos^4\varphi, \\
&= 1 - \frac{1}{2}\sin^2 2\varphi \leq 1. \qquad (6.3.11)
\end{aligned}$$

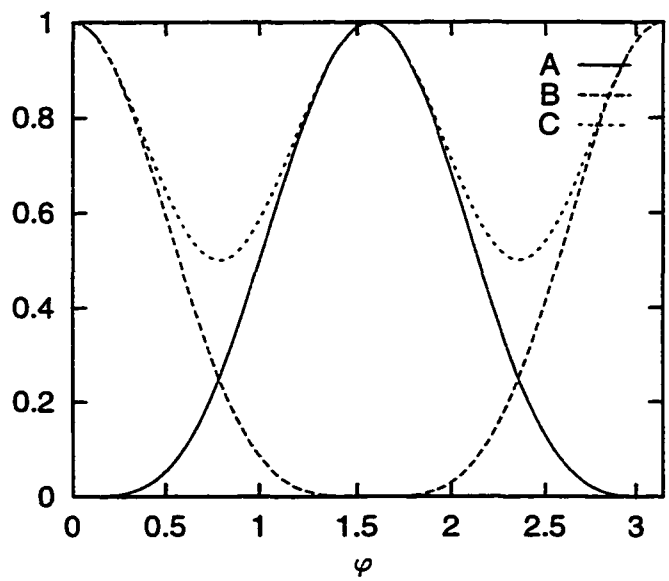

Figure 13: Plots of visibility and distinguishability for the partial which-way scheme exhibiting the fundamental inequality $\mathcal{D}^2 + \mathcal{V}^2 \leq 1$. In the plot $A = \mathcal{D}^2$, $B = \mathcal{V}^2$ and $C = \mathcal{D}^2 + \mathcal{V}^2$.

Depending on the angle φ, the amount of partly "which way" information is in-

creased while the amount of fringe visibility is decreased and vice versa (Fig. 13). For the angle $\varphi = \pi/2$ the amount of "which way" information is equal to one while the fringe visibility is equal to zero corresponding to the extreme situation of full "which way" information and no fringe visibility. For the angle $\varphi = 0$ the amount of partial which-way information is equal to zero while the fringe visibility is equal to one, corresponding to the extreme situation of full fringe visibility and no "which way" information. The intermediate situations of partial "which way" information and partial fringe visibility are realized for every angle φ between the extreme situation $\varphi = 0$ and $\varphi = \pi/2$.

The inequality (6.3.11) is a special case of the Englert inequality [2]. This can be recognized most easily if we consider $\varphi = \pi/4$. In this case the sum of the distinguishability squared and the visibility squared is equal to $1/2$, i.e. smaller than one. That means the upper boundary depends on the angle φ and the inequality for our interferometric scheme has to be modified into

$$\frac{1}{2} \leq \mathcal{D}^2 + \mathcal{V}^2 \leq 1. \tag{6.3.12}$$

The upper boundary is smaller than one because there are two contributions in our interferometer, a π-polarized contribution giving rise to interference and a σ-polarized contribution giving rise to "which way" information. Consequently, the fringe visibility is reduced depending on how much the σ contribution contributes to the scattering processes which determines also the amount of possible "which way" information. But

this σ-contribution cannot contribute to the fringe visibility because of the different polarizations of the two contributions and because of the "which way" information stored in the atoms in the case of σ-scattering processes. This is the reason that the upper boundary is reduced. An upper boundary of one in the inequality (for all polarization angles φ) would be realized if the σ-scattering light would also give rise to interference.

The reason that the lower boundary is not equal to zero is because our measuring of the detector states cannot have a consequence on the fringe visibility. It cannot reduce the fringe visibility but only determine the possible which way information in the limit of this inequality. The reason that we cannot go below this lower boundary is that it is impossible to get "which way" information with our detection scheme from the π-polarized part and consequently the π-polarized part of the scattering light will always give rise to interference and determine the lower boundary of our inequality. However, between these boundaries of our inequality every value can be realized depending on the detector efficiency of the "which way" detector as we will see next.

We denote the detector efficiency with $\epsilon \leq 1$. The detector efficiency determines the amount of available which-way information. In particular the which way-information is reduced to the following maximum likelihood for guessing the way right

$\mathcal{L}^{\varepsilon}_{\rm opt}$

$$\mathcal{L}^{\varepsilon}_{\rm opt} = \frac{1}{2}(1 + \varepsilon \mathcal{D}_{\rm opt}). \tag{6.3.13}$$

The distinguishability is consequently also reduced to

$$\mathcal{D}_{\varepsilon} = \varepsilon \sin^2 \varphi. \tag{6.3.14}$$

However, the fringe visibility $\mathcal{V}$ is not affected by the detector efficiency and is still given by $\mathcal{V} = \cos^2 \varphi$ and the inequality takes the following form,

$$\mathcal{D}^2_{\varepsilon} + \mathcal{V}^2 = \cos^4 \varphi + \varepsilon^2 \sin^4 \varphi. \tag{6.3.15}$$

Consequently, depending on the detector efficiency ε every value of the inequality (6.3.12) can be realized.

As was mentioned in [2] the equal sign of the inequality (6.3.12) always holds if the detector is initially prepared in a pure state (in the case of a 100% detector). We can show this in our scheme if we simulate the detector efficiency with partly a pure initial detector state (in our case $|1\rangle_{AA}\langle 1| \otimes |1\rangle_{BB}\langle 1|$) and a partly mixture of initial detector states as

$$\begin{aligned} \rho^{initial}_{Det} &= \varepsilon \{|1\rangle_{AA}\langle 1| \otimes |1\rangle_{BB}\langle 1|\} \\ &+ \frac{1-\varepsilon}{4}\Big\{|1\rangle_{AA}\langle 1| \otimes |1\rangle_{BB}\langle 1| \\ &\qquad + |2\rangle_{AA}\langle 2| \otimes |1\rangle_{BB}\langle 1| + 1 \leftrightarrow 2\Big\}. \end{aligned} \tag{6.3.16}$$

This determines the final detector states (after the detection of the scattering photon)

after tracing over the atom B because only atom A is measured (see previously)

$$\begin{aligned}\rho_{det}^{final} &= \frac{\varepsilon}{2}\{\cos^2\varphi|1\rangle\langle 1| + \sin^2\varphi|1\rangle\langle 1|\}^{(+)} \\ &+ \frac{\varepsilon}{2}\{\cos^2\varphi|1\rangle\langle 1| + \sin^2\varphi|2\rangle\langle 2|\}^{(-)}, \\ &+ \frac{1-\varepsilon}{4}\{|1\rangle\langle 1| + |2\rangle\langle 2|\}^{(+)} \\ &+ \frac{1-\varepsilon}{4}\{|1\rangle\langle 1| + |2\rangle\langle 2|\}^{(-)}, \end{aligned} \tag{6.3.17}$$

where $^{(+)}$ and $^{(-)}$ denotes the detector states for the upper and lower paths through the interferometer. We recognize from Eq. (6.3.17) that even with a 100% detector for the measuring of the internal atomic states of atom A we can only have a which-way information reduced by the factor ε. From the statistical mixture part of Eq. (6.3.17) we cannot get which way information. In other words a finite detector efficiency can be simulated with a partial mixture of the initial detector states and consequently the equal sign in the inequality (6.3.12) cannot occur, in accordance with the most general results in [2].

6.4 Partial "Which Way" Interferometer Scheme Based on a Quantum Eraser

In this section we discuss a partial "which way" interferometer based on the quantum eraser scheme for two 4-level atoms [33, 34, 35]. The idea to get partial "which way" information from the quantum erasing scheme is the following. The quantum eraser in general erases possible "which way" information and consequently interference is

brought back [6, 22, 23, 24, 26, 27, 28, 29, 30]. We ask in this section what happens when the quantum eraser erases only partly the possible "which way" information and if it is possible to verify the inequalities of Englert in this connection?

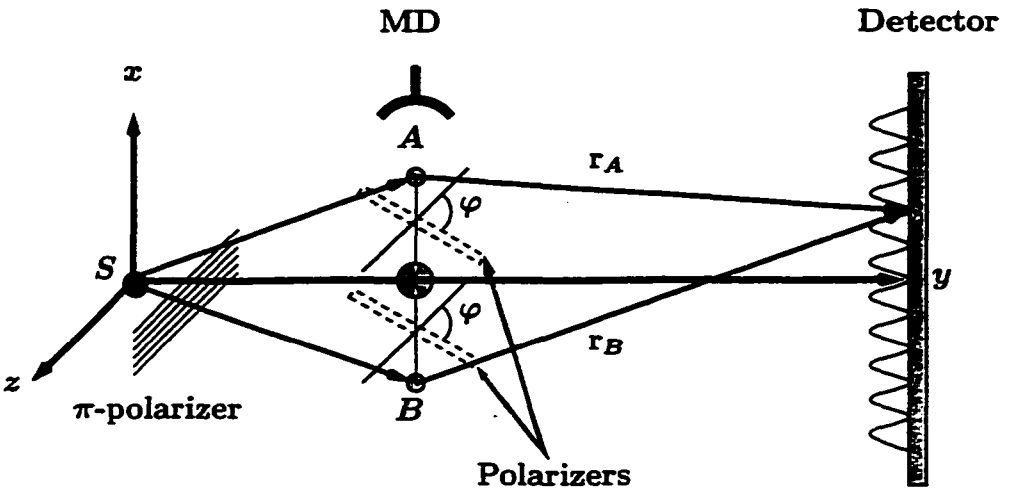

Figure 14: Quantum eraser scheme for a partial "which way" experiment. The experimental setup is identical to the quantum eraser case except for the introduction of polarizers. Due to the polarizers at an angle φ with respect to the z-axis in the $y-z$ plane we have a partial erasing of the information.

The quantum eraser scheme for two 4-level atoms [33, 34, 35] has to be modified, in the following sense with for partial erasing of "which way" information. Instead of measuring the π-polarized photons at the erasing detector, we measure a certain linear polarization direction between the z-polarization and the y-polarization at the erasing detector as indicated in Fig. 14. The polarization direction of the erasing detector is determined by the angle φ with respect to the z-axis in the $z-y$-plane. This modifies

the second-order correlation function derived in [33, 34, 35] to the following

$$\begin{aligned} G^{(2)}(\mathbf{r},t;\boldsymbol{\rho},\tau) &= \langle[\hat{E}_A^{(-)\sigma}(\mathbf{r},t)+\hat{E}_B^{(-)\sigma}(\mathbf{r},t)] \\ &\times \{\cos^2\varphi[\hat{E}_A^{(-)\pi}(\boldsymbol{\rho},\tau)+\hat{E}_B^{(-)\pi}(\boldsymbol{\rho},\tau)] \\ &\quad \cdot[\hat{E}_A^{(+)\pi}(\boldsymbol{\rho},\tau)+\hat{E}_B^{(+)\pi}(\boldsymbol{\rho},\tau)] \\ &+ \sin^2\varphi[\hat{E}_A^{(-)\sigma}(\boldsymbol{\rho},\tau)+\hat{E}_B^{(-)\sigma}(\boldsymbol{\rho},\tau)] \\ &\quad \cdot[\hat{E}_A^{(+)\sigma}(\boldsymbol{\rho},\tau)+\hat{E}_B^{(+)\sigma}(\boldsymbol{\rho},\tau)]\} \\ &\times [\hat{E}_A^{(+)\sigma}(\mathbf{r},'t)+\hat{E}_B^{(+)\sigma}(\mathbf{r},t')]\rangle, \end{aligned} \tag{6.4.1}$$

where π denotes the π-polarized and σ denotes σ-polarized photons, and $\boldsymbol{\rho}$ is the distance of the erasing detector from either atom. The time τ is the time-delay between the detection of the erasing photon and the scattering photon which is σ-polarized. The erasing photon can be π-polarized or σ-polarized with certain probabilities depending on the polarization-direction of the erasing detector. However, complete erasure of the" which way" information is only possible if we detect a π-polarized photon at the erasing detector while the detection of a σ-polarized photon cannot erase the "which way" information and, consequently, no interference occurs. In the above scheme, the probability that a π-polarized photon is measured at the erasing detector is given by $\cos^2\varphi$, while the probability of measuring a σ-polarized photon is given by $\sin^2\varphi$. Consequently, only a part of the "which way" information is erased and interference is brought back only incompletely. There is still "which way" information stored in the atomic internal states which can be read out giving partial

"which way" information, similarly to the previous section.

Calculating the second-order correlation similarly to the second-order correlation function of the quantum eraser scheme in [33, 34, 35], we arrive at

$$
\begin{aligned}
& G^{(2)}(\mathbf{r},t;\boldsymbol{\rho},\tau_2) = \cos^2\varphi\langle|1\rangle_{AA}\langle 1|1\rangle_{BB}\langle 1|\rangle \\
\times\ & |\Psi(\mathbf{r})|^2|\Psi(\boldsymbol{\rho})|^2\Big\{\Theta(t-t_1-|\mathbf{r}_A|/c)\Theta(\tau_2-|\boldsymbol{\rho}|/c) \\
\times\ & e^{-6\gamma(t-t_1-|\mathbf{r}_A|/c)}e^{-6\gamma(\tau_2-|\boldsymbol{\rho}|/c)} + A\leftrightarrow B \\
& +2\Theta(t-t_1-|\mathbf{r}_A|/c)\Theta(t-t_1-|\mathbf{r}_B|/c)\Theta(\tau_2-|\boldsymbol{\rho}|/c) \\
& \times e^{-6\gamma\left[t-t_1-\frac{1}{2}(|\mathbf{r}_A|+|\mathbf{r}_B|)/c\right]}e^{-6\gamma(\tau_2-|\boldsymbol{\rho}|/c)} \\
& \qquad \times\cos[\mathbf{k}(\mathbf{r}_A-\mathbf{r}_B)]\Big\}, \\
& +\sin^2\varphi\langle|2\rangle_{AA}\langle 2|1\rangle_{BB}\langle 1|\rangle \\
\times\ & |\Psi(\mathbf{r})|^2|\Psi(\boldsymbol{\rho})|^2\Theta(t-t_1-|\mathbf{r}_A|/c)\Theta(\tau_2-|\boldsymbol{\rho}|/c) \\
\times\ & e^{-6\gamma(t-t_1-|\mathbf{r}_A|/c)}e^{-6\gamma(\tau_2-|\boldsymbol{\rho}|/c)} + A\leftrightarrow B
\end{aligned}
\tag{6.4.2}
$$

Here, we have introduced the times $t_1 = t_0 + T_D$ which is the time when we expect one of the two photons to be excited by the π-polarized broadband excitation and $\tau_2 = t - t_2$ where $t_2 = t_1 + 5/(6\gamma)$ is the time when we apply the strong σ^- circularly polarized $\pi/2$ pulse [33, 34, 35].

In the second-order correlation function, "which way" information is partially stored in the internal atomic states similar to the first-order correlation function derived in the previous sections. This "which way" information can be read out in

the same fashion as in the previous section giving rise to partial "which way" information. Interestingly the inequality (6.3.12) can also be applied for this experimental setup in spite of the fact that one measures a second-order correlation function. The distinguishability and fringe visibility obey the same inequality for this quantum eraser scheme. The fringe visibility $\mathcal{V}$ and distinguishability $\mathcal{D}$ are given for this interferometric scheme if we measure the internal states of atom A as in the previous sections

$$\begin{aligned} \mathcal{V} &= \cos^2\varphi, \\ \mathcal{D} &= \sin^2\varphi. \end{aligned} \tag{6.4.3}$$

That means the fringe visibility and partial which-way information are identical to the results of the previous section for the first order correlation function and we can apply the same considerations for them concerning, e.g. detector efficiency. This tells us something about the fundamental duality principle between the fringe visibility and which-way information. It is not important, how one derives partial which-way information but an amount of partial "which way" information will always reduce the fringe visibility. Or, to be more precise, the possibility to get partial "which way" information reduces the interference fringes even without an actual partial which-way information which is the starting point of the considered partial "which way" detectors in this section. We have considered schemes for partial which-way information based on an interference experiment of two trapped 4-level atoms [1]. We have

derived a special inequality for this partial "which way" detector similar to the fundamental inequality of Englert [2]. Interestingly, the partial "which way" detection scheme works for the first-order correlation function as well as for the second-order correlation function in connection with the quantum eraser scheme. The considered partial "which way" detectors work on the general duality principle that even the possibility of getting partial "which way" information but not an actual information already reduces the amount of fringe-visibility.

Recently, the equal sign of the inequality of Englert [2] was proved experimentally in connection with interaction free measurements by Karlsson, Björk and Forsberg [40]. Our scheme allows, in addition, to prove the inequality at least between certain boundaries determined by the polarization angle φ of the polarizers in front of the detector. Values different from the equal sign in the inequality arise for detector efficiency less than one. The finite detector efficiency is similar to the assumption of a mixture of initial detector states and, consequently, the results are in accordance with the inequality [2] by Englert who proved that the equality sign always holds for a pure initial detector state but not for a mixture.

Chapter VII

7 Quantum Eraser and the Decoherence Time of a Measurement Process

7.1 Introduction

We have seen in the previous chapter that entanglement of the quantum sub-systems (atoms-photon) is required to implement a quantum eraser. Furthermore, if this entanglement is not stable (if we take into account the decay rates of the states $|1\rangle$ and $|2\rangle$) the erasing pulse must be applied before the decay of the correlation of the sub-system. The stability of the entanglement can be ensured by assuming the states $|1\rangle$ and $|2\rangle$ to be quasi-stable. That is, we assume the lifetimes of the states $|1\rangle$ and $|2\rangle$ to be much longer than the relevant times in the experiment. But now an interesting situation arises concerning the correlations in the expression of the interference Eq. (5.2.3). A measurement of the atomic states of one of the atoms, for example atom B, destroys the entanglement and, therefore, the correlation as well. In other words, a local measurement on one of the atoms and therefore an explicit knowledge of the "which path" information eliminates the possibility to erase the information since the entanglement is destroyed. In principle, this allows us to measure decoherence time (related to the rate at which coherence decays in the measurement process $\tau_c = \frac{1}{\gamma_c}$)

of the local measurement process. During the measurement process the correlation is not completely destroyed, rather it is reduced, and the application of the erasing pulse during the coherence time τ_c of the local measurement process should produce interference in the second order correlation function, albeit, it is reduced as manifested in the reduction of the visibility.

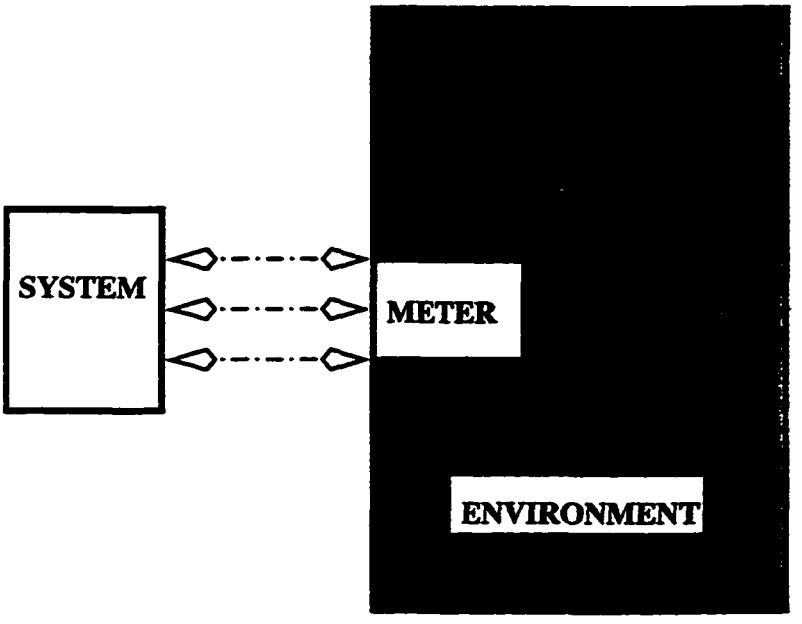

Figure 15: Schematic representation of the measurement scheme. The system is directly coupled to the meter and the meter is coupled to the environment (reservoir).

We now outline the basic ideas of quantum measurement theory and adopt it to the experimental situation of the quantum eraser. The general quantum measurement process has been dealt with in Refs. [44, 45, 46]. In general, the quantum measurement scheme involves a system S, which is to be measured, coupled to a

meter M that reads out the measured quantity, and the meter is coupled to the environment E or reservoir (Fig. 15). The coupling between the meter and the reservoir determines the pointer basis of the meter related to the particular pointer observable of the meter depending on what operator of the system S is measured. Here, we want to implement the quantum eraser as a scheme to probe the decoherence time of a measurement process[41, 42, 43]. The measured system here is the Zeeman split energy of the two degenerate states of one of the atoms, i.e. atom B. We use the quantum eraser scheme of subsection 5.3, valid for non-degenerate atoms which allows us to selectively excite one of the two atoms with a strong, short $\frac{\pi}{2}$-pulse which is σ^- circularly polarized. We start with the following special initial condition of the two atoms system

$$\rho_{AB}(t_0) = |1\rangle_{AA}\langle 1| \otimes |1\rangle_{BB}\langle 1|. \tag{7.1.1}$$

After the application of the BBE field and the subsequent decay of the excited states, we have

$$\begin{aligned} \rho_{AB}(t) &= |2\rangle_{AA}\langle 2| \otimes |1\rangle_{BB}\langle 1| + |2\rangle_{AA}\langle 1| \otimes |1\rangle_{BB}\langle 2| \\ &\quad +1 \leftrightarrow 2. \end{aligned} \tag{7.1.2}$$

The system is coupled to the meter, and we have the system-meter entanglement

$$\begin{aligned} \rho_{S-M} &= |2\rangle_{AA}\langle 2| \otimes |1\rangle_{BB}\langle 1| \otimes |m_1\rangle\langle m_1| \\ &+ |2\rangle_{AA}\langle 1| \otimes |1\rangle_{BB}\langle 2| \otimes |m_1\rangle\langle m_2| + 1 \leftrightarrow 2. \end{aligned} \tag{7.1.3}$$

Here $|m_1\rangle$, $|m_2\rangle$ are pointer bases. The meter is coupled to the environment and the off-diagonal elements decay very fast with a decoherence time γ_{dec}^{-1} of the pointer states. The consequence of this is that the interfering term in the second order correlation function (in the quantum eraser) will decay rapidly due to the coupling to the meter. The erasing pulse is applied at a time δt later after starting the measurement process. It restores the interference but with a reduced visibility. The amount of reduction in fringe visibility is a quantitative measure of the decoherence time (rate). Due to the coupling of the meter system to the environment, the entanglement of correlation decays very rapidly with the same decay rate γ_{dec}. The system-meter state which is "macroscopic" is then given by

$$\begin{aligned} \rho_{S-M} &= |2\rangle_{AA}\langle 2| \otimes |1\rangle_{BB}\langle 1| \otimes |m_1\rangle\langle m_1| \\ &+ e^{-\gamma_{dec}t}(|2\rangle_{AA}\langle 1| \otimes |1\rangle_{BB}\langle 2| \otimes |m_1\rangle\langle m_2|) \\ &+ 1 \leftrightarrow 2. \end{aligned} \tag{7.1.4}$$

The expression of the second order correlation function contains the same entanglement of atomic correlations as in the above meter-system density operator just before application of the erasing pulse. Consequently, these correlations decay rapidly due to the measurement process, i.e. the entanglement of the atomic system to the meter states. The application of the erasing pulse interrupts the measurement because after the application of the erasing pulse the states have the same magnetic quantum number. Therefore a coupling to the measurement apparatus does not exist anymore.

After the delay time δt of the measurement process and application of the erasing pulse afterwards, as will be explicitly shown in the next sections, we get the following for the interference term at the time t, which is the time when we expect a detection event for the interference σ_x-polarized scattering photons

$$\begin{aligned} & G^2(\mathbf{r}, t; \boldsymbol{\rho}, \tau_2) = |\Psi(\mathbf{r})|^2 |\Psi(\boldsymbol{\rho})|^2 \\ \times \; & \Theta(\tau_2 - |\boldsymbol{\rho}|/c)\Theta(t - t_1 - |\mathbf{r}_A|/c)\Theta(t - t_1 - |\mathbf{r}_B|/c) \\ \times \; & e^{-6\gamma[t - t_1 - \frac{1}{2}(|\mathbf{r}_A| + |\mathbf{r}_B|)/c]} e^{-6\gamma(\tau_2 - |\boldsymbol{\rho}|/c)} \\ \times \; & e^{-\gamma_{dec}\delta t} \cos(\mathbf{k} \cdot (\mathbf{r}_A - \mathbf{r}_B)). \end{aligned} \tag{7.1.5}$$

The implication of the above is that the visibility is reduced by a factor related to $e^{-\gamma_{dec}\delta t}$ due to the measurement process. This means the decoherence time is visualized by the reduction of the fringe visibility and that quantum eraser can be used as a tool to study fundamental properties such as the transition from microscopic to macroscopic systems, and the measurement process itself.

7.2 Model of the Measurement Process

The model for the measurement scheme is as follows. We apply a strong magnetic field B_0 which splits the degenerate states (Zeeman splitting) by an amount of Δ (see Fig. 16). In addition we put a high-Q cavity around both of the two atoms in a similar way as the scheme of Ref. [47] proposed for quantum computing. The quantized cavity field is assumed to be x-polarized, i.e. drives σ-transitions and is

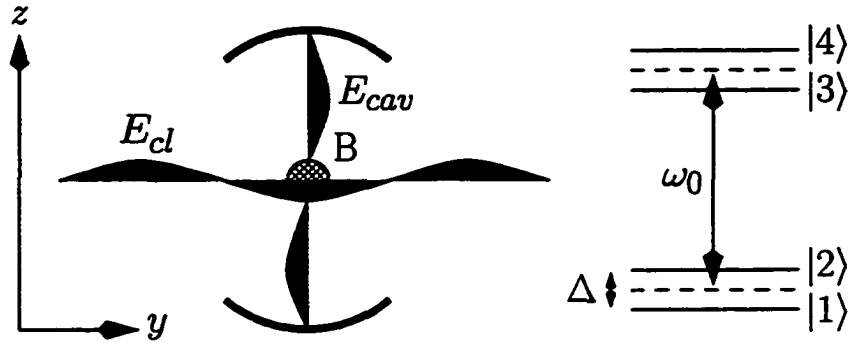

Figure 16: Arrangement for the local quantum measurement process on atom B, where E_{cl} and E_{cav} are x-polarized. Both fields drive the frequency ω_0 as indicated in the right figure. Atom B is selectively driven by the classical laser field. Atom A is behind atom B in x-direction and interacts only with the cavity field.

tuned to the transition frequency ω_0 of the degenerate atoms. Accordingly, the cavity field frequency ω_0 is strongly detuned from the atomic transitions $|2\rangle \leftrightarrow |3\rangle$ by an amount of Δ and $|1\rangle \leftrightarrow |4\rangle$ by an amount of $-\Delta$ for the non-degenerate atoms. In addition to the cavity field, which is initially assumed to be in the vacuum state, we apply a strong classical (coherent state E) driving field also σ_x-polarized and with driving frequency ω_0. The classical field is assumed to have a phase of $\pi/2$ relative to the quantized cavity field. However, we selectively drive with this classical driving field only one of the two atoms, i.e. atom B. The selective driving of one of the two atoms is possible since the two atoms are separated by several wavelengths, i.e. we are far from the Dicke-limit. The coupling to the classical field in the strong detuning limit drives the cavity field into a coherent state. The cavity field will be used as the

meter which is coupled to the atomic system. We can write the total Hamiltonian of the atoms interacting with the cavity field and the classical field as follows

$$\begin{aligned} H &= H_0 + H_{cav} + H_{int}, \\ &= \hbar\frac{\omega_0}{2}(\sigma_{z,A} + \sigma_{z,B}) + \hbar\frac{\Delta}{2}(\tilde{\sigma}_{z,A} + \tilde{\sigma}_{z,B}) + \hbar\omega a^\dagger a \\ &+ \hbar\{g^*_{cav}(\sigma^-_{x,A} + \sigma^-_{x,B})a^\dagger + g_{cav}(\sigma^+_{x,A} + \sigma^+_{x,B})a\} \\ &+ i\hbar g_{cl}E_{cl}\{\sigma^+_{x,B} - \sigma^-_{x,B}\}. \end{aligned} \tag{7.2.1}$$

Here,

$$\begin{aligned} \sigma_z &= |4\rangle\langle 4| + |3\rangle\langle 3| - |2\rangle\langle 2| - |1\rangle\langle 1| \\ \tilde{\sigma}_z &= |4\rangle\langle 4| - |3\rangle\langle 3| + |2\rangle\langle 2| - |1\rangle\langle 1|, \end{aligned} \tag{7.2.2}$$

and g_{cav} is the coupling parameter to the cavity field, $a^\dagger$ and a are the creation and annihilation operators for the cavity field E_{cav} respectively and $g_{cl}E_{cl}$ is the Rabi frequency of the classical driving field. Since the atoms are independent, the state vector for the two atoms can be written as follows

$$|\Psi(t)\rangle = |\Psi_A(t)\rangle \otimes |\Psi_B(t)\rangle. \tag{7.2.3}$$

The equation for atom B is then

$$i\hbar\frac{\partial}{\partial t}|\Psi_B(t)\rangle = H_B|\Psi_A(t)\rangle, \tag{7.2.4}$$

where H_B is the Hamiltonian for atom B and, $|\Psi_B(t)\rangle$ is the state vector for atom B, and we have a similar equation for atom A except it does not contain the classical

driving term. We now consider atom B and, in the interaction picture, we get the following

$$i\hbar\frac{\partial}{\partial t}|\Psi_{IB}(t)\rangle = H_{IB}(t)|\Psi_{IB}(t)\rangle, \tag{7.2.5}$$

where

$$\begin{aligned} H_{IB}(t) &= e^{i\frac{\Delta}{2}\tilde{\sigma}_{z,B}t}\hbar\{g^*_{cav}\sigma^-_{x,B}a^\dagger + g_{cav}\sigma^+_{x,B}a \\ &\quad + ig_{cl}E_{cl}(\sigma^+_{x,B} - \sigma^-_{x,B})\}e^{-i\frac{\Delta}{2}\tilde{\sigma}_{z,B}t}. \end{aligned} \tag{7.2.6}$$

This gives the following interaction Hamiltonian

$$\begin{aligned} H_{IB}(t) &= \hbar\Big\{[(g^*_{cav}a^\dagger - ig_{cl}E_{cl})|1\rangle\langle 4| + (g_{cav}a + ig_{cl}E_{cl})|3\rangle\langle 2|]e^{-i\Delta t} \\ &+ [(g^*_{cav}a^\dagger - ig_{cl}E_{cl})|2\rangle\langle 3| + (g_{cav}a + ig_{cl}E_{cl})|4\rangle\langle 1|]e^{i\Delta t}\Big\}. \end{aligned} \tag{7.2.7}$$

In the strong detuning limit which is valid if $(g_{cav}/\Delta)^2\overline{n} \ll 1$, where $\overline{n}$ is the mean photon number of the cavity field and $(g_{cl}E_{cl}/\Delta)^2 \ll 1$ we use adiabatic elimination to obtain an effective Hamiltonian. We integrate by parts the interaction picture Schröedinger equation and, after dropping the term which is small in the strong limit, we obtain the following for atom B

$$\begin{aligned} H^B_{eff} &= \frac{\hbar}{\Delta}\Big\{(g_{cav}a + ig_{cl}E_{cl})(g^*_{cav}a^\dagger - ig_{cl}E_{cl})[|4\rangle\langle 4| - |3\rangle\langle 3|] \\ &+ (g^*_{cav}a^\dagger - ig_{cl}E_{cl})(g_{cav}a + ig_{cl}E_{cl})[|2\rangle\langle 2| - |1\rangle\langle 1|]\Big\}. \end{aligned} \tag{7.2.8}$$

We also have a similar Hamiltonian for atom A without the classical driving field terms. The two atoms system interacting with the cavity and classical fields is now

described by an effective interaction Hamiltonian H_{eff} given as

$$\begin{aligned} H_{eff} &= \frac{\hbar}{\Delta}\tilde{\sigma}_{z,B}\{|g_{cav}|^2 a^\dagger a + g_{cl}^2|E_{cl}|^2 \\ &+ i(g_{cl}^* g_{cav} E_{cl}^* a - g_{cl} g_{cav}^* E_{cl} a^\dagger)\} \\ &+ \tilde{\sigma}_{z,A}\{|g_{cav}|^2 a^\dagger a\}. \end{aligned} \tag{7.2.9}$$

The above effective interaction Hamiltonian has a simple physical interpretation. The first and last terms are the dynamical Stark-shift and since atom B interacts with the classical field it experiences an additional Stark-shift. The term which includes the classical and cavity fields arises in the strong detuning limit due to two photon processes. These are stimulated absorption by the classical field to a virtual level followed by stimulated or spontaneous emission into the cavity field and vice versa. The factor i in these two terms arises due to the phase difference of $\pi/2$ between the classical and cavity field. We rewrite the effective Hamiltonian by introducing a "normalized" classical field amplitude $|\epsilon| = |g_{cl}E_{cl}/g_{cav}|$ and denoting g_{cav} with g

$$\begin{aligned} H_{eff} &= \hbar\tilde{\sigma}_{z,B}\frac{g^2}{\Delta}(a^\dagger a + |\epsilon|^2 - i\epsilon^* a + i\epsilon a^\dagger) \\ &+ \hbar\tilde{\sigma}_{z,A}\frac{g^2}{\Delta}a^\dagger a. \end{aligned} \tag{7.2.10}$$

7.3 The Decoherence Time

We now consider the full measurement process. The system operator which is measured is $\tilde{\sigma}_z$ (or some function thereof). This effectively is a measurement of the Zeeman split Ted energy. The system is coupled to the meter, cavity field described by H_{eff} and the meter is coupled to the environment. We assume that the cavity field (meter) is coupled to the environment by amplitude coupling

$$H_{ME} = \hbar\left(a\Gamma^{\dagger} + a^{\dagger}\Gamma\right). \tag{7.3.1}$$

Here,

$$\Gamma = \sum_k g_k b_k \ , \ \Gamma^{\dagger} = \sum_k g_k^* b_k^{\dagger}, \tag{7.3.2}$$

where b and $b^{\dagger}$ are reservoir annihilation and creation operators. The meter-environment interaction determines the particular states (pointer basis) to which the meters will reduce. The approximate pointer states in this case are the coherent states [45, 46]. We now have a complete system-meter-environment (atom, cavity field and all modes of the quantized field at zero temperature) process.

The density operator for the system-meter after tracing over the environment at zero temperature satisfies the following equation in the interaction picture

$$\begin{aligned} \frac{d\rho}{dt} &= \frac{1}{i}[H_{eff}, \rho] \\ &+ \gamma_{cav}\left\{2a\rho a^{\dagger} - a^{\dagger}a\rho - \rho a^{\dagger}a\right\}. \end{aligned} \tag{7.3.3}$$

Here γ_{cav} is the cavity decay-rate. We now expand the density operator as follows

$$\rho(t) = \sum_{ij=1}^{2} \rho_{ij}(t) \otimes |i\rangle\langle j|, \tag{7.3.4}$$

where $|i\rangle$ and $|j\rangle$ are the atomic states and $\rho_{ij}(t)$ is the density operator for the cavity field. We start with the initial condition

$$\rho_{ij}(0) = N_{ij}(\alpha_i = 0, \alpha_j = 0)\frac{|0_i\rangle\langle 0_j|}{\langle 0_i|0_j\rangle}. \tag{7.3.5}$$

The system is considered arbitrary, while the meter is in the vacuum state $|\alpha = 0\rangle$. We can solve the master equation using the normally ordered characteristic function[45, 46]. The density operator for the atom system plus meter evolves in the interaction picture into the following where the coherent states are the approximate pointer basis for the meter variable

$$\begin{aligned} \rho(t) &= |2\rangle_{AA}\langle 2| \otimes |1\rangle_{BB}\langle 1| \otimes \frac{|\alpha_1(t)\rangle\langle\alpha_1(t)|}{\langle\alpha_1(t)|\alpha_1(t)\rangle} \\ &+ \exp\Big[(2\alpha)^2\big(1 - \gamma_{cav}t - e^{-\gamma_{cav}t}\big) - i\phi_0 t\Big] \\ &\times |2\rangle_{AA}\langle 1| \otimes |1\rangle_{BB}\langle 2| \otimes \frac{|\alpha_1(t)\rangle\langle\alpha_2(t)|}{\langle\alpha_1(t)|\alpha_2(t)\rangle} + 1 \leftrightarrow 2. \end{aligned} \tag{7.3.6}$$

Here, $\alpha_{1,2} = \mp\alpha(1 - e^{-\gamma_{cav}t})$ are the amplitudes of the ensuing coherent states of the quantized cavity field with opposite phases and with $\alpha = g^2|\epsilon|/(\Delta\gamma_{cav})$ and $\phi_0 = 2g^2|\epsilon|^2/\Delta$. The phase ϕ_0 arises due to the additional dynamical Stark-shift of atom B by the classical field. The decoherence rate between two "macroscopic" states can be related to the distance between them [46], and in this case we have

$$\gamma_{dec} = |\alpha_1(t \to \infty) - \alpha_2(t \to \infty)|\gamma_{cav} = 2\alpha\gamma_{cav}. \tag{7.3.7}$$

The effect of the above in the quantum eraser is the following. In the quantum eraser scheme of Section 5.3 before the application of the erasing pulse the density operator was given by Eq. (5.3.3)

$$\rho_{A,B} = \frac{1}{2}\left(|1\rangle_{AA}\langle 1| \otimes |2\rangle_{BB}\langle 2| + |2\rangle_{AA}\langle 1| \otimes |1\rangle_{BB}\langle 2| + A \leftrightarrow B\right). \tag{7.3.8}$$

Due to the local measurement, the density operator after time δt the density operator is expressed by Eq. (7.3.6). Consequently, the application of the erasing pulse restores the interference, however, due to the local measurement the visibility is reduced from unity. With this we find for the visibility the following after the start of the measurement and the application of the erasing pulse at time δt later

$$\mathrm{V} = \exp\left(-\frac{\gamma_{dec}^2(\delta t)^2}{2}\right)\cos\left[\mathbf{k}\cdot(\mathbf{r}_A - \mathbf{r}_B) - \phi_0\delta t\right]. \tag{7.3.9}$$

Here we have assumed $\gamma_{cav}\delta t \ll 1$ and expanded the exponent in the exponential of Eq. (7.3.6) to second order.

A similar mesoscopic superposition of entangled coherent states has been realized recently in microwave cavities using Rydberg atoms in Ref. [43]. Recent advances in the optical regime in cavity QED allow coupling strength as high as $g \approx 1$ GHz with damping rates limited to $\gamma_{cav} \approx 1$ MHz in a Fabry-Perot cavity [48]. To ensure the strong detuning limit of the interaction Hamiltonian H_{eff} we assume a splitting Δ of the two ground states of around 10 GHz which requires a magnetic field strength

of around 1T. Taking into account a strong classical field $\epsilon \approx 1$ we can realize decoherence rates of $\gamma_{dec} \approx 100$ MHz or decoherence times $1/\gamma_{dec} = T_{dec} \approx 10^{-8}$s. In the long-time regime, $\delta t \gg T_{dec}$, the cavity field is driven into a mesoscopic incoherent superposition of two coherent states with opposite amplitudes $\alpha_{1,2} = \pm 100$. It is therefore allowed to speak of a measurement process on the system because of the generation of a quasi-classical field state as final measurement result.

It is clear that the time-interval of applying the measurement process δt has to be set to a certain value to get enough photon counts to read out the interference in the second order correlation function. After that the time interval δt can be set to another value to collect again enough photon counts and so on. The differences of the visibility of the interference fringes for different time-intervals δt can then be used to determine the decoherence rate of the measurement process. The phase $\phi_0 \delta t$ in the cosine of the interference part of the second order correlation is responsible for a shift of the interference fringes. It is important to recognize that the application of the erasing pulse at the time δt after starting the measurement process interrupts the decoherence process. After the excitation of the atoms with the erasing pulse the density operator contains only atomic states of the same magnetic quantum number $m_j = -1/2$ and consequently no decoherence process takes place. Therefore it is enough to stop the interaction with the measurement device after the detection of the erasing photon. The excitation time T_D to excite the atoms with the broadband scheme is assumed to

be of the order of magnitude of the decay-rate γ_{cav}. This ensures that the cavity field is approximately in the vacuum state when we do the next measurement on atom B and the strong detuning limit of the effective Hamiltonian is fulfilled.

Chapter VIII

8 Conclusion.

The entanglement in the atoms-photon system, as a result of the scattering of a photon, plays a crucial role in the quantum eraser. Entanglement is connected to the nonlocal behavior of quantum systems and, in the case of interference experiments with one photon, to the nonlocal behavior of the photon itself. The entanglement between the atoms-photon system depends on whether there is interference or no interference. In the case of no interference the atoms-photon system is entangled resulting from nonlocal superpositions of the correlated "two atoms-photon" states. The two correlated atomic states in these superpositions are orthogonal and therefore tracing over the atomic density operator gives a vanishing result. In the case of interference there is no entanglement between the atoms-photon system and consequently the atomic density operator can be factored out from the expression of the photon system and tracing over it gives one. As a result interference occurs.

It should be emphasized that even in the case of no interference we do not have an actual knowledge of "which way" the photon took. This is expressed by the nonlocal superpositions of the atoms-photon states. An actual knowledge of the path of the photon would lead to a collapse of the nonlocal superposition of the atoms-photon

states into one specific atoms-photon state. The detection of the photon at the photon detector in the case of non-interference gives us therefore only the possibility of knowing which path the photon has taken. The quantum eraser irreversibly erases this possibility of obtaining "which way" information. In particular the quantum eraser disentangles the atoms-photon system and consequently interference is brought back.

The scheme to obtain partial "which way" information can be implemented with a mere introduction of polarizers to the proposed "which way" experiment or to the experiment of the quantum eraser. The investigation of the intermediate states of the two extreme situations of duality is interesting in as much as it illustrates the principle of complementarity in the cases which are intermediate between the traditional wave-particle boundaries. As pointed out by Englert, the inequality is not a restatement of the uncertainty principle in disguise, rather it is a fundamental relation quantifying the concept of duality. Based on the current experimental advances, an experimental verification of the inequality using the scheme presented is possible.

It is clear that we need the superpositions of nonlocal atoms-photon states to erase the information, i.e. to erase the entanglement between the atoms-photon system or the possibility to obtain "which way" information. If this entanglement is not stable (e. g. finite decay rates of states $|1\rangle$ and $|2\rangle$) the second pulse to erase the information must be applied before the decay of atomic correlations. A local measurement of the

state of one of the atoms, for example atom B, destroys the atomic correlations and therefore the superposition of the nonlocal atoms-photon states. In other words a local measurement on one atom and therefore an explicit knowledge of the way the photon has taken irreversibly destroys the possibility to erase the information because the superpositions of the atoms-photon states leading to interference (after erasing) are destroyed.

The decoherence rate of two "macroscopic" superposition has been observed in a recent experiment by Brune *et al¿* [42] where the decoherence of superposition of two coherent states in a cavity was monitored. It is important to realize that the decoherence in the local measurement process in the scheme of Chapter VII is different. In this case, the decoherence is connected to the measurement process itself. There is a connection between the decoherence of a "macroscopic" superposition and the local measurement process in that in both cases we have superposition of "macroscopic" states which decohere rapidly, but, in the case of the local measurement the decoherence is related to the measurement process. From general principles, a "macroscopic" superposition will have a fast decoherence which depends on the distance between the two states, and in the local measurement scheme, it is a means of monitoring the measurement process itself.

To conclude, we want to point out that the quantum eraser is of fundamental interest in quantum optics because it allows us to explore two important aspects

of quantum mechanics: complementarity and non-locality. We have shown that the nonlocal superpositions of atoms-photon states in the case of non-interference, i.e. the entanglement between the atoms-photon system and the related atomic correlations in the quantum eraser can be used to measure the decoherence time of a macroscopic or mesoscopic measurement apparatus.

Appendix

A Equations of Motion for Two 4-level Atoms Coupled to BBE Field.

The matrix elements of the density operator are denoted by

$$\rho_{ij,kl}(t) = \langle k_A| \otimes \langle i_B|\rho(t)|j_A\rangle \otimes |l_B\rangle \tag{A.1}$$

where $|j_A\rangle$ and $|j_B\rangle$ denote the atomic states of atom A and B respectively. From the master equation Eq. (4.2.4), we get the following equations for the density matrix elements of the ground state population

$$\frac{d}{dt}\rho_{ii,jj}(t) = -4\gamma_D\rho_{ii,jj}(t), \tag{A.2}$$

where $i, j = 1, 2$. These give

$$\rho_{ii,jj}(t) = \rho_{ii,jj}(0)e^{-4\gamma_D t}. \tag{A.3}$$

The other relevant matrix elements of the density operator obey the following equations

$$\begin{aligned}
\frac{d}{dt}\rho_{33,11}(t) &= -\gamma_D[2\rho_{33,11}(t) + \rho_{13,31}(t) + \rho_{31,13}(t) - 2\rho_{11,11}(t)], \\
\frac{d}{dt}\rho_{31,13}(t) &= -\gamma_D[2\rho_{31,13}(t) + \rho_{11,33}(t) + \rho_{33,11}(t) - 2\rho_{11,11}(t)], \\
\frac{d}{dt}\rho_{13,31}(t) &= -\gamma_D[2\rho_{13,31}(t) + \rho_{33,11}(t) + \rho_{11,33}(t) - 2\rho_{11,11}(t)], \\
\frac{d}{dt}\rho_{11,33}(t) &= -\gamma_D[2\rho_{11,33}(t) + \rho_{13,31}(t) + \rho_{31,13}(t) - 2\rho_{11,11}(t)].
\end{aligned} \tag{A.4}$$

These lead to the following equation

$$\begin{aligned} & \frac{d}{dt}\{\rho_{33,11}(t)+\rho_{11,33}(t)+\rho_{13,31}(t)+\rho_{31,13}(t)\} \\ = & -4\gamma_D\{\rho_{33,11}(t)+\rho_{11,33}(t)+\rho_{13,31}(t)+\rho_{31,13}(t)\} \\ + & 8\gamma_D\rho_{11,11}(t). \end{aligned} \tag{A.5}$$

Integrating the above equation we get the following time evolution

$$\begin{aligned} & (\rho_{33,11}(t)+\rho_{11,33}(t)+\rho_{13,31}(t)+\rho_{31,13}(t)) \\ = & (\rho_{33,11}(0)+\rho_{11,33}(0)+\rho_{13,31}(0)+\rho_{31,13}(0))e^{-4\gamma_D t} \\ + & 2(1-e^{-4\gamma_D t})\rho_{11,11}(0). \end{aligned} \tag{A.6}$$

We also have

$$\frac{d}{dt}\{\rho_{33,11}(t)+\rho_{11,33}(t)-\rho_{13,31}(t)-\rho_{31,13}(t)\}=0,$$

$$\rho_{33,11}(t)+\rho_{11,33}(t)=\rho_{13,31}(t)+\rho_{31,13}(t). \tag{A.7}$$

At $t=0$

$$\rho_{33,11}(0)=\rho_{11,33}(0)=\rho_{13,31}(0)=\rho_{31,13}(0). \tag{A.8}$$

If there is no initial excitation, all the above initial conditions are zero and we get

$$\begin{aligned} \rho_{33,11}(t)=\rho_{11,33}(t) &= \rho_{13,31}(t)=\rho_{31,13}(t) \\ &= \frac{1}{2}(1-e^{-\gamma_D t})\rho_{11,11}(0). \end{aligned}$$

Here we may neglect initial evolution due to the vacuum and, since $\gamma \gg \gamma_D$, we cannot have an initially excited state

$$\rho_{33,11}(t) = e^{-\gamma_D t}\rho_{33,11}(0) \to 0. \tag{A.9}$$

The equation for both atoms to be excited is

$$\begin{aligned} \frac{d}{dt}\rho_{33,33}(t) &= 2\gamma_D(\rho_{33,11}(t) + \rho_{11,33}(t) \\ &+ \rho_{13,31}(t) + \rho_{31,13}(t)), \end{aligned} \tag{A.10}$$

and is non zero only if,

$$\rho_{33,11}(0) + \rho_{11,33}(0) + \rho_{13,31}(0) + \rho_{31,13}(0) \neq 0. \tag{A.11}$$

Since we don't have an initial excitation, we have $\rho_{33,33}(t) = 0$, that is we do not have two photon processes.

We consider now

$$\begin{aligned} \frac{d}{dt}\rho_{13,11}(t) &= -\gamma_D(3\rho_{13,11}(t) + \rho_{11,13}(t)), \\ \frac{d}{dt}\rho_{11,13}(t) &= -\gamma_D(3\rho_{11,13}(t) + \rho_{13,11}(t)), \\ \frac{d}{dt}\{\rho_{13,11}(t) + \rho_{11,13}(t)\} &= -4\gamma_D(\rho_{13,11}(t) + \rho_{11,13}(t)), \\ \rho_{13,11}(t) + \rho_{11,13}(t) &= e^{-4\gamma_D t}(\rho_{13,11}(0) + \rho_{11,13}(0)) \\ &= 0. \end{aligned} \tag{A.12}$$

Since $\rho_{13,11}(0) = \rho_{11,13}(0) = 0$, the other terms, $\rho_{13,33}(t), \rho_{33,11}(t)$ etc. give zero.

We consider the initial condition $|1\rangle_{AA}\langle 1| \otimes |2\rangle_{BB}\langle 2|$ and obtain

$$\begin{aligned}
\frac{d}{dt}\rho_{11,44}(t) &= \gamma_D(2\rho_{11,44}(t) - \rho_{31,24}(t) \\
&- \rho_{13,42}(t) - 2\rho_{11,22}(t)), \\
\frac{d}{dt}\rho_{33,22}(t) &= \gamma_D(2\rho_{33,22}(t) - \rho_{13,42}(t) \\
&- \rho_{31,24}(t) - 2\rho_{11,22}(t)), \\
\frac{d}{dt}\rho_{13,42}(t) &= \gamma_D(2\rho_{13,42}(t) - \rho_{33,22}(t) \\
&- \rho_{11,44}(t) - 2\rho_{11,22}(t)), \\
\frac{d}{dt}\rho_{31,24}(t) &= \gamma_D(2\rho_{31,24}(t) - \rho_{33,22}(t) \\
&- \rho_{11,44}(t) - 2\rho_{11,22}(t)).
\end{aligned} \tag{A.13}$$

This gives

$$\frac{d}{dt}\{\rho_{11,44} + \rho_{33,22} + \rho_{13,42} + \rho_{31,24}\} = 0. \tag{A.14}$$

And in a similar fashion as for $\rho_{11,33}(t)$ we get

$$\begin{aligned}
\rho_{11,44}(t) = \rho_{22,33}(t) &= -\rho_{13,42}(t) = -\rho_{31,24}(t) \\
&= \frac{1}{2}(1 - e^{-4\gamma_D t})\rho_{11,22}(0).
\end{aligned}$$

Here we have negative correlation.

B Interference from General Initial Conditions

We start with the general initial conditions, and a $\pi-$polarized BBE field

$$\begin{aligned}\rho_{AB}(t_0) &= P_{11}|1\rangle_{AA}\langle 1|\otimes|1\rangle_{BB}\langle 1| + P_{21}|1\rangle_{AA}\langle 1|\otimes|2\rangle_{BB}\langle 2| \\ &+ P_{21}|2\rangle_{AA}\langle 2|\otimes|1\rangle_{BB}\langle 1| + P_{22}|2\rangle_{AA}\langle 2|\otimes|2\rangle_{BB}\langle 2|.\end{aligned} \tag{B.1}$$

Here, P_{ij} satisfy the following normalization condition

$$\sum_{i=1,j=1}^{2} P_{ij} = 1. \tag{B.2}$$

After a single photon absorption from the BBE we have at time $t_1 \approx t_0 + T_D$

$$\begin{aligned}\rho_{AB}(t_1) &= \frac{1}{2}\Big\{P_{11}\{|1\rangle_{AA}\langle 1|\otimes|3\rangle_{BB}\langle 3| + |3\rangle_{AA}\langle 3|\otimes|1\rangle_{BB}\langle 1| \\ &+ |1\rangle_{AA}\langle 3|\otimes|3\rangle_{BB}\langle 1| + |3\rangle_{AA}\langle 1|\otimes|1\rangle_{BB}\langle 3|\} \\ &+ P_{12}\{|3\rangle_{AA}\langle 3|\otimes|2\rangle_{BB}\langle 2| + |1\rangle_{AA}\langle 1|\otimes|4\rangle_{BB}\langle 4| \\ &- |3\rangle_{AA}\langle 1|\otimes|2\rangle_{BB}\langle 4| - |1\rangle_{AA}\langle 3|\otimes|4\rangle_{BB}\langle 2|\} \\ &+ P_{21}\{|3\rangle_{BB}\langle 3|\otimes|2\rangle_{AA}\langle 2| + |1\rangle_{BB}\langle 1|\otimes|4\rangle_{AA}\langle 4| \\ &- |3\rangle_{BB}\langle 1|\otimes|2\rangle_{AA}\langle 4| - |1\rangle_{BB}\langle 3|\otimes|4\rangle_{AA}\langle 2|\} \\ &+ P_{22}\{|2\rangle_{AA}\langle 2|\otimes|4\rangle_{BB}\langle 4| + |4\rangle_{AA}\langle 4|\otimes|2\rangle_{BB}\langle 2| \\ &+ |2\rangle_{AA}\langle 4|\otimes|4\rangle_{BB}\langle 2| + |4\rangle_{AA}\langle 2|\otimes|2\rangle_{BB}\langle 4|\}\Big\}.\end{aligned} \tag{B.3}$$

The coupling to the vacuum leads to spontaneous emission and, for $\pi-$scattering we reach finally the following for the density operator of the atoms-field system

$$\begin{aligned}\rho_{AB}(t)\otimes\rho_{\gamma}^{f} &= \rho_{AB}(t)\otimes(|\gamma_A\rangle\langle\gamma_A|+|\gamma_B\rangle\langle\gamma_B| \\ &+ |\gamma_A\rangle\langle\gamma_B|+|\gamma_B\rangle\langle\gamma_A|).\end{aligned} \tag{B.4}$$

Here ρ_{γ}^{f} is the density operator for the field and we note that we have no entanglement between the photons and atoms. The scattered photon is not associated with a particular atom. Tracing over the photon states we see that the final density operator at time t is identical with the initial density operator at time $t=0$. The part of the density operator which gives rise to interference for $\pi-$scattering is

$$\begin{aligned}\rho_{AB}^{int}(t_1) &= P_{11}\{|1\rangle_{AA}\langle 3|\otimes|3\rangle_{BB}\langle 1|+|3\rangle_{AA}\langle 1|\otimes|1\rangle_{BB}\langle 3|\} \\ &- P_{12}\{|3\rangle_{AA}\langle 1|\otimes|2\rangle_{BB}\langle 4|+|1\rangle_{AA}\langle 3|\otimes|4\rangle_{BB}\langle 2|\} \\ &- P_{21}\{|3\rangle_{BB}\langle 1|\otimes|2\rangle_{AA}\langle 4|+|1\rangle_{BB}\langle 3|\otimes|4\rangle_{AA}\langle 2|\} \\ &+ P_{22}\{|2\rangle_{AA}\langle 4|\otimes|4\rangle_{BB}\langle 2|+|4\rangle_{AA}\langle 2|\otimes|2\rangle_{BB}\langle 4|\}.\end{aligned} \tag{B.5}$$

The field in the radiation zone (at the detector) is related to the dipole operator as

$$E_{A,B}^{(+)}(t,\mathbf{r})=\Theta(t-|\mathbf{r}_{A,B}|/c)\Psi(\mathbf{r})\sigma_{A,B}^{(-)}(t-|\mathbf{r}_{A,B}|/c),$$

and the interference is given by

$$\begin{aligned} G^{(+)}_{int}(t',\tau) &= |\Psi(\mathbf{r})|^2\Theta(t')\Theta(t'+\tau) \\ &\times \mathrm{Tr}_{A,B}\{\rho^{int}_{AB}(t_1)[\sigma^{(+)}_{A\pi}(t')\sigma^{(-)}_{B\pi}(t'+\tau) \\ &+ \sigma^{(+)}_{B\pi}(t'+\tau)\sigma^{(-)}_{A\pi}(t')]\}, \end{aligned} \tag{B.6}$$

where $t' = t - t_1 - |\mathbf{r}_A|/c$ is the retarded time and $\tau = (|\mathbf{r}_B| - |\mathbf{r}_A|)/c$ is the delay time between the two different propagations for the photon. We first consider the part of the initial density operator connected with P_{11} term:

$$\begin{aligned} G^{(1)}_{11}(t',\tau) &= |\Psi(\mathbf{r})|^2\Theta(t')\Theta(t'+\tau) \\ &\times \mathrm{Tr}_{A,B}\Big\{\big(\rho^A_{13}(t')\rho^B_{31}(t'+\tau)|1\rangle_{AA}\langle 3|\otimes|3\rangle_{BB}\langle 1| \\ &+ \rho^A_{31}(t')\rho^B_{13}(t'+\tau)|3\rangle_{AA}\langle 1|\otimes|1\rangle_{BB}\langle 3|\big) \\ &\times \big(|3\rangle_{AA}\langle 1|\otimes|1\rangle_{BB}\langle 3| + |1\rangle_{AA}\langle 3|\otimes|3\rangle_{BB}\langle 1|\big)\Big\} \\ &= |\Psi(\mathbf{r})|^2\Theta(t')\Theta(t'+\tau) \\ &\times \mathrm{Tr}_{A,B}\Big\{\rho^A_{13}(t')\rho^B_{31}(t'+\tau)|1\rangle_{AA}\langle 1|\otimes|1\rangle_{BB}\langle 1| \\ &+ \rho^A_{31}(t')\rho^B_{13}(t'+\tau)|1\rangle_{AA}\langle 1|\otimes|1\rangle_{BB}\langle 1|\Big\} \\ &= |\Psi(\mathbf{r})|^2\Theta(t')\Theta(t'+\tau)\Big(\rho^A_{13}(t')\rho^B_{31}(t'+\tau) \\ &\qquad + \rho^A_{31}(t')\rho^B_{13}(t'+\tau)\Big) \\ &= 2|\Psi(\mathbf{r})|^2\Theta(t')\Theta(t'+\tau)\cos(\omega\tau)e^{-6\gamma(t'+\tau)}. \end{aligned} \tag{B.7}$$

Next we consider the P_{12} term:

$$\begin{aligned}
G_{12}^{(1)}(t',\tau) &= -|\Psi(\mathbf{r})|^2\Theta(t')\Theta(t'+\tau) \\
&\times \mathrm{Tr}_{A,B}\Big\{(\rho_{13}^{A}(t')\rho_{42}^{B}(t'+\tau)|1\rangle_{AA}\langle 3|\otimes|4\rangle_{BB}\langle 2| \\
&+ \rho_{31}^{A}(t')\rho_{24}^{B}(t'+\tau)|3\rangle_{AA}\langle 1|\otimes|2\rangle_{BB}\langle 4|) \\
&\times -(|3\rangle_{AA}\langle 1|\otimes|2\rangle_{BB}\langle 4|+|1\rangle_{BB}\langle 3|\otimes|4\rangle_{BB}\langle 2|)\Big\} \\
&= |\Psi(\mathbf{r})|^2\Theta(t')\Theta(t'+\tau) \\
&\times \mathrm{Tr}_{A,B}\Big\{\rho_{13}^{A}(t')\rho_{42}^{B}(t'+\tau)|1\rangle_{AA}\langle 1|\otimes|2\rangle_{BB}\langle 2| \\
&+ \rho_{31}^{A}(t')\rho_{24}^{B}(t'+\tau)|1\rangle_{AA}\langle 1|\otimes|2\rangle_{BB}\langle 2|\Big\} \\
&= |\Psi(\mathbf{r})|^2\Theta(t')\Theta(t'+\tau) \\
&\times \Big\{\rho_{13}^{A}(t')\rho_{42}^{B}(t'+\tau)+\rho_{31}^{A}(t')\rho_{24}^{B}(t'+\tau)\Big\} \\
&= 2|\Psi(\mathbf{r})|^2\Theta(t')\Theta(t'+\tau)\cos(\omega\tau)e^{-6\gamma(t'+\tau)}.
\end{aligned} \tag{B.8}$$

The P_{21} term gives identical result as the P_{12} term with $A \leftrightarrow B$ and the P_{22} term gives the same result as P_{11} with $\rho_{13} \leftrightarrow \rho_{24}$ and $\rho_{31} \leftrightarrow \rho_{42}$. The total interference is

$$\begin{aligned}
G_{int}^{(1)}(\tau) &= \sum_{i=1,j=1}^{2} G_{ij}^{(1)}(\tau) \\
&= G_{int}^{(1)}(\tau)\sum_{i=1,j=1}^{2} P_{ij} \\
&= G_{int}^{(1)}(\tau).
\end{aligned} \tag{B.9}$$

Here $G_{int}^{(1)}(\tau)$ is the interference if we started with a pure initial condition $|i\rangle_{AA}\langle i|i\rangle_{BB}\langle i|(i =$

1, 2).

In the $\sigma-$scattering case we have the following final density operator of the atoms-field state

$$\begin{aligned}
\rho^{AB}(t') &= P_{11}[|1\rangle_{AA}\langle 1| \otimes |2\rangle_{BB}\langle 2|\gamma_B\rangle\langle\gamma_B| \\
&+ |2\rangle_{AA}\langle 2| \otimes |1\rangle_{BB}\langle 1|\gamma_A\rangle\langle\gamma_A| \\
&+ |1\rangle_{AA}\langle 2| \otimes |2\rangle_{BB}\langle 1|\gamma_B\rangle\langle\gamma_A| \\
&+ |2\rangle_{AA}\langle 1| \otimes |1\rangle_{BB}\langle 2|\gamma_A\rangle\langle\gamma_B|] \\
&+ P_{12}[|2\rangle_{AA}\langle 2| \otimes |2\rangle_{BB}\langle 2|\gamma_A\rangle\langle\gamma_A| \\
&+ |1\rangle_{AA}\langle 1| \otimes |1\rangle_{BB}\langle 1|\gamma_B\rangle\langle\gamma_B| \\
&+ |2\rangle_{AA}\langle 1| \otimes |2\rangle_{BB}\langle 1|\gamma_A\rangle\langle\gamma_B| \\
&+ |1\rangle_{AA}\langle 2| \otimes |1\rangle_{BB}\langle 2|\gamma_B\rangle\langle\gamma_A|] \\
&+ 1 \leftrightarrow 2. \qquad \text{(B.10)}
\end{aligned}$$

Here, we note the final atoms-field density operator is entangled and consequently we have a which way information. We also note that the final atomic density operator, after tracing over the field is different from the general initial density operator, which was not the case for $\pi-$scattering.

We now consider the calculation for interference from $\sigma-$scattering

$$\begin{aligned} G^{(1)}_{int}(t',\tau) &= |\Psi(\mathbf{r})|^2\Theta(t')\Theta(t'+\tau) \\ &\times \mathrm{Tr}_{A,B}\Big\{\rho^{int}(t_1)[\sigma^{(+)}_{A\sigma}(t')\sigma^{(-)}_{B\sigma}(t'+\tau) \\ &+ \sigma^{(+)}_{B\sigma}(t'+\tau)\sigma^{(-)}_{A\sigma}(t')]\Big\}. \end{aligned} \tag{B.11}$$

We consider first the term of the initial density operator proportional to the P_{11} term:

$$\begin{aligned} G^{(1)}_{11}(t',\tau) &= |\Psi(\mathbf{r})|^2\Theta(t')\Theta(t'+\tau) \\ &\times \mathrm{Tr}_{A,B}\Big\{\big(\rho^A_{13}(t')\rho^B_{31}(t'+\tau)|1\rangle_{AA}\langle 3|\otimes|3\rangle_{BB}\langle 1| \\ &+ \rho^A_{31}(t')\rho^B_{13}(t'+\tau)|3\rangle_{AA}\langle 1|\otimes|1\rangle_{BB}\langle 3|\big) \\ &\times \big(|3\rangle_{AA}\langle 2|\otimes|2\rangle_{BB}\langle 3|+|2\rangle_{AA}\langle 3|\otimes|3\rangle_{BB}\langle 2|\big)\Big\} \\ &= |\Psi(\mathbf{r})|^2\Theta(t')\Theta(t'+\tau) \\ &\times \mathrm{Tr}_{A,B}\Big\{\rho^A_{13}(t')\rho^B_{31}(t'+\tau)|1\rangle_{AA}\langle 2|\otimes|2\rangle_{BB}\langle 1| \\ &\qquad +\rho^A_{31}(t')\rho^B_{13}(t'+\tau)|2\rangle_{AA}\langle 1|\otimes|1\rangle_{BB}\langle 2|\Big\} \\ &= 0. \end{aligned} \tag{B.12}$$

Similary, we derive for the P_{12} term:

$$\begin{aligned} G_{12}^{(1)}(t',\tau) &= |\Psi(\mathbf{r})|^2\Theta(t')\Theta(t'+\tau) \\ &\times \mathrm{Tr}_{A,B}\Big\{\big(\rho_{13}^{A}(t')\rho_{42}^{B}(t'+\tau)|1\rangle_{AA}\langle 3|\otimes|4\rangle_{BB}\langle 2| \\ &+ \rho_{31}^{A}(t')\rho_{24}^{B}(t'+\tau)|3\rangle_{AA}\langle 1|\otimes|2\rangle_{BB}\langle 4|\big) \\ &\times \big(|3\rangle_{AA}\langle 2|\otimes|1\rangle_{BB}\langle 4|+|2\rangle_{AA}\langle 3|\otimes|4\rangle_{BB}\langle 1|\big)\Big\} \\ &= |\Psi(\mathbf{r})|^2\Theta(t')\Theta(t'+\tau) \\ &\times \mathrm{Tr}_{A,B}\Big\{\rho_{13}^{A}(t')\rho_{42}^{B}(t'+\tau)|1\rangle_{AA}\langle 2|\otimes|1\rangle_{BB}\langle 2| \\ &\qquad +\rho_{31}^{A}(t')\rho_{24}^{B}(t'+\tau)|2\rangle_{AA}\langle 1|\otimes|2\rangle_{BB}\langle 1|\Big\} \\ &= 0. \end{aligned} \tag{B.13}$$

Similarly, the P_{21} term gives zero, and the P_{22} term is zero since it the calculations are identical to the P_{11} term, with $1 \leftrightarrow 2$.

C Quantum Eraser with General Initial Conditions

The second order correlation $G^{(2)}(\mathbf{r},t;\boldsymbol{\rho},\tau)$ is defined as

$$\begin{aligned} G^{(2)}(\mathbf{r},t;\boldsymbol{\rho},\tau) &= \langle[E_A^{(-)\sigma}(\mathbf{r},t)+E_B^{(-)\sigma}(\mathbf{r},t)] \\ &\quad\times[E_A^{(-)\pi}(\boldsymbol{\rho},\tau)+E_B^{(-)\pi}(\boldsymbol{\rho},\tau)] \\ &\quad\times[E_A^{(+)\pi}(\boldsymbol{\rho},\tau)+E_B^{(+)\pi}(\boldsymbol{\rho},\tau)] \\ &\quad\times[E_A^{(+)\sigma}(\mathbf{r},t)+E_B^{(+)\sigma}(\mathbf{r},t)]\rangle. \end{aligned} \tag{C.1}$$

In terms of the Heisenberg dipole operators this can be expressed as

$$\begin{aligned} G^{(2)}(\mathbf{r},t';\boldsymbol{\rho},t'') &= \Theta(t'_A)\Theta(t'_B)\Theta(t''-T_o)|\Psi(\mathbf{r})|^2|\Psi(\boldsymbol{\rho})|^2 \\ &\times\langle[\sigma^+_{Ax}(\mathbf{r},t'_A)+\sigma^+_{Bx}(\mathbf{r},t'_B)] \\ &\times[\sigma^+_{Az}(\boldsymbol{\rho},t'')+\sigma^+_{Bz}(\boldsymbol{\rho},t'')] \\ &\times[\sigma^-_{Az}(\boldsymbol{\rho},t'')+\sigma^-_{Bz}(\boldsymbol{\rho},t'')] \\ &\times[\sigma^-_{Ax}(\mathbf{r},t'_A)+\sigma^-_{Bx}(\mathbf{r},t'_B)]\rangle, \end{aligned} \tag{C.2}$$

where we have introduced the retarded times $t'_{A,B} = t - t_1 - |\mathbf{r}_{A,B}|/c$ and $t'' = t' - |\boldsymbol{\rho}|/c$, respectively, and $T_0 = t_2 - t_1$ is the time delay between the excitation of the atoms with the BBE and applyication of the erasing pulse.

We consider first the term of the initial atomic density operator which is proportional to the P_{11} term:

$$\begin{aligned} G^{(2)}_{11}(\mathbf{r},t';\boldsymbol{\rho},t'') &= \Theta(t'_A)\Theta(t'_B)\Theta(t''-T_0)|\Psi(\mathbf{r})|^2|\Psi(\boldsymbol{\rho})|^2 \\ &\times \langle\rho(t_1)[\sigma^+_{Ax}(t'_A)+\sigma^+_{Bx}(t'_B)] \\ &\times[\sigma^+_{Az}(t'')+\sigma^+_{Bz}(t'')] \\ &\times[\sigma^-_{Az}(t'')+\sigma^-_{Bz}(t'')] \\ &\times[\sigma^-_{Ax}(t'_A)+\sigma^-_{Bx}(t'_B)]\rangle \end{aligned} \tag{C.3}$$

The" initial density operator" where we have taken already into account the excitation

with the broad band field is

$$\begin{aligned}\rho(t_1) &= \frac{1}{2}(|1\rangle_{AA}\langle 1| \otimes |3\rangle_{BB}\langle 3| + |1\rangle_{AA}\langle 3| \otimes |3\rangle_{BB}\langle 1| \\ &+ |3\rangle_{AA}\langle 1| \otimes |1\rangle_{BB}\langle 3| + |3\rangle_{AA}\langle 3| \otimes |1\rangle_{BB}\langle 1|). \end{aligned} \tag{C.4}$$

With this we have

$$\begin{aligned} & G_{11}^{(2)}(\mathbf{r}, t'; \boldsymbol{\rho}, t'') = \frac{1}{2}\Theta(t'_A)\Theta(t'_B)\Theta(t'' - T_o) \\ \times\ & |\Psi(\mathbf{r})|^2|\Psi(\boldsymbol{\rho})|^2\langle(|1\rangle_{AA}\langle 1| \otimes |3\rangle_{BB}\langle 3| + |1\rangle_{AA}\langle 3| \otimes |3\rangle_{BB}\langle 1| \\ +\ & |3\rangle_{AA}\langle 1| \otimes |1\rangle_{BB}\langle 3| + |3\rangle_{AA}\langle 3| \otimes |1\rangle_{BB}\langle 1|) \\ \times\ & [U^\dagger(t'_A)(|3\rangle_{AA}\langle 2| + |4\rangle_{AA}\langle 1|)U(t'_A) \\ +\ & U^\dagger(t'_B)(|3\rangle_{BB}\langle 2| + |4\rangle_{BB}\langle 1|)U(t'_B)] \\ \times\ & [\{U^\dagger(t'')(|4\rangle_{AA}\langle 2| - |3\rangle_{AA}\langle 1|)U(t'') \\ +\ & U^\dagger(t'')(|4\rangle_{BB}\langle 2| - |3\rangle_{BB}\langle 1|)U(t'')\}] \\ \times\ & [\{U^\dagger(t'')(|2\rangle_{AA}\langle 4| - |1\rangle_{AA}\langle 3|)U(t'') \\ +\ & U^\dagger(t'')(|2\rangle_{BB}\langle 4| - |1\rangle_{BB}\langle 3|)U(t'')\}] \\ \times\ & [U^\dagger(t'_A)(|2\rangle_{AA}\langle 3| + |1\rangle_{AA}\langle 4|)U(t'_A) \\ +\ & U^\dagger(t'_B)(|2\rangle_{BB}\langle 3| + |1\rangle_{BB}\langle 4|)U(t'_B)]\rangle. \end{aligned} \tag{C.5}$$

Here, $U(t) = U_A(t) \otimes U_B(t)$ is the time evolution operator for the two atoms-system, where each atom evolves independently. From time $t_1 \rightarrow t_2$, that is immediately before the application of the $\sigma-$polarized erasing pulse, we use cyclic permutation

inside the trace and free evolution until $t' = T_0$ and get the following

$$
\begin{aligned}
& G^{(2)}_{11}(\mathbf{r}, t' = T_0; \boldsymbol{\rho}, t'') = \frac{1}{2}\Theta(t'_A)\Theta(t'_B) \\
\times\ & \Theta(t'' - T_0)|\Psi(\mathbf{r})|^2|\Psi(\boldsymbol{\rho})|^2 \\
\times\ & \langle (e^{-6\gamma t'_A}|2\rangle_{AA}\langle 2| \otimes |1\rangle_{BB}\langle 1| + e^{-6\gamma t'_B}(|1\rangle_{AA}\langle 1| \otimes |2\rangle_{BB}\langle 2|) \\
\times\ & \left[\{U^\dagger_A(\tau'')(|4\rangle_{AA}\langle 2| - |3\rangle_{AA}\langle 1|)\right. \\
\times\ & U_A(\tau'') + U^\dagger_B(\tau'')(|4\rangle_{BB}\langle 2| - |3\rangle_{BB}\langle 1|) \\
\times\ & \left. U_B(\tau'')\}\right]\left[\{U^\dagger_A(\tau'')(|2\rangle_{AA}\langle 4| - |1\rangle_{AA}\langle 3|)\right. \\
\times\ & U_A(\tau'') + U^\dagger_B(\tau'')(|2\rangle_{BB}\langle 4| - |1\rangle_{BB}\langle 3|) \\
\times\ & \left. U_B(\tau'')\}\right]\rangle \\
+\ & \Theta(t'_A)\Theta(t'_B)\Theta(\tau'')|\Psi(\mathbf{r})|^2|\Psi(\boldsymbol{\rho})|^2 \\
\times\ & e^{-6\gamma \bar{t}'_{A,B}}\langle (|2\rangle_{AA}\langle 1| \otimes |1\rangle_{BB}\langle 2| \\
+\ & |1\rangle_{AA}\langle 2| \otimes |2\rangle_{BB}\langle 1|)\left[\{U^\dagger_A(\tau'')(|4\rangle_{AA}\langle 2| - |3\rangle_{AA}\langle 1|)\right. \\
\times\ & U_A(\tau'') + U^\dagger_B(\tau'')(|4\rangle_{BB}\langle 2| - |3\rangle_{BB}\langle 1|) \\
\times\ & \left. U_B(\tau'')\}\right]\left[\{U^\dagger_A(\tau'')(|2\rangle_{AA}\langle 4| - |1\rangle_{AA}\langle 3|)\right. \\
\times\ & U_A(\tau'') + U^\dagger_B(\tau'')(|2\rangle_{BB}\langle 4| - |1\rangle_{BB}\langle 3|) \\
\times\ & \left. U_B(\tau'')\}\right]\rangle .
\end{aligned}
$$

Here, we have introduced the delay time $\tau'' = t'' - T_0$, as well as the average retarded time $\bar{t}'_{A,B} = t - (|\mathbf{r}_A| + |\mathbf{r}_B|)/2c$. Immediately after the excitation with $\sigma-$polarized

erasing pulse we have

$$
\begin{aligned}
& G^{(2)}_{11}(\mathbf{r},t';\boldsymbol{\rho},t'') = \frac{1}{4}\Theta(t'_A)\Theta(\tau'')|\Psi(\mathbf{r})|^2|\Psi(\boldsymbol{\rho})|^2 \\
\times\ & \langle\{e^{-6\gamma t'_A}(|3\rangle_{AA}\langle 3|\otimes|1\rangle_{BB}\langle 1| + |2\rangle_{AA}\langle 2|\otimes|4\rangle_{BB}\langle 4|)\} \\
\times\ & [U^{\dagger}_A(\tau'')(|4\rangle_{AA}\langle 2| - |3\rangle_{AA}\langle 1|U_A(\tau'') \\
+\ & U^{\dagger}_B(\tau'')(|4\rangle_{BB}\langle 2| - |3\rangle_{BB}\langle 1|)U_B(\tau'')] \\
\times\ & [U^{\dagger}_A(\tau'')(|2\rangle_{AA}\langle 4| - |1\rangle_{AA}\langle 3|)U_A(\tau'') \\
+\ & U^{\dagger}_B(\tau'')(|2\rangle_{BB}\langle 4| - |1\rangle_{BB}\langle 3|)U_B(\tau'')]\rangle \\
+\ & \{A\leftrightarrow B\} \\
+\ & \Theta(t'_A)\Theta(t'_B)\Theta(\tau'')|\Psi(\mathbf{r})|^2|\Psi(\boldsymbol{\rho})|^2 \\
\times\ & e^{-6\gamma\bar{t}'_{A,B}} \\
\times\ & \langle(|3\rangle_{AA}\langle 1|\otimes|1\rangle_{BB}\langle 3| + |2\rangle_{AA}\langle 4|\otimes|4\rangle_{BB}\langle 2| \\
+\ & A\leftrightarrow B)[\ldots][\ldots]\rangle. \qquad \text{(C.6)}
\end{aligned}
$$

Here, $[\ldots]$ is the same as the previous expression in the relevant brackets (time-evolution operators and dipole moment operators). After free evolution and the detection of the $\sigma-$polarized interference photon and the $\pi-$polarized erasing photon,

we obtain the results for the second order correlation in section 5.2

$$
\begin{aligned}
G_{11}^{(2)}(\mathbf{r},t;\boldsymbol{\rho},\tau_2) &= \frac{1}{4}\Theta(t-t_1-|\mathbf{r}_A|/c)\Theta(\tau_2-|\boldsymbol{\rho}|/c) \\
&\times |\Psi(\mathbf{r})|^2|\Psi(\boldsymbol{\rho})|^2 e^{-6\gamma(t-t_1-|\mathbf{r}_A|/c)}e^{-6\gamma(\tau_2-|\boldsymbol{\rho}|/c)} \\
&\times \langle(|1\rangle_{AA}\langle 1|\otimes|1\rangle_{BB}\langle 1|+|2\rangle_{AA}\langle 2|\otimes|2\rangle_{BB}\langle 2|)\rangle + A\leftrightarrow B \\
&+ \frac{1}{4}\Theta(t-t_1-|\mathbf{r}_A|/c)\Theta(t-t_1-|\mathbf{r}_B|/c)\Theta(\tau_2-|\boldsymbol{\rho}|/c) \\
&\times |\Psi(\mathbf{r})|^2|\Psi(\boldsymbol{\rho})|^2 e^{-6\gamma[t-t_1-(|\mathbf{r}_A|+|\mathbf{r}_B|)/2c]} \\
&\times e^{-6\gamma(\tau_2-|\boldsymbol{\rho}|/c)}\cos[\mathbf{k}\cdot(\mathbf{r}_A-\mathbf{r}_B)] \\
&\times \langle(|1\rangle_{AA}\langle 1|\otimes|1\rangle_{BB}\langle 1|+|2\rangle_{AA}\langle 2|\otimes|2\rangle_{BB}\langle 2|+A\leftrightarrow B)\rangle \\
&= \frac{1}{2}\Theta(t-t_1-|\mathbf{r}_A|/c)\Theta(\tau_2-|\boldsymbol{\rho}|/c)|\Psi(\mathbf{r})|^2|\Psi(\boldsymbol{\rho})|^2 \\
&\times e^{-6\gamma(t-t_1-|\mathbf{r}_A|/c)}e^{-6\gamma(\tau_2-|\boldsymbol{\rho}|/c)} + A\leftrightarrow B \\
&+ \Theta(t-t_1-|\mathbf{r}_A|/c)\Theta(t-t_1-|\mathbf{r}_B|/c)\Theta(\tau_2-|\boldsymbol{\rho}|/c) \\
&\times |\Psi(\mathbf{r})|^2|\Psi(\boldsymbol{\rho})|^2 e^{-6\gamma(t-t_1-(|\mathbf{r}_A|+|\mathbf{r}_B|)/2c)} \\
&\times e^{-6\gamma(\tau_2-|\boldsymbol{\rho}|/c)}\cos[\mathbf{k}\cdot(\mathbf{r}_A-\mathbf{r}_B)], \qquad \text{(C.7)}
\end{aligned}
$$

where $\tau_2 = t - t_2$. The interfering part of the second-order correlation function which gives rise to an interference picture, also contributes to σ-scattering events. The entanglement between the photon and atomic system is erased and interference occurs as a result of the selective behavior of the measurement on the second-order correlation it selects fringes out of the two possibilities fringes, and anti-fringes [22, 25].

The calculation of the second order correlation with initial density operator pro-

portional to the P_{12} term is similar to the above calculation and we give therefore here only an abbreviated version considering only the time evolution of the atomic density operator. However, the atomic density operator immediately after the excitation with the broad band light reads as the following, due to the different initial condition

$$\begin{aligned}\rho(t_1) &= \frac{1}{2}(|3\rangle_{AA}\langle 3| \otimes |2\rangle_{BB}\langle 2| + |1\rangle_{AA}\langle 1| \otimes |4\rangle_{BB}\langle 4| \\ &- |3\rangle_{AA}\langle 1| \otimes |2\rangle_{BB}\langle 4| - |1\rangle_{AA}\langle 3| \otimes |4\rangle_{BB}\langle 2|). \end{aligned} \tag{C.8}$$

After the excitation with the BBE, free evolution takes place leading to the σ-polarized scattering photon. After this free evolution our density operator is of the following form

$$\begin{aligned}\rho(t') &= \frac{1}{2}(e^{-6\gamma t'_A}|2\rangle_{AA}\langle 2| \otimes |2\rangle_{BB}\langle 2| \\ &+ e^{-6\gamma t'_B}|1\rangle_{AA}\langle 1| \otimes |1\rangle_{BB}\langle 1| \\ &- e^{-6\gamma \bar{t'}_{A,B}+i\omega\tau}|2\rangle_{AA}\langle 1| \otimes |2\rangle_{BB}\langle 1| \\ &- e^{-6\gamma \bar{t'}_{A,B}-i\omega\tau}|1\rangle_{AA}\langle 2| \otimes |1\rangle_{BB}\langle 2|). \end{aligned} \tag{C.9}$$

Here, $\tau = |\mathbf{r}_A|/c - |\mathbf{r}_B|/c$ is the time delay between the two different photon propagations $\mathbf{r}_A$ and $\mathbf{r}_B$, respectively, which can lead in, the relevant photon correlation function, to the interference. Then, the application of the σ-polarized erasing pulse

at the time $t' = T_0$ leads to

$$\begin{aligned}
\rho(t') = \frac{1}{4}\Big[& e^{-6\gamma t'_A}(|3\rangle_{AA}\langle 3| \otimes |2\rangle_{BB}\langle 2| + |2\rangle_{AA}\langle 2|3\rangle_{BB}\langle 3|) \\
+ \; & e^{-6\gamma t'_B}(|4\rangle_{AA}\langle 4|1\rangle_{BB}\langle 1| + |1\rangle_{AA}\langle 1| \otimes |4\rangle_{BB}\langle 4|) \\
- \; & e^{-6\gamma \bar{t}'_{A,B} + i\omega\tau}(|3\rangle_{AA}\langle 1| \otimes |2\rangle_{BB}\langle 4| + |4\rangle_{AA}\langle 2| \otimes |1\rangle_{BB}\langle 3|) \\
+ \; & e^{-6\gamma \bar{t}'_{A,B} - i\omega\tau}(|2\rangle_{AA}\langle 4| \otimes |3\rangle_{BB}\langle 1| + |1\rangle_{AA}\langle 3| \otimes |4\rangle_{BB}\langle 2|)\Big].
\end{aligned} \tag{C.10}$$

After the detection of the erasing photon, which is detected as a π-polarized light another minus sign in the interference part occurs, and we have overall plus sign, finally, which leads to interfernce fringes (not anti-fringes). Th final density operator after detection of the second-order correlation function is given by taking into account the free evolution after the erasing pulse

$$\begin{aligned}
\rho(t', t'') = \; & \frac{1}{4}\Big[\Theta(t'_A)\Theta(t'' - T_0)e^{-6\gamma t'_A}e^{-6\gamma(t''-T_0)} \\
& \times \; (|1\rangle_{AA}\langle 1| \otimes |2\rangle_{BB}\langle 2| + 1 \leftrightarrow 2) \\
& + \; \Theta(t'_B)\Theta(t'' - T_0)e^{-6\gamma t'_B}e^{-6\gamma(t''-T_0)} \\
& \times \; (|2\rangle_{AA}\langle 2| \otimes |1\rangle_{BB}\langle 1| + 1 \leftrightarrow 2) \\
& + \; \Theta(t'_A)\Theta(t'_B)\Theta(t'' - T_0)e^{-6\gamma \bar{t}'_{A,B} + i\omega\tau}e^{-6\gamma(t''-T_0)} \\
& \times \; (|1\rangle_{AA}\langle 1| \otimes |2\rangle_{BB}\langle 2| + |2\rangle_{AA}\langle 2| \otimes |1\rangle_{BB}\langle 1|) \\
& + \; \Theta(t'_A)\Theta(t'_B)\Theta(t'' - T_0)e^{-6\gamma \bar{t}'_{A,B} - i\omega\tau}e^{-6\gamma(t''-T_0)} \\
& \times \; (|2\rangle_{AA}\langle 2| \otimes |1\rangle_{BB}\langle 1| + |1\rangle_{AA}\langle 1| \otimes |2\rangle_{BB}\langle 2|)\Big].
\end{aligned} \tag{C.11}$$

We recognize immediately that the tracing over the atomic density operator leads in the second order correlation function of the photons to an interfering part (term proportional to $e^{i\omega\tau}$). In other words we have erased the entanglement between the atomic system and the photon system and consequently get back the interference. The calculations for the other terms P_{ij} of our initial density operator can be done in the same way. The erasing scheme is independent from the initial conditions and leads to interference also for σ-scattering events if we measure the second order correlation of the correlated scattering and erasing photons.

References

[1] U. Eichmann, J. C. Bergquist, J.J. Bollinger, J.M Gilligan, W.M. Itano, D. J. Wineland, and M. G. Raizen, Phys. Rev. Lett. **70**, 2359 (1993).

[2] B. G. Englert, Phys. Rev. Lett. **77**, 2154 (1996).

[3] N. Bohr, Naturwissenschaften **16**, 245 (1928); Nature (London) **121**, 580 (1928).

[4] J. A. Wheeler and W. H. Zurek, *Quantum Theory and Measurement* (Princeton University Press, Princeton, NJ, 1983).

[5] R. P. Feynman, R. B. Leighton, and M. Sand, *The Feynman Lectures on Physics* (Addison Wesley, Reading, MA, 1965), Vol. III

[6] M. O. Scully and K. Drühl, Phys. Rev. A**25**, 2208 (1982).

[7] H. W. Wiseman, F. E. Harrison, M. J. Collet, S. M. Tan, D. F. Walls, and R. B. Killip, Phys. Rev. A **56**, 55 (1997).

[8] H. W. Wiseman, F. E. Harrison Phys. Rev. A **58**, 1740 (1997).

[9] G. M. Meyer and G. Yeoman, Phys. Rev. Lett. **79**, 2650 (1997).

[10] W. M. Itano, J. C. Bergquist, J. J. Bollinger, D. J. Wineland, U. Eichmann, and M. G. Raizen, Phys. Rev. A **57**, 4176 (1998).

[11] D. Polder and M. F. H. Schuurmans, Phys. Rev. A **14**, 1468 (1976).

[12] T. Wong, S. M. Tan, M. J. Collett, and D. F. Walls, Phys. Rev. A **55**, 1288 (1997).

[13] G. S. Agrawal, in *quantum Statistical Theories of Spontaneous Emission and their Relations to Other Approaches*, Springer Tracts Mod. Phys.,Vol 70 (Springer, Berlin, Heidelberg 1974)

[14] W. Heitler, *The Quantum Theory of Radiation*, 3rd ed. (Clarendon, Oxford, 1954).

[15] M. G. Raizen, J. M. Gilligan, J. C. Bergquist, W. M. Itano, and D. J. Wineland, Phys. Rev. A **45**, 6493 (1992).

[16] M. Itano and D.J. Wineland, Phys. Rev. A **25**, 36 (1982).

[17] B. R. Mollow, Phys. Rev. A **188**, 1969 (1969).

[18] C. Cohen-Tannoudji, in *Frontiers in Laser Spectroscopy, Les Houches Lectures 1975, Session XXVII*, edited by R. Balian *et al.* (North-Holland, Amsterdam, 1976).

[19] Th. Richter, Opt. Commun. **80**, 285 (1991).

[20] P. Kochan, H. J. Carmichael, P.R. Morrow, and M. G. Raizen, Phys. Rev. Lett. **75**, 45 (1995).

[21] B. C. Sanders and G. M. Milburn, Phys. Rev. A **39**, 2208 (1989).

[22] M. O. Scully, B. G. Englert, and H. Walther, Nature (London) **351**, 111 (1991); and references therein.

[23] M. Hillery and M. O. Scully, in *Quantum Optics, Experimental Gravity, and Measurement Theory* (Plenum, NY,1983) p.65.

[24] A. G. Zajonc, L. J. Wang, X. Y. Zou, and L. Mandel, Nature (London) **353**, 507 (1991).

[25] M. O. Scully and M. S. Zubairy, *Quantum Optics* (Cambridge University Press, Cambridge, UK, 1997)

[26] P. G. Kwiat, A. M. Steinberg, and R. Y. Chiao, Phys. Rev. A **11**, 7729 (1992).

[27] B. G. Englert, M. O. Scully, and H. Walther, Nature (London) **375**, 367 (1995); Sci. Am. **271** (6), 86 (1994).

[28] Th. J. Herzog, P. G. Kwiat, H. Weinfurter, and A. Zeilinger, Phys. Rev. Lett. **75**, 3034 (1995).

[29] H.-J. Briegel, B. G. Englert, M. O. Scully, and H. Walther in *Atom Interferometry*, ed. P. Bergmann (Academic Press, New York (1997)); and references therein.

[30] U. Mohrhoff, Am. J. Phys. **64**, 1468 (1997); B.-G. Englert, M. O. Scully, and H. Walther, Am. J. Phys., to appear (1998); B.-G. Englert, European J. Phys., to appear (1998).

[31] P. Storey, S. Tan, M. Collet, and D. Walls, Nature (London) **367**, 626 (1994).

[32] E. P. Storey, S. M. Tan, M. J. Collet, and D. F. Walls, Nature (London) **375**, 368 (1995).

[33] Y. Abranyos, M. Jakob, and J. Bergou, submitted to Phys. Rev. A. RC..

[34] Y. Abranyos, M. Jakob, and J. Bergou, submitted to Phys. Rev. A.

[35] Y. Abranyos, M. Jakob, and J. Bergou, Acta Phys. Slov. **48**, 255 (1998).

[36] D. M. Greenberger and A. Yasin, Phys. Lett. A **128**, 391 (1988).

[37] W. K. Wooters and W. H. Zurek, Phys. Rev. D **19**, 473 (1979).

[38] L. Mandel, Opt. Lett. **16** 1882 (1991).

[39] H. Rauch and J. Summhammer, Phys. Lett. A **104**, 44 (1984); J. Summhammer, H. Rauch,, and D. Tuppinger, Phys. Rev. A **36**, 4447 (1987).

[40] A. Karlsson, G. Björk, and E. Forsberg, Phys. Rev. Lett. **80**, 1198 (1998).

[41] S. Bose, K. Jacobs, and P. L. Knight, Los Alamos Preprint, quant-ph/9712017.

[42] L. Davidovich, M. Brune, J. M. Raimond, and S. Haroche, Phys. Rev. A **53**, 1295 (1996).

[43] M. Brune, E. Hagley, J. Dreyer, X. Maître, A. Maali, C. Wunderlich, J. M. Raimond, and S. Haroche, Phys. Rev. Lett. **77**, 4887 (1996).

[44] W. H. Zurek, Phys. Rev. D **26**, 1862 (1982).

[45] D. F. Walls, M. J. Collett, and G. J. Milburn, Phys. Rev. D **32**, 3208 (1985).

[46] D. F. Walls and G. J. Milburn, *Quantum Optics* (Springer, Berlin, 1994).

[47] T. Pellizari, S. A. Gardiner, J. I. Cirac, and P. Zoller, Phys. Rev. Lett. **75**, 3788 (1995).

[48] C. J. Hood, M. S. Chapman, T. W. Lynn, and H. J. Kimble, Phys. Rev. Lett. **80**, 4157 (1998).

IMAGE EVALUATION
TEST TARGET (QA-3)

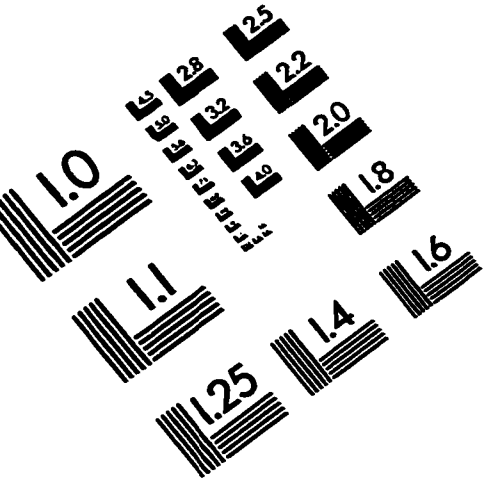

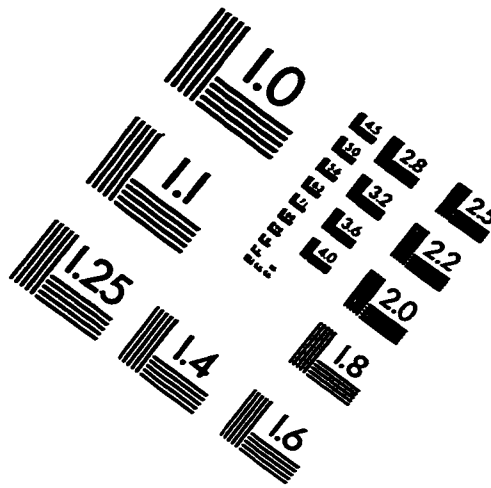

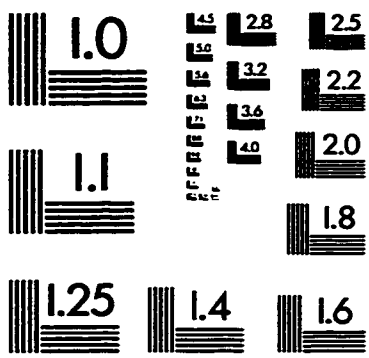

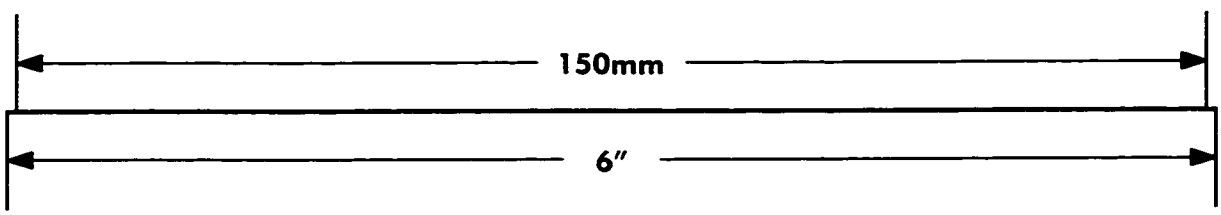

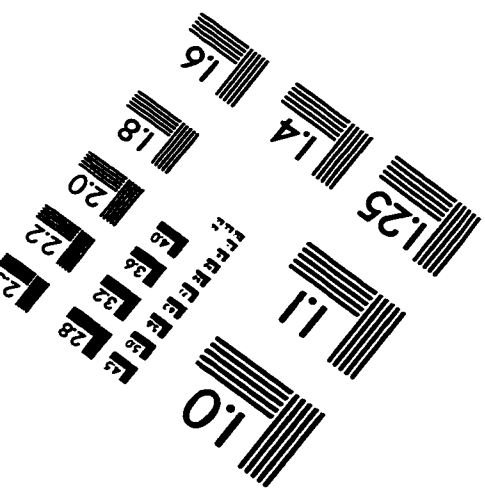

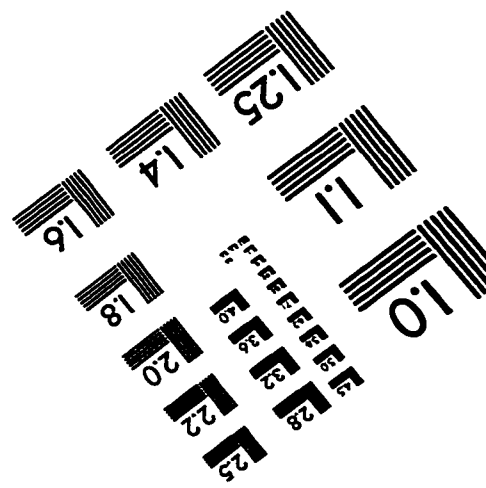

APPLIED IMAGE, Inc
1653 East Main Street
Rochester, NY 14609 USA
Phone: 716/482-0300
Fax: 716/288-5989